Aus der Klinik für Anästhesiologie - Anästhesie-, Intensiv-, Notfall- und Schmerzmedizin

(Direktor Univ.- Prof. Dr. Hahnenkamp)

der Universitätsmedizin der Universität Greifswald

Effects of Poloxamer 188 on Direct Mitochondrial Protection in Isolated Mitochondria after Ischemia Reperfusion Injury in Rat Isolated Hearts

Inauguraldissertation

zur

Erlangung des akademischen

Grades

Doktor der Medizin

(Dr. med.)

der

Universitätsmedizin

der

Universität Greifswald

2024

vorgelegt von: Josephine Eskaf

geb. am: 25.07.1996

in: Neubrandenburg

Dekan: Prof. Dr. med. Karlhans Endlich

1. Gutachter: Prof. Dr. med. Klaus Hahnenkamp

2. Gutachter: Prof. Dr. med. Maria Deja

Tag der Disputation: 18.03.2024

Table of content

List of Abbreviations

A	Aorta
ADP	Adenosine diphosphate
AHA	American Heart Association
ANT	Adenine nucleotide translocator
ATP	Adenosine triphosphate
BN	Brown Norway (rat strain)
BSA	Bovine serum albumin
Ca^{2+}	Calcium
CAC	Citric acid cycle
CCMS	Copolymer cell membrane stabilizers
CHD	Coronary heart disease
CO_2	Carbon dioxide
CORE	Collaborative Organization for RheothRx Evaluation
CPR	Cardiopulmonary resuscitation
CRC	Calcium retention capacity
CsA	Cyclosporine A
CVD	Cardiovascular disease
Cyt c	Cytochrome c
DAP	Diadenosine pentaphosphate
DMSO	Dimethyl sulfoxide
DNA	Deoxyribonucleic acid
dys	Dysferlin
EGTA	Ethylene glycol tetraacetic acid
ETC	Electron transport chain
F_1F_0- ATP synthase	ATP synthase
FAD	Flavin adenine dinucleotide (oxidized)
$FADH_2$	Flavin adenine dinucleotide (reduced)
FDA	Food and Drug Administration
g	Gram
g	Gravity
H^+	Proton
H_2O	Water
HR	Heart rate

i.c.	Intracoronary
i.v.	Intravenous
IACUC	Institutional Animal Care and Use Committee
IF_1	Inhibitor protein IF_1
IMM	Inner mitochondrial membrane
IMS	Intermembrane space
IR	Ischemia-reperfusion
IR+	Ischemia-reperfusion with 1 mM P188
Isc	Ischemia
IVC	Inferior vena cava
K^+	Potassium
KB	Krebs buffer
LA	Left atrium
LAD	Left anterior descending
LDH	Lactate dehydrogenase
LPC	Lysophosphatidylcholine
LV	Left ventricle
LVP	Left ventricular pressure
MI	Myocardial infarction
MM	Mitochondrial matrix
MOMP	Mitochondrial outer membrane permeabilization
MOPS	3-(N-Morpholino)- propanesulfonic acid
mPT	Mitochondrial permeability transition
mPTP	Mitochondrial permeability transition pore
MVO	Microvascular obstruction
Na^+	Sodium
NAD^+	Nicotinamide adenine dinucleotide (oxidized)
NADH	Nicotinamide adenine dinucleotide (reduced)
NCE	Na^+-Ca^{2+}-exchanger
NHE	Na^+-H^+- exchanger
O_2	Oxygen
$O_2^{-\bullet}$	Superoxide anion
OMM	Outer mitochondrial membrane
OXPHOS	Oxidative phosphorylation

P188	Poloxamer 188
PA	Pulmonary artery
PEG	Polyethylene glycol
PEO	Polyethylene oxide
P_i	Inorganic phosphate
PMF	Proton motive force
PPO	Polypropylene oxide
PTCA	Percutaneous transluminal coronary angioplasty
Q	Ubiquinone
QH_2	Ubiquinol
RA	Right atrium
RCI	Respiratory control index
ROS	Reactive oxygen species
RPP	Rate pressure product
RV	Right ventricle
SD	Sprague Dawley (rat strain)
SEM	Standard error of the mean
SR	Sarcoplasmic reticulum
SS	Dahl Salt Sensitive (rat strain)
SVC	Superior vena cava
TBI	Traumatic brain injury
TCH	Time control heart
VUMC	Vanderbilt University Medical Center

List of Figures

List of Tables

List of Equations

1. Introduction

1.1. Myocardial Infarction

As of 2018, the American Heart Association (AHA) defines acute myocardial infarction (MI) as an acute myocardial injury with clinical evidence of myocardial ischemia [1].

1.1.1. Epidemiology

MI is a leading cause for mortality and morbidity in Europe and worldwide [2]. It is the most common form of coronary heart disease (CHD) and, thus, of cardiovascular disease (CVD) which summarizes conditions affecting the heart and blood vessels.

Age- and gender-standardized mortality rate of CHD in Germany was 132.0 per 100,000 inhabitants in 2019 with the age-standardized mortality rate of men (176.3) being significantly higher than that of women (87.6). Of that the mortality rate of MI was at 48.5 per 100,000 inhabitants with a 52% difference between genders in favor of women [3].

Notably, regions in eastern Germany, such as Mecklenburg-Western Pomerania (65) and Saxony-Anhalt (67), have the highest mortality rates of MI per 100,000 inhabitants. This is probably due to confounding factors like smoking, unemployment rate and prevalence of comorbidities [3]. The INTERHEART study (2004) [4] identified nine risk factors that account for more than 90% of the population attributable risk of MI. These include elevated blood pressure, diabetes and smoking, hypercholesterolemia, obesity, physical inactivity as well as alcohol and low vegetable and fruit consumption [2,4].

The mortality rate for CHD in European high-income countries has been steadily declining for more than 25 years while it is increasing in low- and middle-income countries due to approaching lifestyles with remaining deficits in treatment [2,5]. Positive impacts on lowered MI mortality in Germany are mostly attributed to a shortened ischemic time. This has been achieved by numerous factors including optimized procedures in emergency systems in sparsely populated regions, reduction of pre-hospital time and “door-to-balloon-time”, as well as a well-informed population regarding symptoms of MI through national information agencies [3].

1.1.2. Clinical Manifestation of Myocardial Infarction

Myocardial injuries occur through an imbalance in oxygen (O_2) supply and demand, when either myocardial perfusion is reduced or demand is increased and cannot be sufficiently met (Fig. 1).

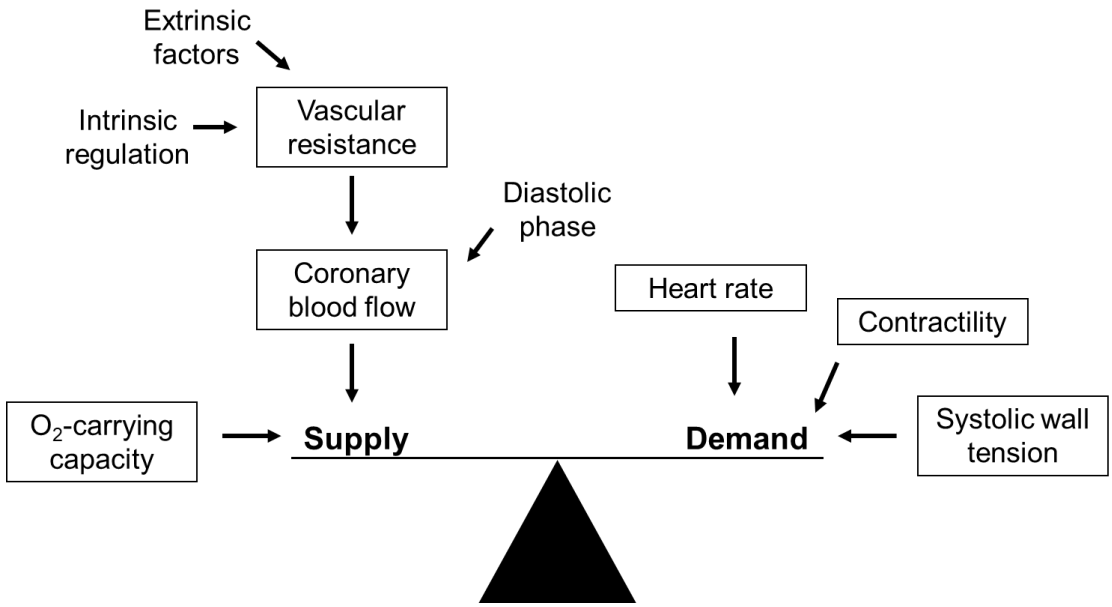

Figure 1: **Factors influencing myocardial oxygen supply and demand**. *Adapted from Ardehali A, Ports TA: Myocardial oxygen supply and demand* [6].

Myocardial perfusion can be reduced by coronary embolisms, atherosclerotic lesions, artery dissection, respiratory failure, myocardial injury as well as systemic conditions like sepsis and stroke [1,7]. When the ischemic condition prevails without prompt reperfusion, reversible turns into irreversible damage which is then called infarction [7].

However, reperfusion presents with a paradoxical exacerbation of tissue injury including mitochondrial and cellular dysfunction [8]. Four types of reperfusion injury in myocardial infarction can be separated from the primary ischemic insult. Reperfusion-induced arrhythmia and myocardial stunning are reversible and self-terminating whereas microvascular obstruction (MVO) and lethal reperfusion injury are not [9]. MVO is described as the “disturbance of myocardial circulation after temporary ischemia” [10] despite an open infarct-related coronary artery and is correlated with larger infarct size and higher mortality rate [11]. Lethal myocardial reperfusion injury is defined as the death of not yet irreversibly damaged cardiomyocytes caused by reperfusion [9]. In total this is called ischemia reperfusion (IR) injury.

1.1.3. Pathophysiology of Ischemia Reperfusion Injury

IR injury consists of two time periods: ischemia and reperfusion (Fig. 2).

Ischemia

Severed blood flow during ischemia results in deprivation of O_2 and nutrient supply to cardiomyocytes. Cellular consequences are a deficit in high-energy phosphate compounds like adenosine triphosphate (ATP), changes from aerobic glycolysis to anaerobic glycolysis with a resulting decrease in intracellular pH, and a disturbance of ion homeostasis. This makes the ischemic period a mainly metabolic event [7,12].

Anaerobic glycolysis severely decreases the cell's efficiency in ATP production compared to oxidative phosphorylation (OXPHOS) in oxygenated cells and rapidly depletes cellular energy resources. Pyruvate is increasingly converted to lactate in an effort to regenerate nicotinamide adenine dinucleotide (NAD^+) [13]. This lactate accumulation, a rise in protons (H^+), from ATP hydrolysis, and carbon dioxide (CO_2), produced by residual aerobic respiration, rapidly decrease cellular pH [7,14].

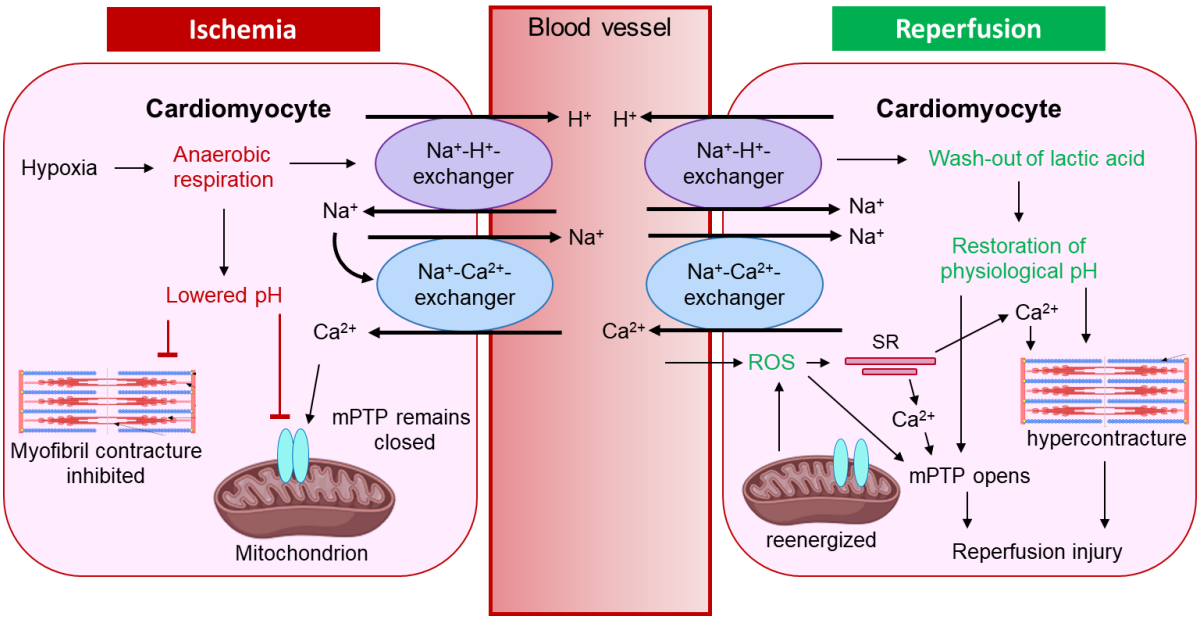

Figure 2: **Events of ischemia reperfusion injury in cardiomyocytes.** *Adapted from Hausenloy et al. 2013* [14].

During ATP deprivation active transport proteins in the cell membrane, like the sodium-potassium-ATPase (Na^+-K^+-ATPase) and calcium-pumps (Ca^{2+}-pumps), cease to work while secondary active transport proteins, like the Na^+-H^+-exchanger (NHE) and Na^+-Ca^{2+}-exchanger (NCE), stay operational. NHE is triggered by high H^+

concentration and exchanges intracellular H^+ for extracellular Na^+, accumulating Na^+, amplified by lack of function of the Na^+-K^+-ATPase [15]. To rid itself of Na^+, the NCE in cardiomyocytes extrudes 3 Na^+ in exchange for 1 Ca^{2+}, loading the cell up with Ca^{2+} [16]. High intracellular Ca^{2+}-concentrations lead to membrane leakage and trigger activation of lysosomal proteases, production of reactive oxygen species (ROS), and activation of Ca^{2+}-dependent ATPases. This results in ultrastructural injury, apoptosis and myocardial hypercontracture [7,17].

Cellular creatine phosphate levels rapidly decrease while inorganic phosphate (P_i) levels increase, further enhancing glycolysis [18]. Intracellular accumulation of lactate, H^+, P_i and ammonium ions steer the cell into osmotic shock which leads to membrane disruption [7], deteriorating function and premature cell death through necrosis [19]. These damages are reinforced by reperfusion [20].

Reperfusion

When blood flow is restored, cells are supplied with O_2 and nutrients again. This reperfusion reduces ischemia and limits ischemic injury but also initiates reactions that lead to further damage of heart tissue and loss in function. Some cells are inevitably lost during ischemia, while others remain definitely viable, and others are potentially viable and could be saved through reperfusion (Fig. 3). However, reperfusion activates mechanisms for apoptosis and necrosis in potentially viable cells in this “risk zone”, resulting in an extended period of apoptosis with a considerable amount of cell loss that advances the development of heart failure [21,22].

Energy production is resumed quickly upon reperfusion and initially leads to further increase in Ca^{2+}-overload. ATP dependent Ca^{2+}-pumps now increasingly pump Ca^{2+} into the sarcoplasmic reticulum (SR) and mitochondria. Once the SR’s Ca^{2+}-capacity is reached, Ca^{2+} is extruded, causing a frequent shift of Ca^{2+} between SR and cytosol [23]. Since Ca^{2+}-extrusion is closely linked to intracellular Na^+-levels, the Ca^{2+}-shift is only terminated when the physiological Na^+-gradient has been reestablished by the Na^+-K^+-ATPase and the NCE is able to eject Ca^{2+} from the cell [24]. Elevated Ca^{2+}-levels in already reenergized cells are cause for hypercontracture of the heart muscle which is associated with membrane disruption and cell death. A low pH during reperfusion has been shown to be beneficial through inhibition of the contractile apparatus and prevention of hypercontracture until the ion balance is restored [9].

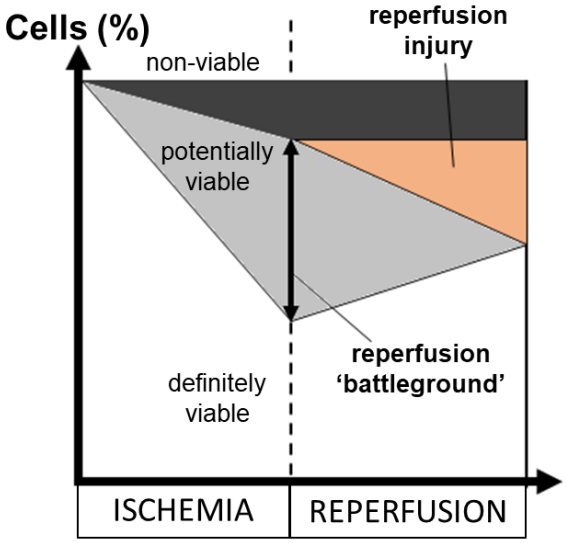

Figure 3: Reperfusion 'battleground'. During ischemia, non-viable cells (black) are inevitably lost. Others remain definitely (white) or potentially viable (grey). Reperfusion injury (orange) consists of potentially viable cells that cannot be salvaged during reperfusion. The extent of reperfusion injury can be influenced in the interval known as reperfusion 'battleground'. *Adapted from Maxwell et al. 1997* [22].

The intracellular pH can drop well below 7.0 during ischemia. Extracellular pH normalizes quickly through lactate wash-out during reperfusion, while the intracellular pH lags behind [25]. Due to this pH gradient H^+ is extruded from the cell, e.g. through the NHE, in an effort to normalize intracellular pH. The resulting increase in intracellular Na^+ hinders normalization of the Na^+-gradient [9]. Thus, although crucial in reestablishing cellular homeostasis, a rapid rise in pH enhances IR injury [9,25].

Similarly, quickly normalizing tissue osmolality causes water influx that leads to cell swelling and membrane disruption of already mechanically injured cells [26]. This effect has been shown to be attenuated with highly hyperosmotic reperfusion [9].

Myocardial O_2 partial pressure rises with reperfusion and enhances formation of ROS and oxidative stress. Oxidative stress describes the damaging processes that occur upon an imbalance of excess ROS production and the cellular antioxidant defense mechanisms [27]. ROS are free radicals derived from molecular O_2 that act as strong oxidants and play a role in intracellular signaling. During reintroduction of O_2 upon reperfusion, ROS are increasingly generated through oxidases and the mitochondrial electron transport chain (ETC) [17,28]. They cause cellular damage by altering membrane permeability and enzyme function. This interrupts the physiological ionic environment and accelerates cell death through necrosis [8,29]. ROS are thought to be partially responsible for arrhythmia, myocardial stunning and cell death [30,31].

1.1.4. Therapy and Treatment

Management of myocardial infarction is built on prompt reperfusion via percutaneous transluminal coronary angioplasty (PTCA) or thrombolysis. This is followed by pharmacological treatment to prevent in-stent restenosis, improving myocardial oxygen supply and reducing oxygen demand.

A critical determinant of infarct size is the duration of myocardial ischemia. Timely reperfusion is the only treatment of MI and essential in preventing heart failure by rescuing still viable cardiomyocytes, reducing infarct size, and preserving myocardial function. This makes it a viable therapeutic target [8,9,14]. Attempts have been made in two major directions: pre- and post-conditioning.

Ischemic pre-conditioning refers to short, alternating cycles of ischemia and reperfusion before prolonged ischemic conditions occur. It has been shown to reduce infarct size and incidence of arrhythmia and to improve recovery of contractile and endothelial function in several species, including man. However, benefits could only be observed upon timely reperfusion (< 3 h). Ischemic pre-conditioning is only a viable treatment for planned episodes of ischemia, e.g. during cardiac surgery [32].

Ischemic post-conditioning attempts to reduce infarct size through intermittent reperfusion. Cardiac protection can be observed when cycles of 30 sec reperfusion and 30 sec reocclusion are administered immediately at the onset of reperfusion [33]. Outcome is dependent on the time of the ischemic insult, time frame between onset of reperfusion, and post-conditioning procedure [34] as well as the amount of cycles of reperfusion and reocclusion [35].

Besides ischemic (‘mechanical’) post-conditioning, there are efforts pursuing pharmacological post-conditioning where drugs are administered directly before or during reperfusion to rescue potentially viable cells. Numerous possible targets have been identified and tested in experimental settings such as cyclosporine A (CsA) as an inhibitor of the mitochondrial permeability transition pore (mPTP) [36,37], and copolymer cell membrane stabilizers (CCMS) like Poloxamer 188 (P188) [31,38]. Post-conditioning would be feasible in clinical conditions of acute MI and is therefore a vital part of future research in search for a treatment of IR injury.

1.2. Isolated Heart Model

The isolated heart model allows observations and interventions of the heart ex-vivo without external neuronal and hormonal influences. The method of isolated mammal hearts was first established by Oskar Langendorff in 1895 (Fig. 4) and is still being used today (Fig. 5). It is referred to as the ‘Langendorff Heart Model’ [39].

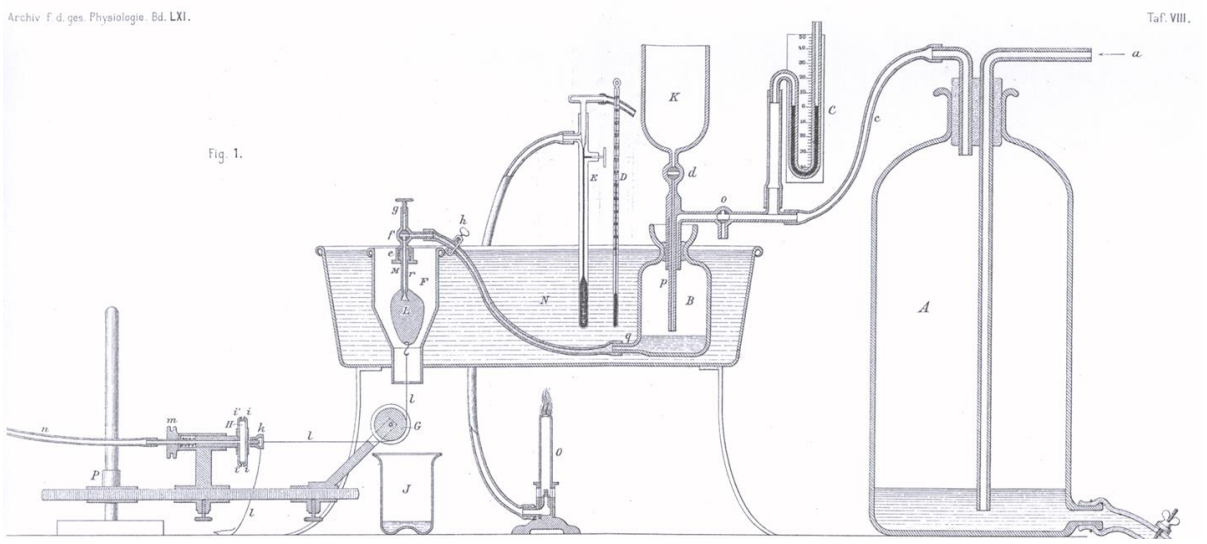

Figure 4: Original Langendorff set-up by Oskar Langendorff in 1895 [39].

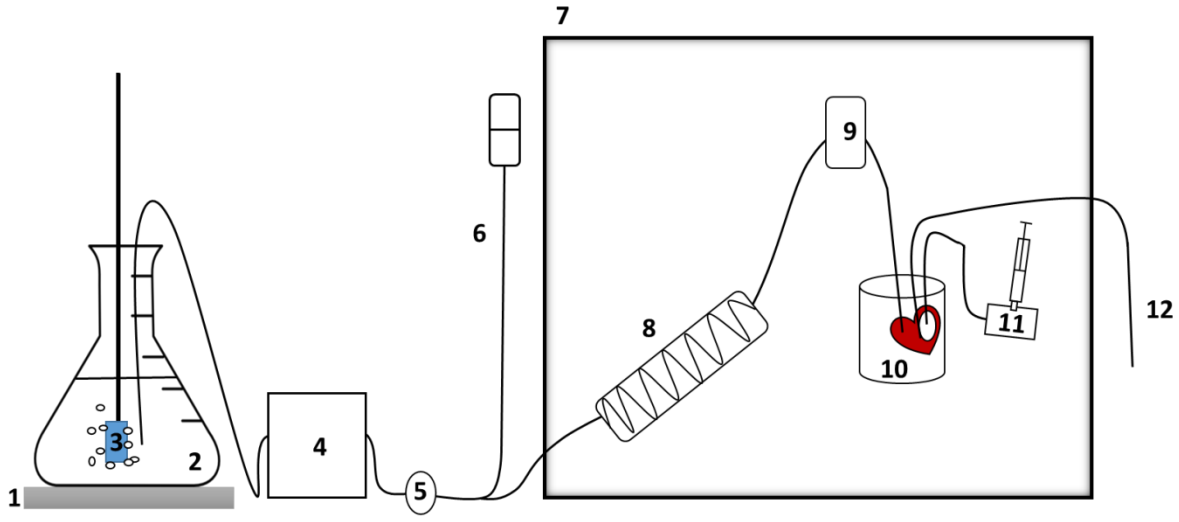

Figure 5: Schematic set-up of Langendorff apparatus used in this study. 1 heating plate, 2 Erlenmeyer flask containing Krebs buffer, 3 gas diffusing stone, 4 roller pump, 5 membrane filter, 6 pressure column, 7 light resistant cage, 8 heating coil, 9 bubble trap, 10 tissue bath with isolated heart, 11 pressure transducer connected to saline filled balloon, 12 effluent collection

In contrast to physiological perfusion of the heart (Fig. 6), hearts in the Langendorff apparatus are retrogradely perfused with oxygenated Krebs buffer through a cannula inserted into the aorta, just distal of the aortic valves (Fig. 7). The retrograde perfusion

is achieved at either a constant pressure or with a constant flow [40]. In this study, the constant pressure model was utilized and attained with a pressure column at a set height (6 in Fig. 5). The buffer provides the tissue with essential metabolites and O_2.

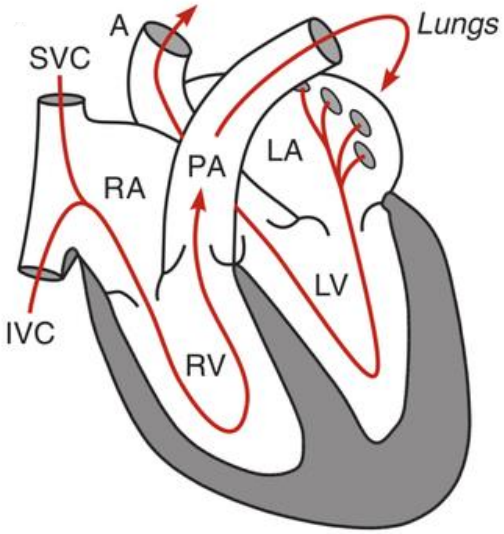

Figure 6: Physiological perfusion of the human heart. Blood is drained from the systemic venous system via the inferior and superior venae cavae (IVC, SVC) into the right atrium (RA). From the right ventricle (RV) the pulmonary artery (PA) transports the blood into the lungs where it is oxygenated and then flows back into the left atrium (LA) and ventricle (LV). From the LV the aorta (A) originates and distributes the oxygenated blood into the systemic circulation. *According to Klabunde et al. 2011* [41].

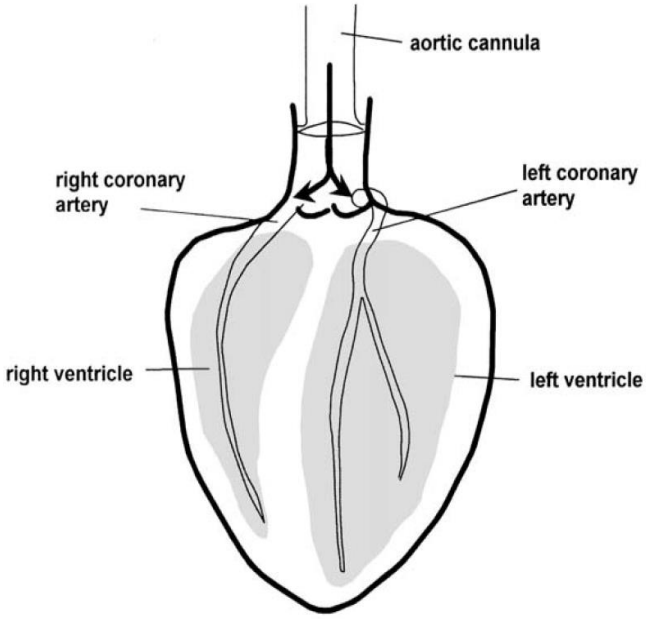

Figure 7: Retrograde perfusion of the isolated heart. In the isolated heart, the aortic cannula is placed just distal of the aortic valves. The pressure forces the valves to shut and the perfusate to flow into the coronary arteries, sustaining the heart tissue. It is drained via the coronary sinus into the right atrium and ventricle. It finally passes the cannulated pulmonary artery (not shown) where effluent is collected. *According to Dhein 2005* [40].

The aortic valves are forced shut, allowing the perfusate to flow through the coronary arteries and sustain the heart tissue. The buffer enters the right atrium via the coronary sinus in the physiological way of venous drainage. With the superior and inferior venae cavae (SVC, IVC) tied off, the buffer takes the physiological way through the right ventricle and pulmonary artery (PA). Here, the effluent can be collected with a cannula placed in the PA.

The contractions of the isolated heart are isovolumic, as opposed to physiological conditions, allowing for control of hemodynamic and mechanical variables, and ensuring a constant afterload. This is achieved with a saline filled balloon that is inserted into the left ventricle and connected to a pressure transducer (11 in Fig. 5).

1.3. Mitochondria

Mitochondria are double-membrane bound organelles that average around 0.5-1 µm in width and 1-2 µm in length [42]. Their numerous metabolic functions include ATP synthesis, ROS production and disposal, Ca^{2+}-signaling and initiation of apoptosis [42,43]. About 30-35 % of the total cell volume in cardiomyocytes is made up of mitochondria [42,44]. Mitochondria have a smooth outer mitochondrial membrane (OMM) that comprises an intermembrane space (IMS) as well as an inner mitochondrial membrane (IMM) that is convoluted and folded into cristae and tubuli to amplify functional area (Fig. 8). The IMM contains the mitochondrial matrix (MM) [45]. The OMM contains porins that allow a relatively unhindered exchange of molecules < 10 kDa [42] while the IMM is impermeable even for small molecules except CO_2, O_2 and water (H_2O). Energy for all transport processes between IMS and MM derives from the electrochemical gradient the ETC upholds [46]. Enzyme complexes for mitochondrial respiration and OXPHOS are embedded in the IMM. The MM is an important Ca^{2+}-reservoir and holds the mitochondrial deoxyribonucleic acid (DNA), ribosomes, enzymes as well as cofactors crucial to metabolic processes like the citric acid cycle (CAC), OXPHOS and oxidation of pyruvate [46].

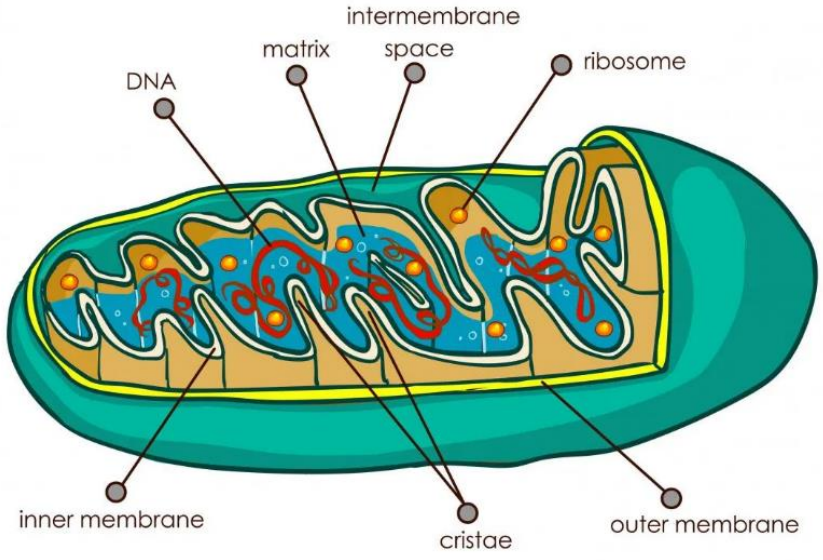

Figure 8: Mitochondrial structure with inner and outer mitochondrial membrane, intermembrane space and mitochondrial matrix containing deoxyribonucleic acid (DNA) and ribosomes [47].

Mitochondrial fission and fusion allow dynamic changes in response to cellular stress signals [42,45]. This is vital for cell survival and plays an important role in normal heart function [21]. Excessive mitochondrial fission has been linked to increased ROS production, impaired mitochondrial function and activation of cell death [21].

ROS are a byproduct of the ETC and can potentially damage mitochondria [45]. However, mitochondria have various antioxidant defenses, including a low pH in the IMS that facilitates the spontaneous dismutation of superoxide anion ($O_2^{-\bullet}$) [27]. While mitochondria can repair small damages, autophagy occurs when damage is too severe [45]. The removal of dysfunctional mitochondria is critical to cell survival as damaged mitochondria are a source for ROS and pro-apoptotic signals [21].

Mitochondria are especially vital in cells with a high ATP turnover like cardiomyocytes and sustain the critical cardiac function of contraction and relaxation. They are furthermore responsible for crucial processes during myocardial injury like Ca^{2+}-homeostasis, ROS generation and apoptosis [12,48].

1.3.1. Mitochondrial Respiration

Mitochondrial respiration is achieved by the ETC, also known as respiratory chain, that consists of four enzyme complexes (I-IV), cytochrome c (cyt c) and ubiquinone (Q). Complex I-IV catalyze redox reactions and facilitate electron transfer. Complex I, III and IV operate as H^+-pumps that generate and maintain a H^+-gradient across the IMM by relocating H^+ from the MM into the IMS. The H^+-gradient is the foundation for the ATP synthesis.

NAD^+ is reduced to NADH during breakdown of carbohydrates, fats, and amino acids and transports two electrons to complex I of the ETC. The fully reduced flavin adenine dinucleotide ($FADH_2$) provides complex II of the ETC with two electrons [46].

Complex I ultimately transfers electrons from NADH to Q, reducing it to ubiquinol (QH_2). The ensuing conformational change is coupled to the transport of 4 H^+ across the IMM [49]. Complex I specific substrates used in experiments with isolated mitochondria are pyruvate and malate (Fig. 9). Malate is oxidized to oxaloacetate in the CAC under formation of NADH. Pyruvate is the final product of glycolysis and is fed into the CAC where it is degraded, among others, to 3 mol NADH [46]. Rotenone is an inhibitor of complex I and inhibits electron transport [46,49]. When exclusively looking at complex II in this study, rotenone is used to inhibit complex I.

Complex II accepts electrons through $FADH_2$ and transfers them to Q. Complex II does not serve as a H^+-pump but is part of the CAC as the succinate dehydrogenase that oxidizes succinate to fumarate [46]. This establishes succinate as the substrate used for complex II experiments (Fig. 9). Complex III transfers electrons from QH_2 to cyt c.

Complex IV accepts electrons from cyt c and transfers them to O_2. O_2 takes up H^+ from the MM and creates H_2O. This reaction leads to relocation of another two H^+ to the IMS and contributes to the proton motive force (PMF). The PMF is made up of the electrochemical energy built through the difference in H^+-concentration and separation of charge across the IMM [50]. Adenosine diphosphate (ADP) boosts mitochondrial respiration [46] and is key in assays for mitochondrial O_2-consumption.

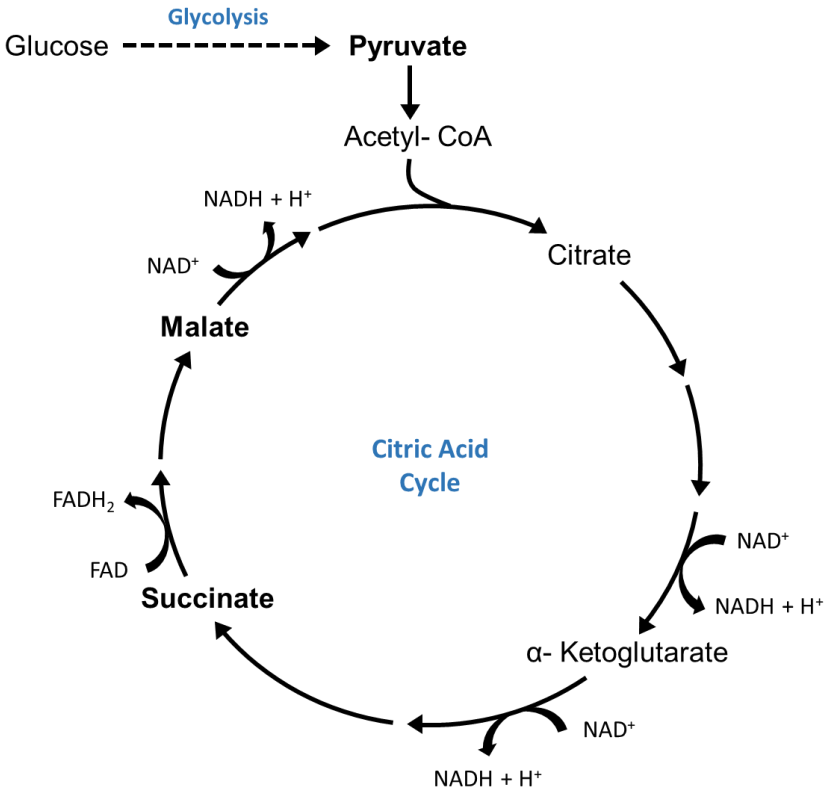

Figure 9: Simplified schematic of glycolysis and citric acid cycle. Complex specific substrates pyruvate, malate (complex I), succinate (complex II) and synthesis of NADH and $FADH_2$ are highlighted.

1.3.2. Oxidative Phosphorylation and ATP Synthesis

ATP provides energy for a multitude of physiological processes, e.g. contraction of cardiomyocytes and various transports to sustain cellular homeostasis. ATP cannot be stored which links its synthesis closely to its consumption and makes it one of the most frequent processes occurring in the body [46,50]. ATP is generated in the IMM through phosphorylation of ADP using the energy of the PMF. This OXPHOS is catalyzed by the F_1F_0- ATP synthase (ATP synthase) [50]. The mitochondrial ATP synthase is an enzyme complex with two main units, F_0 and F_1 (Fig. 10). F_1 contains three catalytic units of one α and one β unit each that enclose a shaft (γ unit) that is rooted in the rotor

of F_0. F_0 is a rotary H^+-channel and is fixated to F_1 by a stator [50–52]. H^+ translocation from the IMS to the MM puts the rotor into a clockwise rotation. This leads to conformational changes in the catalytic units of F_1 enabling them to synthesize ATP. In one 360° rotation, the catalytic units generate three ATP [46,50–52].

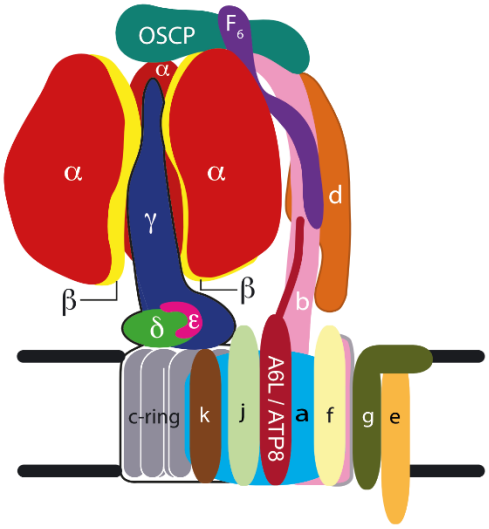

Figure 10: **ATP synthase.** F_0 is fully embedded into the inner mitochondrial membrane, F_1 protrudes into the mitochondrial matrix. F_1 consists of 3α, 3β, γ, δ and ε subunits. The α and β units form a tight circle and three catalytic units. They enclose the γ unit which functions as the shaft and is rooted in the c-ring of F_0 (rotor). F_0 is fixated to F_1 by a- and b-units (stator). *According to the Mitochondrial Biology Unit website by the University of Cambridge* [50,51].

1.3.3. Mitochondrial Permeability Transition Pore

The mPTP is a non-specific voltage-dependent channel in the IMM that is triggered open upon high Ca^{2+}-concentration in the MM and is responsible for an abrupt increase in IMM permeability. It has a diameter of 2.3 nm and is permeable to molecules < 1.5 kDa [53,54]. Research on the molecular identity of mPTP is not yet conclusive but different proteins could serve as pore-forming components, e.g. ATP synthase dimers, and the mitochondrial P_i carrier [43,55,56]. Transient openings of the mPTP are vital in physiological regulation of mitochondrial Ca^{2+}-levels and ROS homeostasis [21,56] and have been suggested to play a role in cardiomyocyte development and mitochondrial maturation (Fig. 11) [55].

Prolonged openings of mPTP have been linked to mitochondrial dysfunction. Increased permeability of the IMM leads to uncoupling of the ETC, dissipation of the H^+-gradient and a subsequent stop of ATP synthesis [53,55]. The colloidal osmotic pressure from proteins within the MM causes mitochondrial swelling. This can lead to

rupture of the OMM and release of NADH, proapoptotic signals and Ca^{2+} (Fig. 11) which causes irreversible cellular damage [17,53,55,56]. MPTP opening occurs during myocardial IR and is a major determinant for the extent of injury during reperfusion [53].

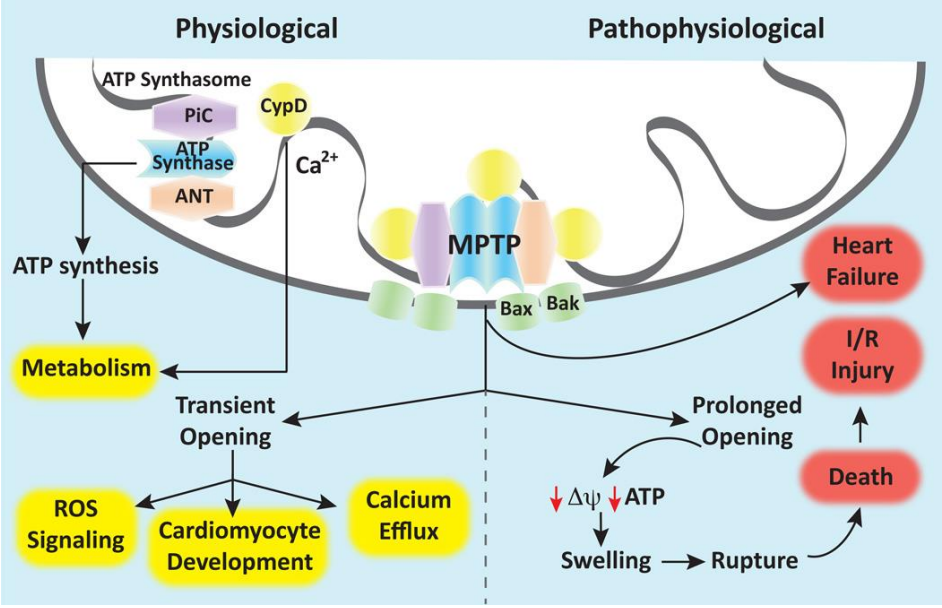

Figure 11: Role of mitochondrial permeability transition pore (mPTP) in physiological and pathophysiological heart function. ATP synthase, adenine nucleotide translocator (ANT) and phosphate carrier (P_iC) are crucial for adenosine triphosphate (ATP) synthesis. They are thought to be components of the mPTP. Transient opening sustains reactive oxygen species (ROS) signaling, cardiomyocyte development and Ca^{2+}-homeostasis. Prolonged opening leads to mitochondrial dysfunction through increased membrane permeability, loss of membrane potential (Δψ) and release of pro-apoptotic proteins (bax/bak). (CypD - cyclophilin D). *According to Kwong et al. 2015* [55].

MPTP opening can be inhibited by inhibition of the Ca^{2+}-trigger site through H^+ or divalent cations. Oxidative stress, high P_i, as well as ATP and ADP depletion increase the mPTP's sensitivity to Ca^{2+}, while ATP, ADP and CsA decrease it [53,56].

1.3.4. Mitochondria in IR Injury

Mitochondrial dysfunction in injured cells includes changes in mitochondrial respiration, ROS production, ATP synthesis, Ca^{2+}-, and autophagy regulation as well as apoptosis. In cardiac mitochondria, this ultimately results in reduced cardiac performance [57].

Oxygen depletion during ischemia inhibits ETC and stops OXPHOS [17]. This leads to depolarization of the IMM, collapse of the electro chemical gradient and ATP depletion [14,58]. The ATP synthase further contributes to the fast decline in cellular ATP levels by hydrolyzing ATP to ADP. However, the inhibitor protein IF_1 inhibits activity of F_1 of the ATP synthase when the cellular pH falls below 6.5 [59]. Prolonged ischemia and

energy depletion cause functional and structural alterations, mitochondrial fragmentation and induction of apoptosis [18,57,60].

Mitochondrial O_2-consumption quickly recovers to baseline upon reperfusion while ATP levels and the heart's contractile function do not due to a dissociation of ATP synthesis from electron transport, called uncoupling [22,61]. This results in enhanced ROS production, can take days to normalize and is a reason for development of irreversible damage in IR injury [12].

The mPTP stays closed during ischemia but is primed due to intracellular Ca^{2+}-overload, high P_i and low ATP concentrations. Oxidative stress, mitochondrial Ca^{2+}-accumulation and pH increase during reperfusion facilitate opening [17,53,62]. To prevent impairment of mitochondrial function through mPTP opening, Ca^{2+}-concentration is regulated in the MM. However, Ca^{2+} cycles across the IMM at the cost of the H^+-gradient. Ca^{2+} is transferred into the MM via Ca^{2+}-uniporters [14]. Ca^{2+}-efflux is then mediated by the NCE working in reverse, and the accumulating Na^+ is removed from the MM via the NHE. Ultimately H^+ accumulates in the MM [12,21].

Thus, both ROS and Ca^{2+}-overload lead to failure of the electrochemical gradient and further disruption of ETC activity [57]. Moreover, ROS promote Ca^{2+}-overload by damaging OXPHOS and inhibiting anaerobic glycolysis while Ca^{2+}-overload damages ETC and activates Ca^{2+}-dependent proteases that lead to activation of oxidases and ROS production [22].

In summary, mitochondria have protective mechanisms against IR injury, like IF_1 and antioxidants but also possess elements that exacerbate the damage, e.g. ROS generation, mPTP opening and the release of apoptotic factors. Furthermore, remaining mitochondrial function provides the energy for myocardial hypercontracture that leads to membrane disruption and cell death [12].

1.4. Poloxamer 188

P188 has been approved by the Food and Drug Administration (FDA) since the 1950s as a therapeutic reagent to reduce blood viscosity before transfusions and inhibit thrombosis [63,64]. It has more recently been shown to stabilize membranes [65], a pivotal part of IR injury.

P188 is a synthetic, non-ionic, linear triblock copolymer with a molecular weight of 8,400 Da. It is composed of one chain of hydrophobic polypropylene oxide (PPO) that is flanked by two chains of hydrophilic polyethylene oxide (PEO) with the chemical structure $PEO_{75}PPO_{30}PEO_{75}$ (Fig. 12). The hydrophilic blocks make up a relatively large part of the molecule compared to the hydrophobic centerpiece [66].

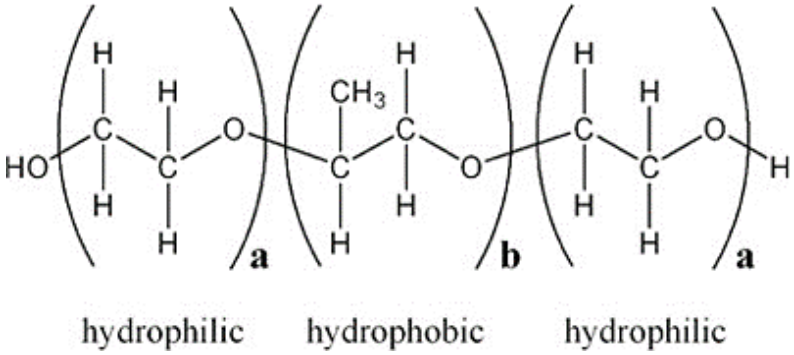

Figure 12: Chemical structure of a triblock copolymer. For Poloxamer 188: a = 75 units of hydrophilic polyethylene oxide, b = 30 units of hydrophobic polypropylene oxide. *According to Walsh et al. 2006* [67].

P188 is used in wound care [68], improves microvascular blood flow [69], facilitates fibrin clot lysis and prevents lipid peroxidation [70]. Recent studies show P188 to stabilize and seal cellular membranes [31,60,65,68] and to enhance the repair of skeletal muscle cells [71], cardiomyocytes [72], neurons [73] and endothelial cells [74,75] after IR injury as well as other physicochemical insults that lead to membrane permeabilization, e.g. heat, electroporation, mechanical puncture and radiation [76]. P188 has shown beneficial effects in in-vitro [31,72,77], ex-vivo [78,79] and in-vivo [80,81] cardiac IR models, as well as in clinical studies upon immediate [82] but not delayed [83] reperfusion.

A study of the Riess' study group determined P188's protective effects in cardiac IR injury on rat strains with different endogenous resistance to IR injury [79]. Myocardial function and infarct size improved in hearts from both Brown Norway (BN) and Dahl

Salt Sensitive (SS) rats with 120 min of 1mM P188 post-conditioning after 30 min of no-flow ischemia (Fig.13).

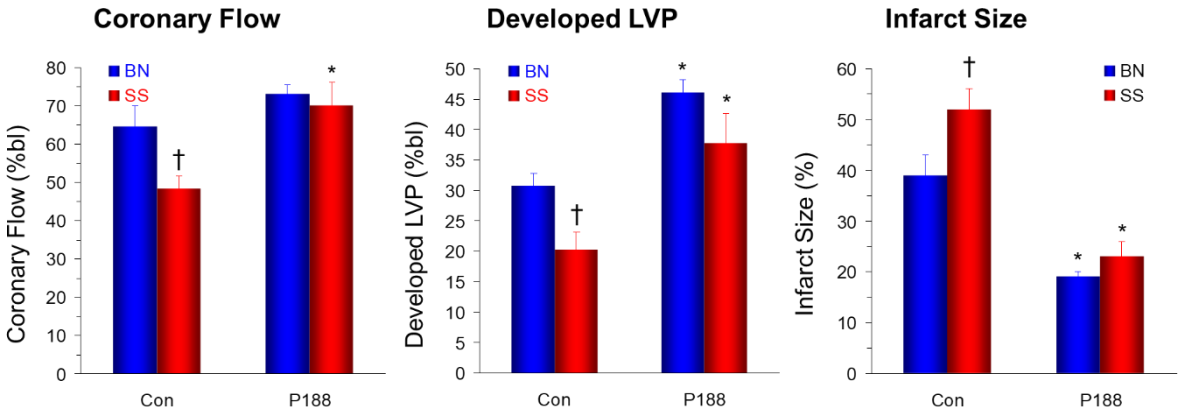

Figure 13: Improved myocardial function and decreased infarct size after ex-vivo P188 post-conditioning in hearts from Brown Norway (BN) and Dahl Salt Sensitive (SS) rats [79]. Myocardial function in coronary flow and developed left ventricular pressure [LVP]). * vs control, † vs BN**.**

Membrane damage is a critical hallmark of cardiac IR injury in which the internal hydrophobic area of the bilayer is exposed. The PPO structure of P188 adheres to the damaged site and converts the hydrophobic tails of the membrane lipids into a hydrated surface that closely resembles the surface of normal cells. The PEO chains serve as a barrier to the damaged cell surfaces and prevent them from approaching each other [82,84]. In doing so, P188 does not penetrate the bilayer core [63,76] but adsorbs to the outer surface of the membrane as a patch stabilizing the surface (Fig. 14). This reduces permeability and shields the cell against secondary injuries even under conditions of oxidative stress [31,76]. The effect of P188 is localized to damaged membranes and has little to no effect on non-affected membranes [60,76]. After reestablishing membrane integrity, P188 is ejected from the membrane [85].

Moreover, studies have found that P188 improves mitochondrial function in in-vitro neurons [86] and a porcine model of myocardial infarction [38] and it has been shown to be active in mitochondrial membranes in neurons [87]. However, P188 has shown no beneficial effect on rat brain isolated mitochondria [88].

A preliminary study conducted by the Riess study group [89], that most closely resembles our current one, incubated mitochondria in 100 µM P188 after isolating them from an ex-vivo rat heart subjected to IR injury (30 min ischemia, 10 min reperfusion). No improvement of mitochondrial function could be found with the used mitochondrial

dose of P188. When reperfused with 1 mM P188 during the 10 min of reperfusion, an inclination towards an additive protective of ex-vivo and mitochondrial P188 administration could be seen. This prompted this study to further investigate both P188 administrations using another concentration for mitochondrial treatment.

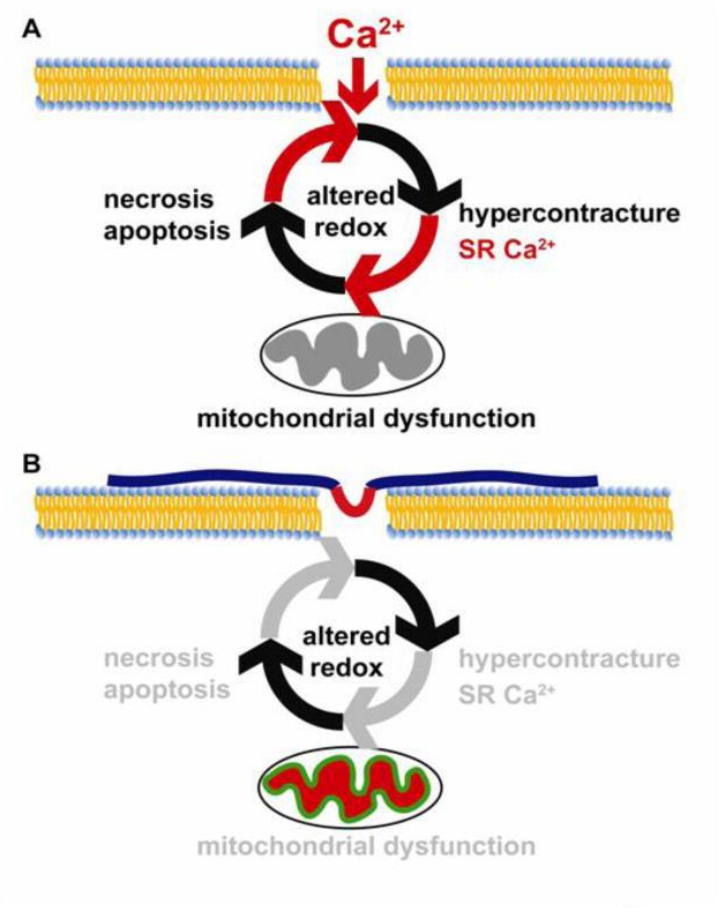

Figure 14: Poloxamer 188 (P188) preserves cellular and mitochondrial function by reducing membrane permeability. A: Injured cellular membrane with Ca^{2+} influx and resulting damage. **B:** Injured cellular membrane with P188. The hydrophobic structure (red) of P188 adheres to the damaged site while the hydrophilic chains (blue) serve as a barrier to prevent the cell surfaces from approaching each other. *According to Martindale et al. 2014* [31].

1.5. Polyethylene Glycol

Polyethylene Glycol (PEG) is utilized as a viscosity control for P188 in this study because of its similar composition. It is a non-toxic, synthetic, hydrophilic polymer that is made up of a variable amount of PEO blocks (Fig. 15) and has been FDA approved for use in cosmetics, foods, and drugs [90,91]. It has a widespread use in biomedical settings, applications including coating gene therapy vectors, such as viruses, to protect them from inactivation by the immune system, drug delivery, surface functionalization, bioconjugation and bowel preparation for colonoscopy [90,91].

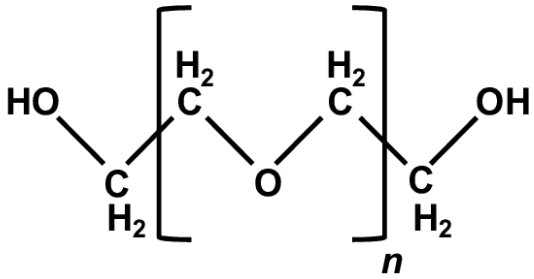

Figure 15: Chemical structure of polyethylene glycol. *According to Sigma Aldrich* [92].

PEG has been investigated in the fusion of membranes and its ability to lower water molecule activity at the membrane-solvent interface. It has been shown to be effective in membrane stabilization and sealing only in very high concentrations (mM-M) or with a high-molecular-weight (15-20 kDa) that appears to have a protective effect from myocardial IR injury in pre-conditioning studies [93]. This indicates an essential role of the hydrophobic block of poloxamers at a lower concentration [66,94]

PEG 8,000 Da is used as a control for P188 because of its molecular weight and similar composition that lead to a similar reduction in blood viscosity for both molecules [38]. However, studies have shown that PEG in this dosage does not mirror P188's protective effects on mitochondrial function or infarct size reduction in a porcine IR model [38] and also did not prevent lactate dehydrogenase (LDH) release in an IR in-vitro study in cardiomyocytes [31].

2. Aim and Hypotheses

Mitochondria play a crucial role in energy maintenance of cardiomyocytes and are damaged in IR injury. Mitochondrial dysfunction results in cellular dysfunction and subsequent cell death. Due to their high dependence on mitochondrial energy production, cardiomyocytes are highly susceptible to mitochondrial dysfunction by IR injury.

P188 is a triblock copolymer that has been shown to protect against IR injury in myocardial models in-vitro, ex-vivo and in-vivo. P188 is thought to improve cellular and mitochondrial function by stabilizing membranes with its amphiphilic structure.

This study aims to identify whether P188 has a direct protective effect on mitochondrial function. We utilize an ex-vivo model of rat isolated heart that is subjected to no-flow ischemia and reperfusion. Mitochondria are isolated and mitochondrial function is assessed through ATP synthesis, Ca^{2+}-retention capacity (CRC) and O_2-consumption.

Hypotheses:

1. P188 improves mitochondrial function when given immediately upon reperfusion in rat isolated hearts.

2. P188 improves mitochondrial function when given during isolation of mitochondria after IR injury in rat isolated hearts.

3. The effect of P188 is not purely osmotically, but depends on its hydrophobic portion and cannot be substituted with the completely hydrophilic molecule PEG.

3. Materials and Methods

All experiments were performed at Vanderbilt University Medical Center (VUMC), Nashville, TN, at the Department of Anesthesiology in the laboratory of Matthias Riess, MD, PhD.

3.1. Animals

This study was performed with approval by the VUMC's Institutional Animal Care and Use Committee (IACUC) in accordance with U.S. National Institutes of Health standards (NIH Publication 95-23, revised 1996) under the protocol number M1600012-00 (29 January 2018). For all experiments, a total of 79 male Sprague Dawley (SD) Rats (Charles River Laboratories, Inc., Wilmington, Massachusetts, USA) with an average age of 92 ± 4.2 d standard error of the mean (SEM) and an average weight of 426.9 ± 13.9 g SEM were used.

The rats were housed at VUMC's animal facility in rat-specific rooms maintained at a temperature between 20-26 °C, humidity between 30-70%, with 10-15 fresh air changes per hour and a 12 h light/dark cycle. They were maintained in solid-bottom ventilated cages containing appropriate bedding material and environmental enrichment objects. Pelleted rat chow and fresh water were available at all times for the rats, and they were group housed according to size and sex. Cages were cleaned at least twice per week [VUMC Division Animal Care].

3.2. Isolated Heart Model

3.2.1. Equipment

Table 1: Isolated Heart Model. Equipment.

Name	Catalog No.	Company
Heating Plate	11-100-49SH	Thermo Fisher Scientific Inc., Waltham, MA, USA
Roller Pump	REGLO Digital MS-2/8	Ismatec, Cole-Parmer GmbH, Vernon Hills, IL, USA
Membrane Filter	SMWP02500	Merck Millipore, Merck KGaA, Darmstadt, Germany
Light-Resistant Cage	custom-built	Vanderbilt Mechanic Store
Gas Diffusing Stone	11-139A	Fisher Scientific, part of Thermo Fisher Scientific

Heating Coil	158822	Radnoti, Covina, CA, USA
Bubble Trap Compliance Chamber	130149	Radnoti
Tissue Organ Bath	1583-201	Radnoti
Latex Balloon	170404	Radnoti
Aortic Cannula	140163-24	Radnoti
Pressure Transducer	PX600F	Edwards Lifesciences Corporation, Irvine, CA, USA
Pressure Monitor	BPM-832,	CWE Inc., Ardmore, PA, USA
LabVIEW Full Development System 2014		National Instruments, Austin, TX, USA
Tubing Flow Module	TS410	Transonic Systems Inc., Ithaca, NY
Flow Meter	ME1PXN	Transonic Systems Inc.
Polystat	EW-12121-02	Cole-Parmer
Gas Mix (95% O_2, 5% CO_2)	UN3156	A-L Compressed Gases, Spokane, WA, USA
Surgical Scissors	14075-09	Cueto & Stanek, Newark, NJ, USA
Standard Surgical Forceps	MC32B	Moria Surgical, Antony, France
Curved Forceps	RS-5138	Roboz Surgical Instrument Co., Inc., Gaithersburg, MD, USA
Fine Forceps	11370-31	Fine Science Tools GmbH, Heidelberg, Germany
Curved Scissors	14075-09	Fine Science Tools
Fine Scissors	14090-09	Fine Science Tools
Braided Silk Suture, black, 2-0	113S	Teleflex Incorporated, Wayne, PA, USA
Rodent Guillotine	DCAP	World Precision Instruments, Sarasota, FL, USA

3.2.2. Chemicals

Table 2: **Isolated Heart Model. Chemicals.**

Name	**Catalog No.**	**Company**
VetaKet (Ketamine Hydrochloride)	NDC: 59399-114-10	Akorn, Inc., Lake Forest, IL, USA
Heparin	NDC: 0641-0391-12	West-Ward Pharmaceuticals, Eatontown, NJ, USA
Lidocaine 1%	491237	Fresenius Kabi AG, Bad Homburg, Germany

Kolliphor P 188	15759	Sigma-Aldrich, St. Louis, MO, USA
Antifoam A concentrate	A5633	Sigma-Aldrich

Modified Krebs Buffer (Riess laboratory [95]) pH 7.4 (includes addition of CO_2)

Table 3: Isolated Heart Model. Krebs Buffer.

119 mM NaCl (sodium chloride)	S9625	Sigma-Aldrich
24 mM $NaHCO_3$ (sodium bicarbonate)	S8875	Sigma-Aldrich
5.5 mM D-Glucose	G8270	Sigma-Aldrich
1.6 mM $CaCl_2$ (calcium chloride dihydrate)	C3881	Sigma-Aldrich
4.7 mM KCl (potassium chloride)	P4505	Sigma-Aldrich
1.17 mM $MgSO_4$ (magnesium sulfate heptahydrate)	230391	Sigma-Aldrich
1.16 mM NaH_2PO_4 (sodium phosphate monobasic)	S0751	Sigma-Aldrich
5 units/L insulin	183311	Novo Nordisk, Bagsværd, Denmark
1.19 mM sodium pyruvate	P2256	Sigma-Aldrich
0.026 mM 1% ethylenediaminetetraacetic acid (EDTA)	E1644	Sigma-Aldrich

3.2.3. Set-Up

The Krebs buffer was oxygenated using a gas diffusing stone (95% O_2, 5% CO_2) and held at a temperature of about 40 °C on a heating plate outside the Langendorff chamber. A roller pump was used to pump the buffer into the light-blocking Faraday cage (see Fig. 5, chapter 1.2.). Inside the chamber, the perfusate passed a heating coil kept at 37 °C with help of a temperature-controlled circulating water bath, as well as a bubble trap that was kept at the same temperature before it supplied the aortic cannula once the heart was introduced to the apparatus. The heart was immersed continuously in Krebs buffer also kept at 37 °C and perfused at a constant pressure of 70 mmHg. A temperature sensor inserted into the tissue bath ensured continuous temperature control. A latex balloon filled with saline was connected to a pressure transducer and a pressure monitor recorded changes in left ventricular pressure (LVP).

3.2.4. Anesthesia

All rats were intraperitoneally injected with 30 mg/kg ketamine hydrochloride and anesthesia was evaluated after 10 min with the toe pinch method. With no reaction to

toe pinch, the animals were intraperitoneally injected with 1,000 units/kg heparin. The animals were euthanized by decapitation 5 min after heparin administration.

3.2.5. Preparation of Isolated Heart

The following methods have been published previously [96–98]. Once decapitated, the rats were taped down with both front legs spread superior-laterally and the rear legs bundled together with the tail to give access to the ventral torso (Fig. 16). The fur and skin were trimmed before cutting into the abdomen. The rib cage was opened along the sternum and the opened chest cavity cleaned briefly with cold, oxygenated Krebs buffer (Fig. 17).

The tissue surrounding the aorta was removed and curved forceps were used to guide a 2-0 suture behind the aorta to tie a double overhand knot that was left loose. Distal to the cannulation site, the ascending aorta was grabbed with curved forceps and a small incision made proximal to it.

Figure 16: Taped down rat with access to the ventral torso.

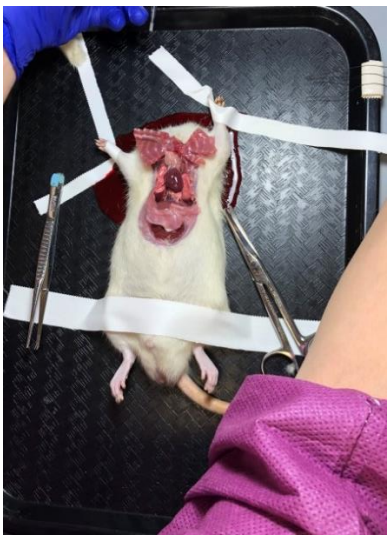

Figure 17: Opened chest cavity.

A cannula was inserted into the incision close to the aortic sinus to perfuse the coronary arteries without damaging the aortic valves. The previously started overhand knot was tightened around the aorta, keeping the cannula in place (Fig. 18). The stopcock to the cannula was opened to start perfusing the heart with ice cold, oxygenated Krebs buffer. Lungs were cut away quickly to avoid pressure building up in the heart (Fig. 19). IVC and SVC were ligated using curved forceps, 2-0 sutures and two single overhand knots. Vessels were cut distal to the ligations.

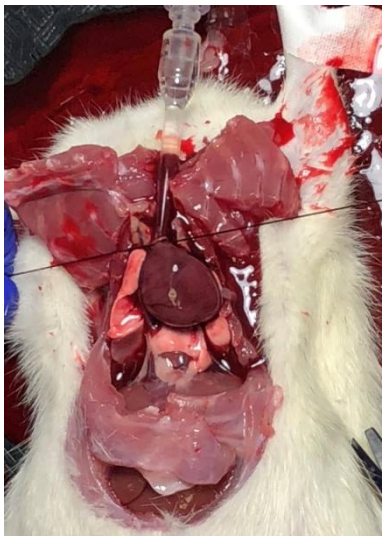

Figure 18: Fixation of the aortic cannula.

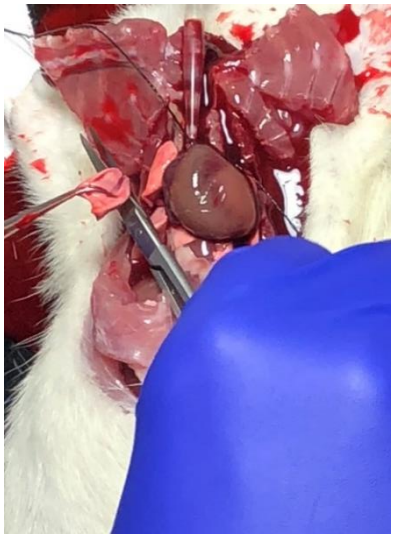

Figure 19: Removal of lung to avoid pressure build-up in the heart.

The heart was removed from the body by lifting it up by the aortic cannula and using curved scissors to cut away all other tissue without causing damage to the heart. For cannulation of the PA the heart was hung at a height for better access and the curved forceps were used to push the suture through the pulmonary trunk without damaging the aorta. Similar to the cannulation of the aorta, a double overhand knot was tied and left loose. A small incision was made using the curved forceps in the superior part of the right ventricle and the PA cannula inserted into the incision. Once the PA was cannulated, perfusate could be seen pumping out of the cannula and the position was adjusted to maximize flow (Fig. 20). The position of the PA cannula was fixated by taping it to the aortic cannula and tightening the knot to secure it to the heart by pulling in enough cardiac tissue to hold it in place while minimizing possible ischemic insult to the heart.

The stop-cock to the heart was turned off and the aortic cannula was removed from the tubing to place the heart into the Langendorff apparatus with the roller pump turned on, running at a flow of 13-17 mL/min. The hemostats were unclamped from the pressure column immediately after connecting the heart to the pump to avoid pressure building up in the heart. The LabView program was running while the heart was placed in the apparatus so coronary flow could be checked to make sure the aorta was not twisted during set-up.

Figure 20: Cannulation of pulmonary artery (PA). Krebs buffer is pumped out of the PA.

Figure 21: Immersion of the prepared heart in the organ tissue bath.

Part of the left atrium was trimmed. The collapsed latex balloon was inserted into the left ventricle through the mitral valve, inflated with saline to a diastolic pressure of 10 mmHg and taped to the aortic cannula with a narrow piece of tape. The organ bath filled with Krebs buffer was raised to heart level (Fig. 21).

A 20 min stabilization period was started and myocardial function was mirrored closely. Once stabilization finished and recordings started, position changes and adjustments were avoided. Potential ventricular fibrillation was treated with a 0.2 mL bolus of lidocaine 1%. Functional data collected (Fig. 22) include diastolic and systolic pressure, developed LVP (devLVP), heart rate (HR), rate pressure product (RPP), contractility, and coronary flow. Calculations are illustrated in equations 1-3. Diastolic pressure was adjusted to 10 mmHg baseline. All other data were analyzed as percentage to baseline (% bl). Data was recorded and analyzed using LabVIEW Full Development System 2014.

$$devLVP = systolic\ pressure - diastolic\ pressure \quad (1)$$

$$RPP = HR \times devLVP \quad (2)$$

$$Contractility = \frac{\Delta LVP}{\Delta t_{max}} \quad (3)$$

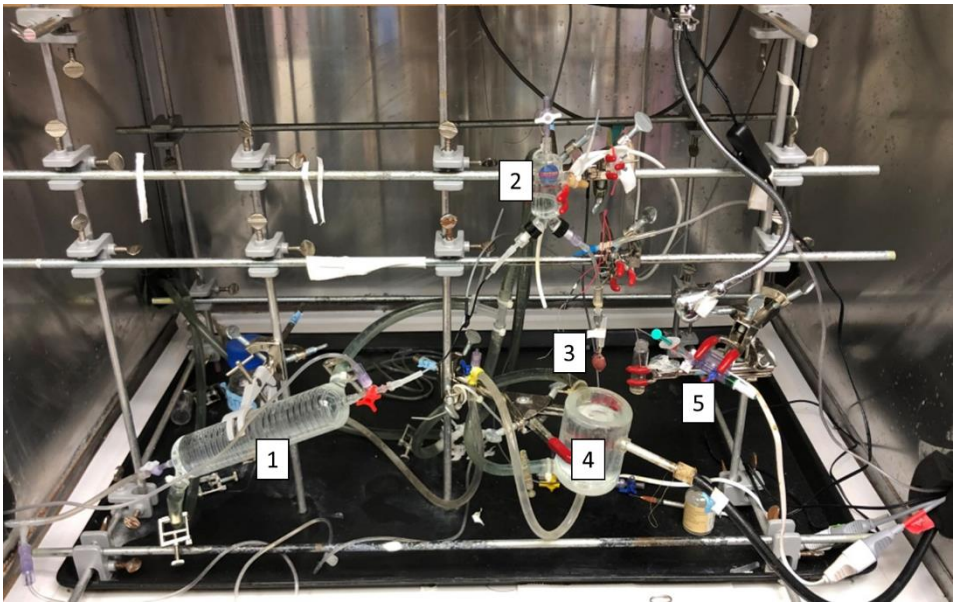

Figure 22: Placement of the heart into the Langendorff apparatus. For schematic set up see Fig. 5, chapter 1.2. 1 heating coil, 2 bubble trap, 3 cannulated heart, 4 organ tissue bath, 5 pressure transducer with saline-filled syringe, connected to latex balloon.

3.3. Groups

The rats were randomized into 5 groups (Fig. 23).

TCH 60 Time Control Heart, 60 min perfusion with Krebs buffer

TCH 50 Time Control Heart, 50 min perfusion with Krebs buffer

Isc Ischemia, 20 min perfusion with Krebs buffer, 30 min no-flow ischemia

IR Ischemia/Reperfusion, 20 min perfusion with Krebs buffer, 30 min no-flow ischemia, 10 min reperfusion with Krebs buffer

IR+ Ischemia/Reperfusion with 1 mM P188, 20 min perfusion with Krebs buffer, 30 min no-flow ischemia, 10 min reperfusion with 1 mM P188 in Krebs buffer

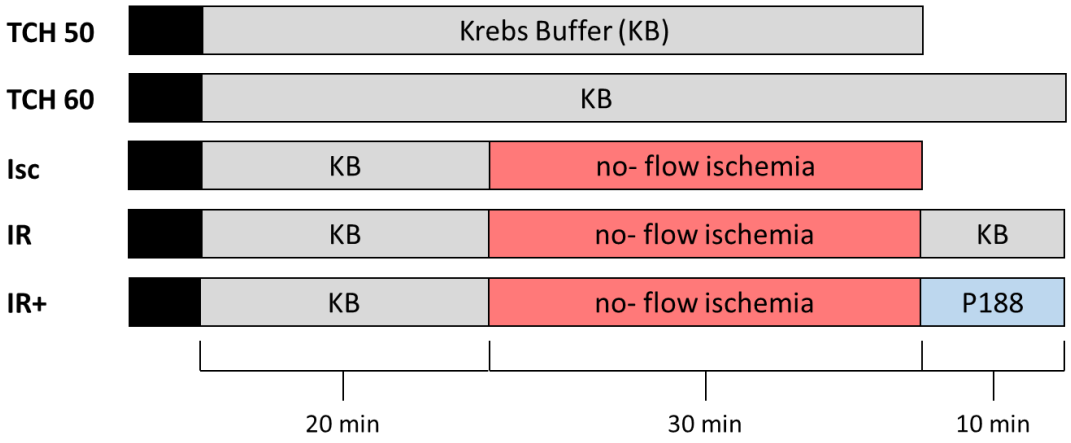

Figure 23: Timeline of experimental protocol. The 5 experimental groups are shown as a timeline starting with decapitation. The different colors represent treatment of the heart. Black – preparation time of the isolated heart; grey – perfusion with Krebs buffer in the Langendorff apparatus; red – no-flow ischemia; blue – perfusion with 1 mM P188 in Krebs buffer. TCH – time control heart; Isc – ischemia; IR – ischemia/reperfusion; IR+ - IR with 1 mM P188 during reperfusion

Readings of myocardial function were done at the same time points in all groups (Fig. 24).

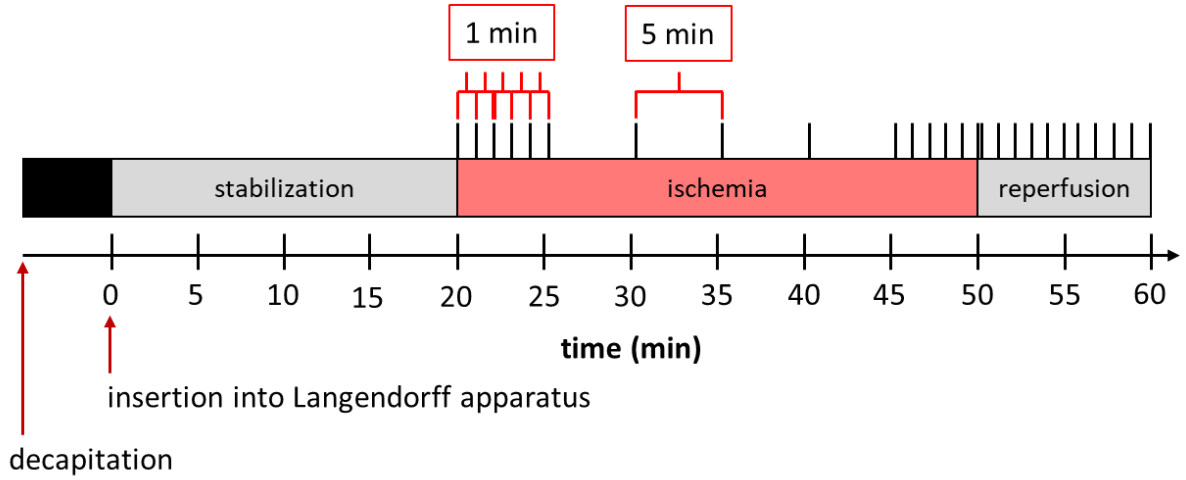

Figure 24: Representative time points for readings of myocardial function in all groups indicated by black marks.

Each ex-vivo group was further divided into three groups which received different treatments during isolation of mitochondria. Those were: a) without treatment, b) with 1 mM P188, or c) 1 mM PEG.

To ensure that cannulation and ex-vivo perfusion did not compromise mitochondrial function in time controls, preliminary studies were done comparing mitochondrial function of freshly excised cannulated and un-cannulated hearts to time controls. No

significant difference could be shown and, thus, TCH were used as undamaged comparison in all experiments. The data is not shown here.

3.4. Isolation of Mitochondria

3.4.1. Equipment

Table 4: Isolation of Mitochondria. Equipment.

Name	Catalog No.	Company
Surgical Scissors	14075-09	Cueto & Stanek
Blade Homogenizer	Type X120	CAT Engineering, Ballrecht-Dottingen, Germany
Avanti J-E Centrifuge	369001	Beckman Coulter Inc., Brea, CA, USA
Rocking Platform	1660719	Bio-Rad Laboratories Inc., Hercules, CA, USA
Plate Reader	H1MF	BioTek Instruments Inc., Winooski, VT, USA
Clear 96-well Plate	12-565-226	Fisher Scientific
pH 700 Benchtop Meter	WD-35419-03	OAKTON Instruments, Vernon Hills, IL, USA

3.4.2. Chemicals

Isolation Buffer (pH adjusted to 7.15 with KOH) [99]

Table 5: Isolation of Mitochondria. Isolation Buffer.

Name	Catalog No.	Company
200 mM Mannitol	Sigma M-4125	Sigma-Aldrich
50 mM Sucrose	Sigma S-7903	Sigma-Aldrich
5 mM KH_2PO_4 (potassium dihydrogen phosphate)	P-5379	Sigma-Aldrich
5 mM 3-(N-Morpholino)- propane sulfonic acid (MOPS)	M-3183	Sigma-Aldrich
0.1% bovine serum albumin (BSA)	BP1600-100	Thermo Fisher Scientific
1 mM ethylene glycol tetraacetic acid (EGTA)	E-4378	Sigma-Aldrich
KOH (potassium hydroxide)	P1767	Sigma-Aldrich

Table 6: Isolation of Mitochondria. Chemicals.

Name	Catalog No.	Company
Protease (Bacillus licheniformis)	P-5380	Sigma-Aldrich
Kolliphor P188	15759	Sigma-Aldrich
Polyethylene Glycol 8000	1546605	Sigma-Aldrich
Protein Assay Kit	500-0002	Bio-Rad Laboratories

3.4.3. Procedure

To isolate mitochondria from the isolated heart all devices were removed, the heart was blot dry and cut into two halves that were stored separately in ice cold isolation buffer. Both heart halves were isolated separately with only isolation buffer, isolation buffer containing 1 mM P188 or 1 mM PEG.

The tissue was minced with scissors and rinsed clear of blood and debris with cold isolation buffer. The isolation buffer was removed, the tissue transferred to a homogenizing vessel, and 5 mL of 5 U/mL protease (*Bacillus licheniformis*) were added to promote breakdown of the cellular structure. The tissue was homogenized for 30 sec with a blade homogenizer. The protease was deactivated by dilution with 15 mL of cold isolation buffer. The tissue was homogenized until smooth.

The mitochondria were isolated by differential centrifugation with an Avanti Centrifuge at 4 °C. The protease was removed in 10 min at 8,000 *g*, followed by resuspension of the pellet in 25 mL isolation buffer. The resuspended pellet was centrifuged at 750 *g* for another 10 min to remove cellular debris. The resultant supernatant was centrifuged at 8,000 *g* for 10 min leaving a pellet of the isolated mitochondria. The pellet was resuspended and the protein concentration estimated via the Protein Assay by Bradford et al. [100].

Protein Assay for Isolated Mitochondria

A protein standard was prepared with BSA and isolation buffer in the following concentrations: 0, 0.1, 0.25, 0.5, 1, 2.5, and 5 mg/mL. 2 µL of each standard were pipetted into a clear 96-well plate in triplicates and 2 µL of each sample in duplicates. 200 µL of protein assay dye reagent, prepared as described in the kit, were added using a multi-channel pipet.

The plate was incubated at room temperature and light-protected on a rocker platform for 10 min. Absorbance was measured at 595 nm with a plate reader. Concentration of protein was calculated by linear regression of the standard. For further experiments the mitochondria were diluted to a final concentration of 2.5 mg protein/mL with experimental buffer (see below) and kept on ice.

For comparison the mitochondrial yield was calculated as percentage in dependence on heart weight.

3.5. Tests for Mitochondrial Function

3.5.1. Equipment

Table 7: Test for Mitochondrial Function. Equipment.

Name	Catalog No.	Company
GloMax 20/20 Luminometer	E5311	Promega Corporation, Madison, WI, USA
Mitocell Respirometry System	S200; MT200A; SI130; SI021	Strathkelvin Instruments Ltd., North Lanarkshire, Scotland
10µL glass syringe	80365	Hamilton Company, Reno, NV, USA
5 µL glass syringe	87919	Hamilton Company
Fluorescence spectrophotometer	custom	Horiba, Piscataway, NJ, USA
FelixG software	Ver 4.2.2.5265	Horiba
Macro Quartz Cuvette	14958128	Fisher Scientific
Various volume pipets; Rainin Classic; single and multichannel	17008708	Mettler-Toledo Rainin, LLC, Columbus, OH, USA

3.5.2. Chemicals

Experimental Buffer (pH adjusted to 7.15 with KOH)

Table 8: Test for Mitochondrial Function. Experimental Buffer.

Name and concentration	Catalog No.	Company
130 mM KCl	P4504	Sigma-Aldrich
5 mM K_2HPO_4	P5504	Sigma-Aldrich
20 mM MOPS	M3183	Sigma-Aldrich
0.1% BSA	BP1600-100	Thermo Fisher Scientific
KOH	P1767	Sigma-Aldrich

ATP Assay Buffer (Added to Experimental buffer (see above) on day of experiment)

Table 9: Test for Mitochondrial Function. ATP Assay Buffer.

Name and concentration	Catalog No.	Company
0.2 µM diadenosine pentaphosphate (DAP)	D4022	Sigma-Aldrich
30 µM ADP	A5285	Sigma-Aldrich
0.1 mg/mL Luciferin	5427	Tocris Bioscience, Bristol, UK
1.25 µg/mL Luciferase	786-1309	G-Biosciences, St. Louis, MO, USA

No-Phosphate Buffer (pH adjusted to 7.15 with KOH)

Table 10: Test for Mitochondrial Function. No Phosphate Buffer.

Name and concentration	Catalog No.	Company
130 mM KCl	P4504	Sigma-Aldrich
20 mM MOPS	M3183	Sigma-Aldrich
0.1% BSA	BP1600-100	Thermo Fisher Scientific
KOH	P1767	Sigma-Aldrich

Table 11: Test for Mitochondrial Function. Chemicals.

Name	Catalog No.	Company
Sodium pyruvate	P2256	Sigma-Aldrich
L-malic acid disodium salt	M9138	Sigma-Aldrich
Sodium succinate dibasic hexahydrate	S2378	Sigma-Aldrich
Rotenone	R8875	Sigma-Aldrich
Dimethyl sulfoxide (DMSO)	D5879-1L	Sigma-Aldrich
ATP	A2383-5G	Sigma-Aldrich
Na_2SO_3	S0505	Sigma-Aldrich
Sodium tetraborate decahydrate	S9640	Sigma-Aldrich
ADP	A5285	Sigma-Aldrich
Calcium Green™-5N, hexapotassium salt	C3737	Thermo Fisher Scientific
$CaCl_2$	C3881	Sigma-Aldrich

To assess mitochondrial function, three end-point assays were performed assessing ATP synthesis, mitochondrial respiration and CRC in the isolated mitochondria. They have been described previously [38,101,102]. For all assays the complex I substrates pyruvate and malate and the complex II substrate succinate (all suspended in experimental buffer) together with the complex I inhibitor rotenone (suspended in DMSO) were used.

3.5.3. Mitochondrial ATP Synthesis Assay

The rate of mitochondrial ATP synthesis was determined by measuring bioluminescence in a GloMax 20/20 Luminometer utilizing the ATP-dependent reaction of firefly luciferase and luciferin (Fig. 25). The ATP assay buffer was made fresh from experimental buffer on the day of the experiment and kept on ice.

The ATP standard curve consisted of 8 defined ATP concentrations (0, 2.5, 5, 10, 25, 50, 100, 250 µM) that were diluted in experimental buffer. 5 µL of each standard and

500 µL ATP assay buffer were pipetted into a micro centrifuge tube without cap and luminescence was measured.

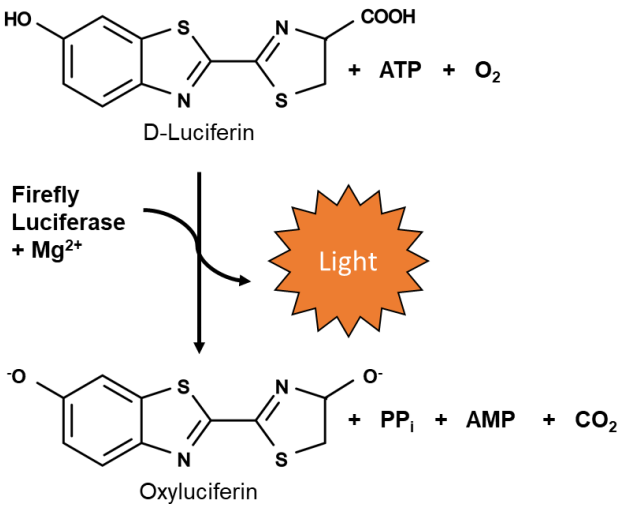

Figure 25: The reaction of D-Luciferin to Oxyluciferin in the presence of adenosine triphosphate (ATP) and firefly luciferase. The emission of light is directly proportional to ATP and is used to calculate the amount of ATP synthesized. *Adapted from Thermo Fisher website*. [103].

For complex I experiments, 2.5 µL 1 mM pyruvate/ malate, and for complex II experiments 2.5 µL 1 mM succinate as well as 2.5 µL 1 µM rotenone were added to 500 µL ATP assay buffer. The addition of 5 µL mitochondria (2.5 mg/mL) initiated the reaction of Luciferin to Oxyluciferin by providing ATP (Fig. 26). The emitted light was measured for 120 sec in 10 recordings. The samples were done in triplicates for each complex.

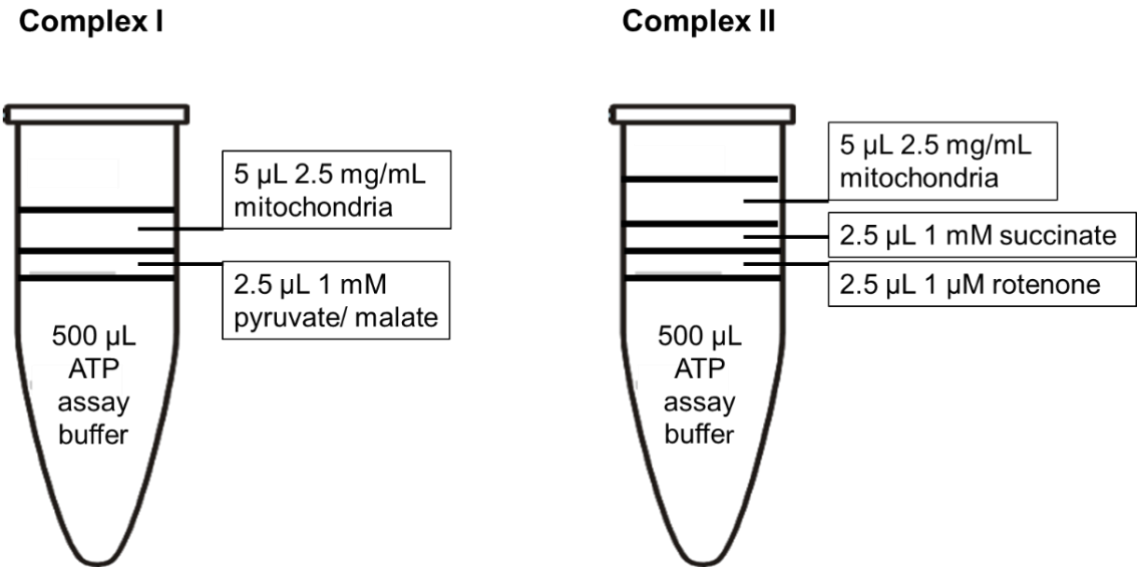

Figure 26: Schematics of chemicals added in the adenosine triphosphate (ATP) synthesis assay in complex I and II runs. Listed in order of addition into micro centrifuge tube from bottom to top.

As a result of ATP being the limiting factor in the reaction, the amount of light emitted in the oxidation of luciferin was proportional to the rate of ATP produced in the sample. This allowed calculation of the rate of mitochondrial ATP synthesis with linear regression of the standard curve. Accordingly, mitochondria synthesizing more of ATP would get higher readings than ones with impaired ATP synthesis.

3.5.4. Mitochondrial O_2-Consumption

Mitochondrial O_2-consumption was measured at room temperature using Strathkelvin's Mitocell Respirometry System that comprises of an O_2-meter, O_2-electrode and a MT200 respirometer as well as FEP membranes. The included software was used for analysis.

The system was calibrated for high consumption measurements with air-saturated MilliQ H_2O and with 2% Na_2SO_3 in 0.01 M sodium tetraborate decahydrate (in MilliQ H_2O) for zero O_2 readings.

280 µL of experimental buffer and 70 µL mitochondria (2.5 mg/mL) were added to two water-jacketed chambers equipped with a Teflon-coated magnetic stirring bar. The chambers were sealed with a plexiglass plug, removing potential air bubbles (t = 0 min). After a stabilization period of 60 sec, state 2 respiration was initiated by addition of complex specific substrates for complex I (10 mM pyruvate/malate) or complex II (10 mM succinate with 10 µM rotenone, complex I inhibitor) of the mitochondrial respiratory chain using small volume glass syringes. Addition of 250 µM ADP 60 sec later triggered respiratory state 3. Once phosphorylation of APD to ATP was complete state 4 could be observed. O_2-concentration in the chambers was monitored for 60 sec after state 4 was reached or until the O_2-concentration was 0. Fig. 27 shows a representative timeline of the mitochondrial oxygen consumption. The assay was completed twice for each complex.

O_2-consumption in each respiratory state was calculated from the slope of the curve. The respiratory control index (RCI) was calculated as the ratio of state 3 to state 4 respiration.

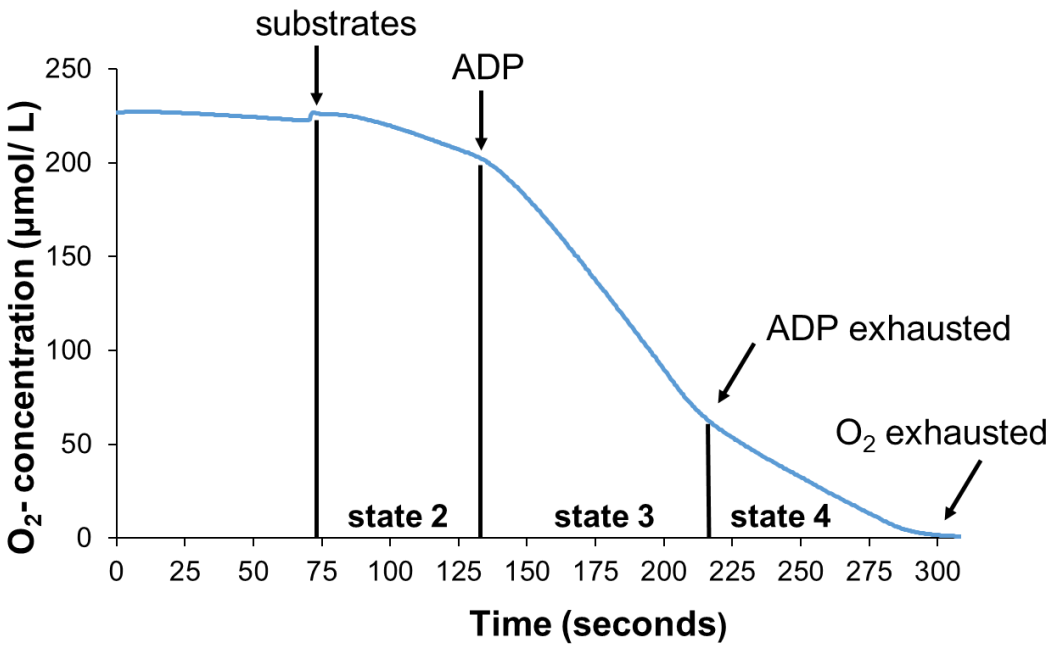

Figure 27: Timeline of mitochondrial O_2-consumption. After 60 sec stabilization, complex specific substrates were added to the chamber, initiating state 2 respiration. Addition of adenosine diphosphate (ADP) 60 sec later initiated state 3 respiration. Upon exhaustion of ADP, the curve flattened, signaling beginning of state 4 respiration until exhaustion of O_2.

3.5.5. Mitochondrial Calcium Retention Capacity

The mitochondrial CRC is a form of measurement of mitochondrial membrane integrity and general mitochondrial function. It is defined as the amount of calcium required to trigger opening of the mPTP. Upon binding Ca^{2+} the cell-impermeant Ca^{2+}-indicator Calcium Green™-5N exhibits an increase in fluorescence emission intensity and can be used to monitor extra-mitochondrial Ca^{2+}.

To measure mitochondrial CRC, a cuvette-based fluorescence spectrophotometer was used. The slit widths were set to 299 mm and 210 mm and the assay wavelengths set to 504 nm excitation and 532 nm emission, respectively.

5 mM and 10 mM $CaCl_2$ were prepared in no-phosphate buffer on the day of the experiment.

1.8 mL of 100 nM Calcium Green™-5N in experimental buffer and 200 µL of the mitochondria sample (2.5 mg/mL) were pipetted into a 3 mL 4-sided rectangular cuvette that was placed in the spectrophotometer along with a magnetic stirring bar.

For complex I, 10 mM pyruvate and malate were added. For complex II, 10 mM succinate with 10 µM rotenone were used. Recordings were started after addition of

the substrates. After 1 min of stabilization, 10 µL boli of 5 mM $CaCl_2$ (complex I) or of 10 mM $CaCl_2$ (complex II) were added at 1 min intervals. After each bolus, a sudden increase with following decrease in intensity of fluorescence could be observed, suggesting mitochondrial calcium intake after bolus administration (Fig. 28). An influx in extra-mitochondrial Ca^{2+} after the initial $CaCl_2$ bolus occurred later in the experiment due to opening of the mPTP and the subsequent leakage of small molecules (including Ca^{2+}) into the buffer.

The decrease in intensity was calculated in percentage of each bolus until opening of mPTP. The calculated values were plotted and the x-intercept determined (Fig. 29). The CRC was estimated by multiplying the calculated intercept with the amount of Ca^{2+} delivered and normalized to mitochondrial protein levels.

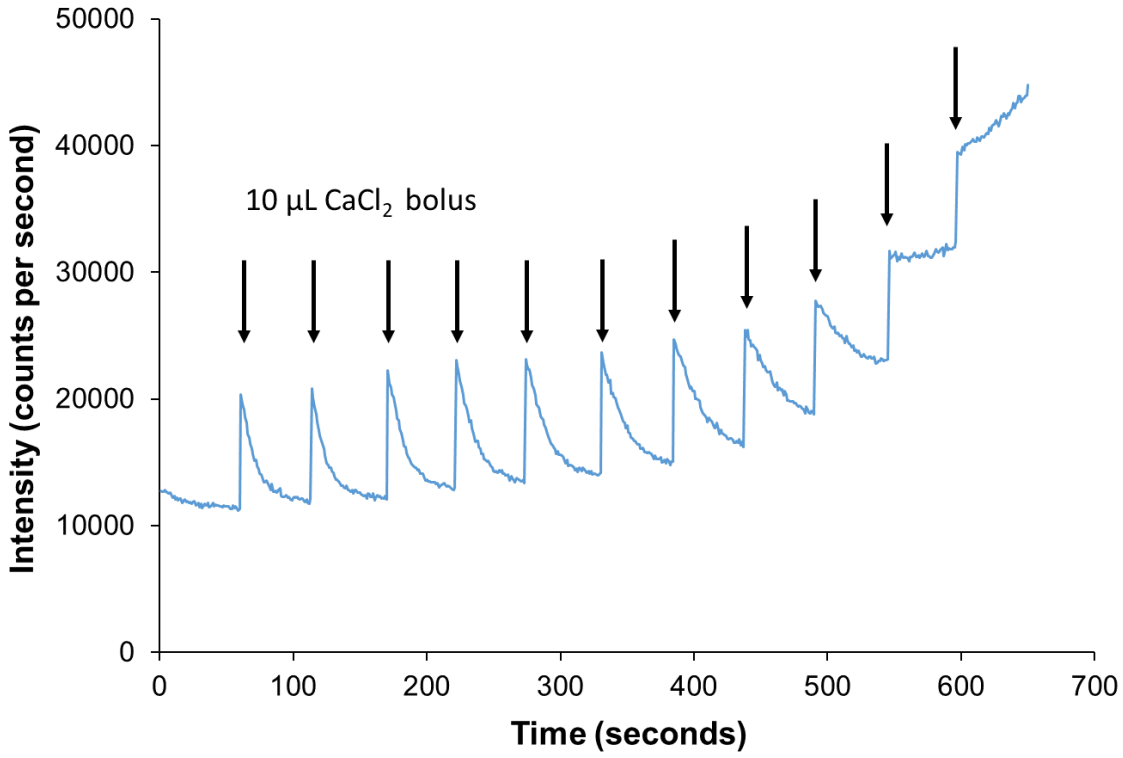

Figure 28: Recording example of Ca^{2+}-retention until opening of the mitochondrial permeability transition pore (mPTP). After 1 min of stabilization, $CaCl_2$ bolus administration begun in 1 min intervals (indicated by black arrows). The increase in fluorescence after each bolus indicates an increase in extra-mitochondrial Ca^{2+}, the subsequent decrease indicates Ca^{2+}-uptake by the mitochondria. In this example, after the eleventh bolus, a further increase can be observed marking the opening of the mPTP.

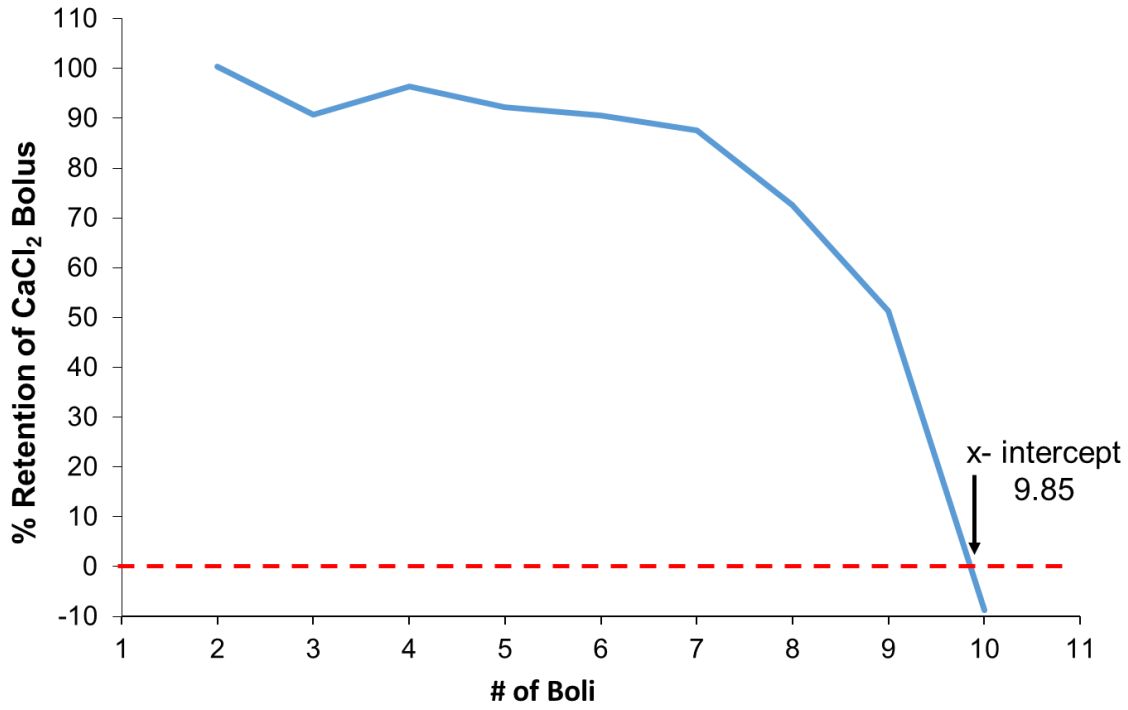

Figure 29: Percentage of retention of each $CaCl_2$ bolus plotted with the x-intercept calculated. For each bolus the amount retained by the mitochondria was calculated in percent and plotted. The x-intercept was calculated and then used for calculation of the total amount calcium retained.

3.6. Statistical Analysis

Statistical analysis was performed with SigmaStat (version 4.0, Systat Software Inc, San Jose, CA, USA). All data were tested for normal distribution with the Shapiro-Wilk test. Due to the majority of data failing the Shapiro-Wilk test ($p > 0.05$), all data were further analyzed using nonparametric testing with the Kruskal-Wallis test. If a significant difference ($p < 0.05$) was found among the groups by Kruskal-Wallis, post-hoc comparisons were performed by Dunn's test.

Graphically, data of myocardial function over time are presented as mean percentages to baseline with SEM for easier comprehension. Mitochondrial data are presented as box plots. Box limits define the interquartile range. The horizontal line within the boxes represents the median value, and the error bars define the 10^{th} and 90^{th} percentiles. Outliers are shown as circles outside the box. Statistically significant differences ($p < 0.05$, two-tailed) are indicated by * (TCH vs IR), † (TCH 60 vs IR+), and ‡ (TCH 50 vs Isc) in myocardial data and as brackets in mitochondrial data.

4. Results and Findings

4.1. Myocardial Function

Functional data of the heart were collected ex-vivo in the isolated heart during stabilization, ischemic and reperfusion intervals. End points collected include: diastolic and systolic pressure, devLVP, contractility, HR, RPP and coronary flow. All data are shown as percentage to baseline (% bl) except for diastolic pressure.

In all data collected and shown, time controls (TCH 50, TCH 60) are analogous to each other and their function was steady over the duration of the experiment. Myocardial function decreased during the ischemic interval and showed significant damage in Isc, IR and IR+ equally. Reperfusion slightly improved function of the myocardium in IR and IR+. Therefore, it can be concluded that the Langendorff model works as expected and the parameters recorded show deteriorating function upon IR injury in the isolated rat heart. This will be depicted in detail below.

4.1.1. Diastolic Pressure

Diastolic pressure (Fig. 30) was normalized to 10 mmHg at baseline (t = 0 min) in all groups. Time controls (TCH 50, TCH 60) stayed at baseline levels throughout the experiment. Diastolic pressure increased equally in Isc, IR and IR+ hearts during ischemia and reached its ischemic maximum at approximately 45 mmHg after 25 min of no-flow ischemia. An instantaneous increase could be observed upon reperfusion in IR (67 mmHg) and IR+ hearts (73 mmHg). While no significance was found between IR and IR+ at 10 min reperfusion (t = 40 min), IR showed a slightly slower rise in diastolic pressure during the first 2 min of reperfusion than IR+ with a drop to 61 mmHg at t = 31 min that was not matched in IR+ hearts.

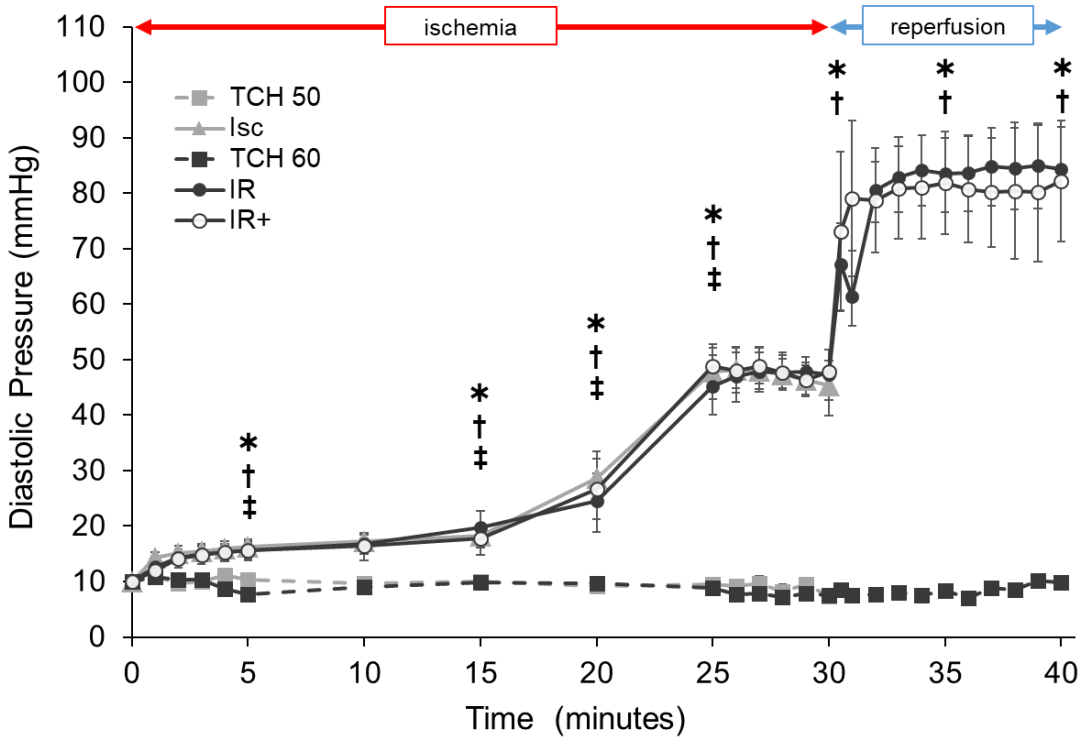

Figure 30: Change in diastolic pressure in rat isolated hearts during ischemia (Isc; n=9) and reperfusion (IR; n=9), compared to IR with P188 post-conditioning (IR+; n=10) and time controls perfused for 50 or 60 min (TCH 50, TCH 60; each with n=8) with Krebs buffer. Diastolic pressure was normalized to 10 mmHg at baseline in all hearts. For easier comprehension, non-parametric data are presented as mean ± SEM. Statistically significant difference ($p < 0.05$), as tested with Kruskal-Wallis testing and post-hoc comparison by Dunn's test, is indicated by * (TCH vs IR), † (TCH 60 vs IR+) and ‡ (TCH 50 vs Isc). Of note, there was no statistically significant difference between IR and IR+ at any time.

4.1.2. Systolic Pressure

Systolic pressure (Fig. 31) decreased fivefold with start of ischemia in all injured groups. A subsequent increase could be observed over the duration of ischemia that leveled at approximately 50% bl 25 min into ischemia. With start of reperfusion, systolic pressure increased in IR and IR+ to about time control levels. There was no significant difference between both groups at 10 min reperfusion (t = 40 min). Though not statistically significant, the increase in both IR and IR+ concluded above time control levels at the end of the experiment.

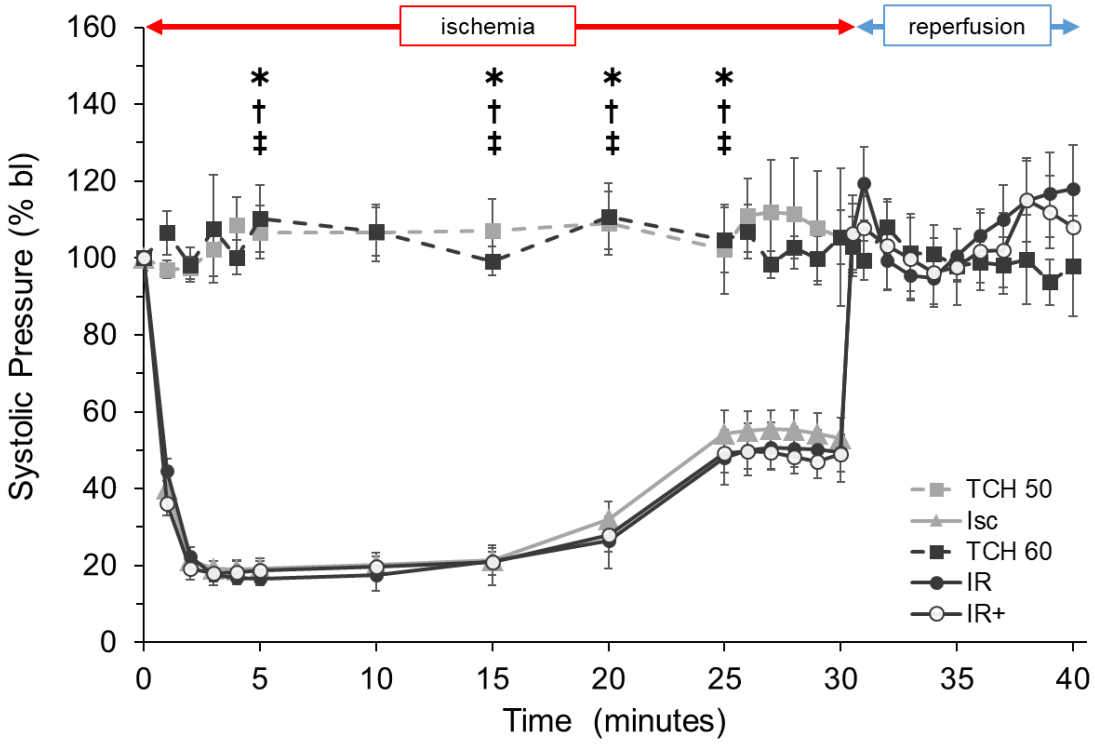

Figure 31: Change in systolic pressure in rat isolated hearts during ischemia (Isc; n=9) and reperfusion (IR; n=9), compared to IR with P188 post-conditioning (IR+; n=10) and time controls perfused for 50 or 60 min (TCH 50, TCH 60; each with n=8) with Krebs buffer. Systolic pressure is represented as percentage to baseline in all hearts. For easier comprehension, non-parametric data are presented as mean ± SEM. Statistically significant difference ($p < 0.05$), as tested with Kruskal-Wallis testing and post-hoc comparison by Dunn's test, is indicated by * (TCH vs IR), † (TCH 60 vs IR+), and ‡ (TCH 50 vs Isc). Of note, there was no statistically significant difference between IR and IR+ at any time.

4.1.3. Developed Left Ventricular Pressure

As a result of the gradual increase in diastolic and the instantaneous decrease in systolic pressure, devLVP (Fig. 32) rapidly decreased in Isc, IR and IR+ hearts during ischemia and was not measurable for most of the ischemic period. During reperfusion devLVP increased in IR and IR+ hearts but stayed at 40% bl and significantly below TCH 60 in both groups. The peak to 64% bl in IR hearts in the first minute of reperfusion (t = 31 min) can be related to a similar, although less pronounced, peak in systolic pressure and a slower increase in diastolic pressure during reperfusion compared to IR+. However, no significant difference could be observed between IR and IR+ after 10 min reperfusion (t = 40 min).

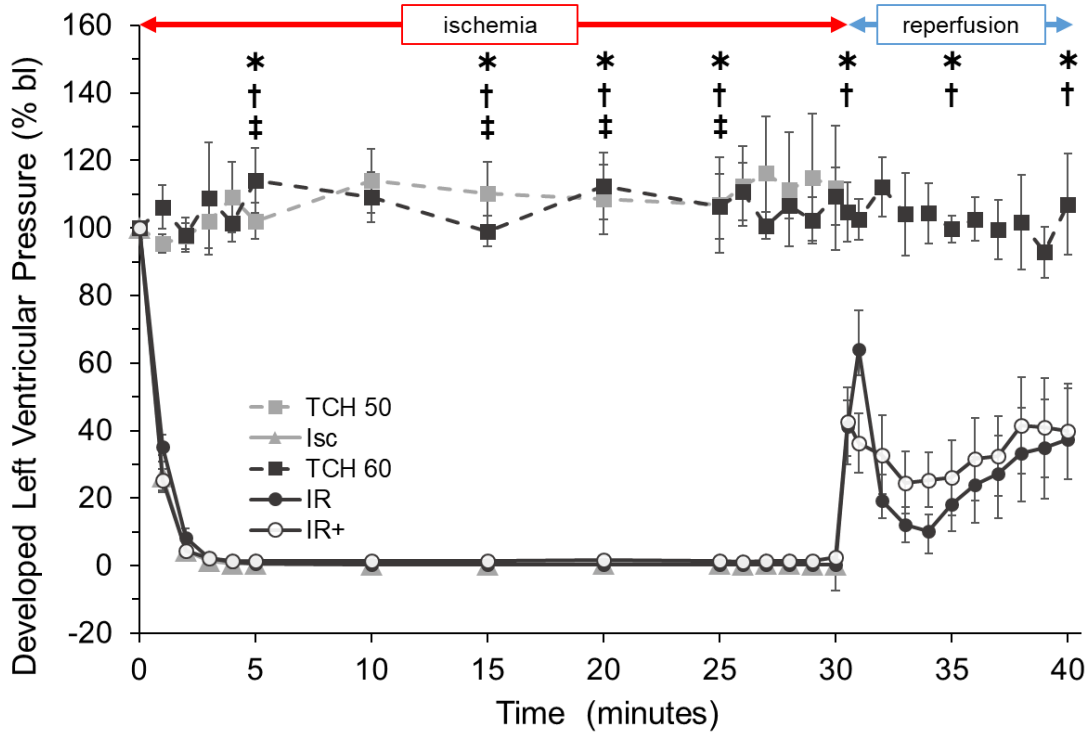

Figure 32: Change in developed left ventricular pressure (devLVP) in rat isolated hearts during ischemia (Isc; n=9) and reperfusion (IR; n=9), compared to IR with P188 post-conditioning (IR+; n=10) and time controls perfused for 50 or 60 min (TCH 50, TCH 60; each with n=8) with Krebs buffer. DevLVP is calculated by subtracting the diastolic from the systolic pressure and is represented here as percentage to baseline in all hearts. For easier comprehension, non-parametric data are presented as mean ± SEM. Statistically significant difference ($p < 0.05$), as tested with Kruskal-Wallis testing and post-hoc comparison by Dunn's test, is indicated by * (TCH vs IR), † (TCH 60 vs IR+), and ‡ (TCH 50 vs Isc). Of note, there was no statistically significant difference between IR and IR+ at any time.

4.1.4. Contractility

Myocardial contractility (Fig. 33) was calculated as the maximal first derivative of devLVP (see Equation 3, chapter 3.2.) and shows the rate of change in devLVP in respect to time. Therefore, the results are similar to devLVP when presented as percentage to baseline. Contractility decreased drastically in Isc, IR and IR+ upon ischemia. Contractility increased in IR and IR+ at the beginning of reperfusion but stayed below 40% bl at t = 40 min and was significantly reduced compared to TCH 60. IR+ recovered contractility more evenly and showed a slight improvement compared to IR in the first 8 min of reperfusion. However, there was no difference between IR and IR+ after 10 min of reperfusion (t = 40 min).

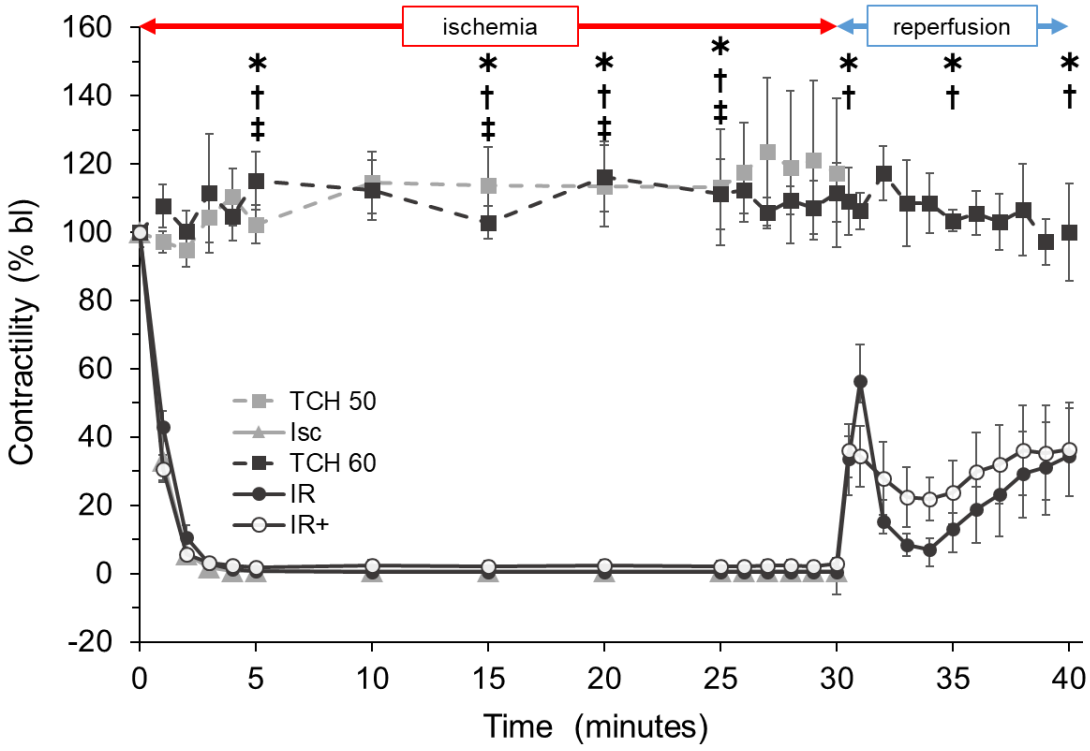

Figure 33: Change in contractility in rat isolated hearts during ischemia (Isc; n=9) and reperfusion (IR; n=9), compared to IR with P188 post-conditioning (IR+; n=10) and time controls perfused for 50 or 60 min (TCH 50, TCH 60; each with n=8) with Krebs buffer. $dLVP/dt_{max}$ is calculated as the maximal rise of left ventricular pressure and is represented here as percentage to baseline in all hearts. For easier comprehension, non-parametric data are presented as mean ± SEM. Statistically significant difference ($p < 0.05$), as tested with Kruskal-Wallis testing and post-hoc comparison by Dunn's test, is indicated by * (TCH vs IR), † (TCH 60 vs IR+), and ‡ (TCH 50 vs Isc). Of note, there was no statistically significant difference between IR and IR+ at any time.

4.1.5. Heart Rate

HR (Fig. 34) dropped in Isc, IR and IR+ groups to 0% bl after 5 min of ischemia and stayed unchanged for the whole ischemic period. IR and IR+ initially increased to approximately 75% bl upon reperfusion without reaching time control levels. The subsequent decrease in HR after 2 min of reperfusion was less pronounced in IR+ (30% bl) compared to IR (12% bl) and showed slightly better results for the majority of reperfusion. Both groups reapproached each other at approximately 55% bl towards the end of reperfusion. At the end of reperfusion (t = 40 min), no significant difference between IR and IR+ could be observed.

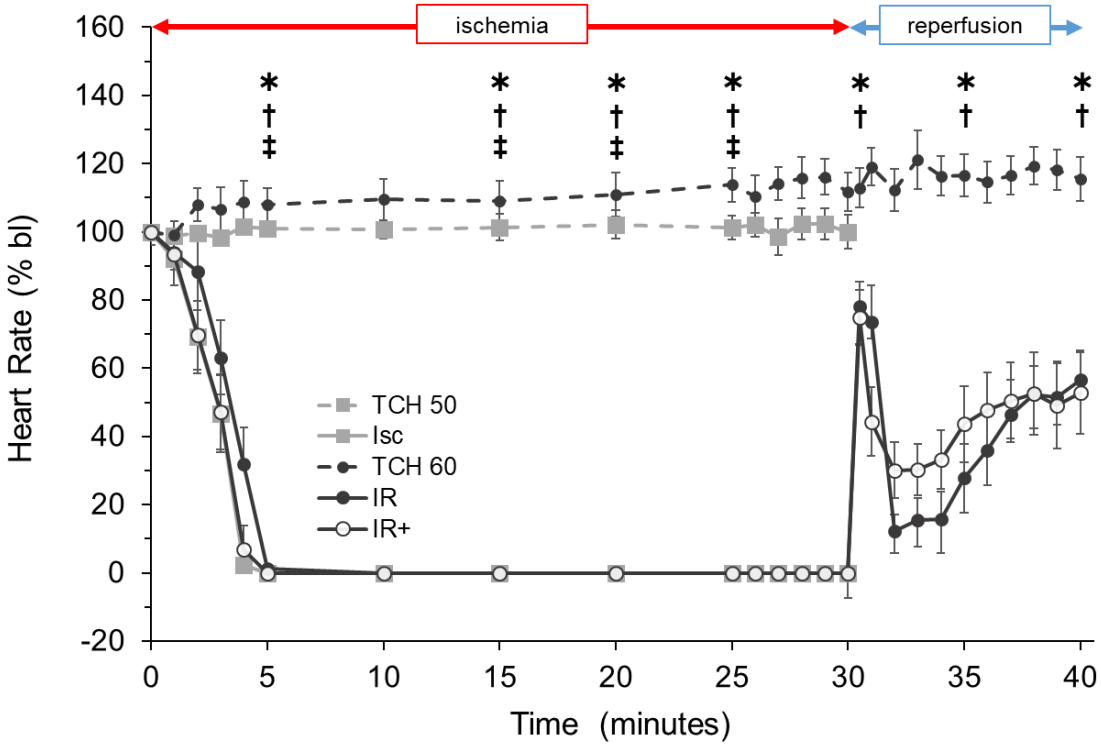

Figure 34: Change in heart rate (HR) in rat isolated hearts during ischemia (Isc; n=9) and reperfusion (IR; n=9), compared to IR with P188 post-conditioning (IR+; n=10) and time controls perfused for 50 or 60 min (TCH 50, TCH 60; each with n=8) with Krebs buffer. HR is shown here as percentage to baseline in all hearts. For easier comprehension, non-parametric data are presented as mean ± SEM. Statistically significant difference ($p < 0.05$), as tested with Kruskal-Wallis testing and post-hoc comparison by Dunn's test, is indicated by * (TCH vs IR), † (TCH 60 vs IR+), and ‡ (TCH 50 vs Isc). Of note, there was no statistically significant difference between IR and IR+ at any time.

4.1.6. Rate Pressure Product

RPP (Fig. 35) is calculated as the product of HR and devLVP (see Equation 2, chapter 3.2.). It is an indication for myocardial workload and energy demand of the heart. Parallel to both devLVP and heart rate, RPP decreased in Isc, IR and IR+ groups to 0% bl after 5 min of ischemia and remained low for the whole duration of ischemia. IR and IR+ initially increased upon reperfusion, with a pronounced peak in IR to 51% bl after 2 min of reperfusion that was not matched in IR+. Both groups showed a subsequent decrease in RPP which had a greater extent in IR (4% bl) compared to IR+ (13% bl). This corresponds to a greater peak in devLVP and larger drop in HR in IR compared to IR+ hearts at 2 min reperfusion. At 4 min of reperfusion, RPP increased again in both groups with IR+ showing slightly better results than IR, though not statistically significant. Neither group reached time control levels after 10 min of reperfusion (t = 40 min).

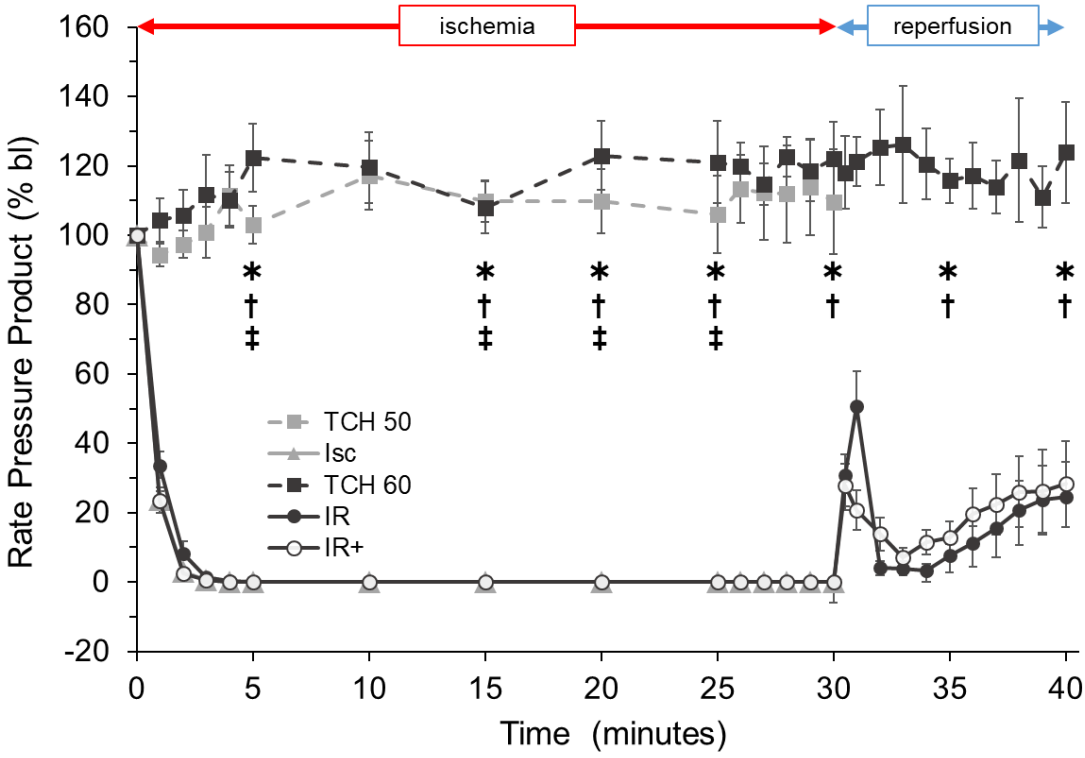

Figure 35: Change in rate pressure product (RPP) in rat isolated hearts during ischemia (Isc; n=9) and reperfusion (IR; n=9), compared to IR with P188 post-conditioning (IR+; n=10) and time controls perfused for 50 or 60 min (TCH 50, TCH 60; each with n=8) with Krebs buffer. RPP is calculated as systolic pressure multiplied by heart rate and is represented here as percentage to baseline in all hearts. For easier comprehension, non-parametric data are presented as mean ± SEM. Statistically significant difference ($p < 0.05$), as tested with Kruskal-Wallis testing and post-hoc comparison by Dunn's test, is indicated by * (TCH vs IR), † (TCH 60 vs IR+), and ‡ (TCH 50 vs Isc). Of note, there was no statistically significant difference between IR and IR+ at any time.

4.1.7. Coronary Flow

Coronary flow (Fig. 36) was stopped to create the ischemic interval in Isc, IR and IR+ hearts and was therefore 0 during the ischemic period until the beginning of reperfusion. During reperfusion, coronary flow increased instantly to 50% bl in IR and IR+ hearts but did not return to preischemic levels after 10 min. Although coronary flow was lower in IR+ compared to IR starting at 2 min of reperfusion and over the remainder of the reperfusion period, there was no statistically significant difference between IR (54% bl) and IR+ (42% bl) at the end of reperfusion.

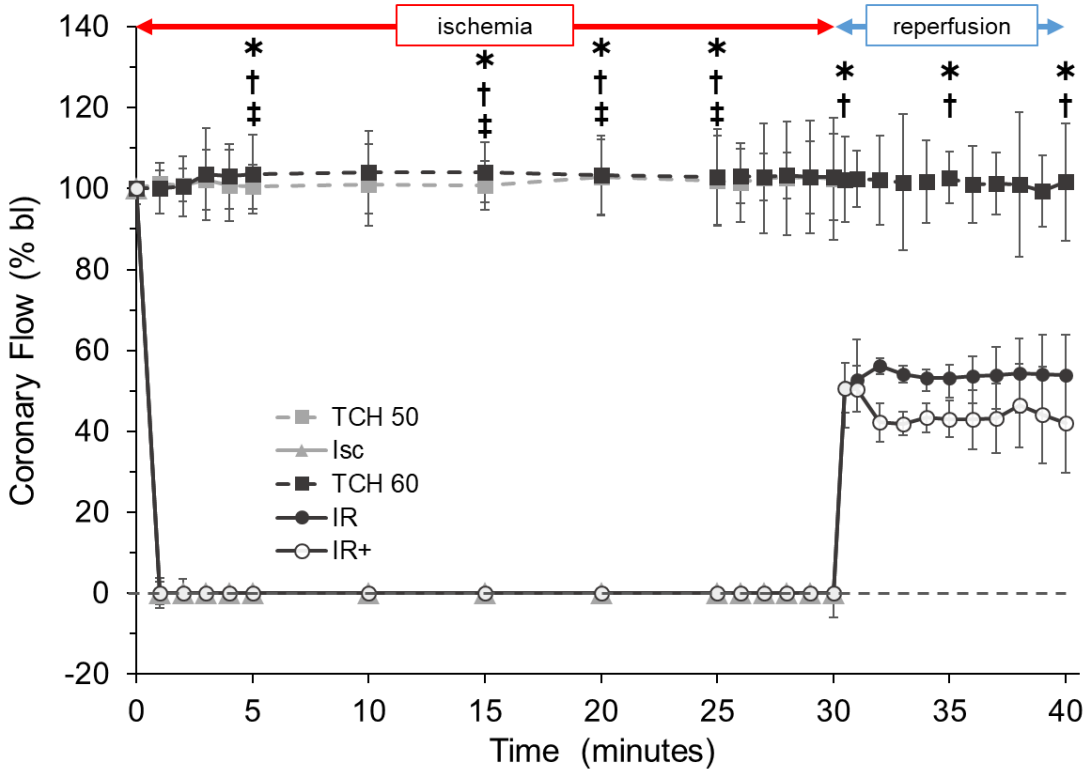

Figure 36: Change in coronary flow in rat isolated hearts during ischemia (Isc; n=9) and reperfusion (IR; n=9), compared to IR with P188 post-conditioning (IR+; n=10) and time controls perfused for 50 or 60 min (TCH 50, TCH 60; each with n=8) with Krebs buffer. Coronary flow is shown as percentage to baseline. For easier comprehension, non-parametric data are presented as mean ± SEM. Statistically significant difference ($p < 0.05$), as tested with Kruskal-Wallis testing and post-hoc comparison by Dunn's test, is indicated by * (TCH vs IR), † (TCH 60 vs IR+), and ‡ (TCH 50 vs Isc). Of note, there was no statistically significant difference between IR and IR+ at any time.

4.2. Mitochondrial Function

Mitochondria were isolated from time control hearts and hearts subjected to IR injury. They were randomized into treatment groups during isolation with isolation buffer (no-treatment), 1 mM P188 or 1 mM PEG in isolation buffer. Values of mitochondrial function are presented as box plots. The digital values for the graphical data can be found in the appendix (chapter 8.1.).

4.2.1. Mitochondrial ATP Synthesis

Complex I

Mitochondrial ATP synthesis with complex I-specific substrates pyruvate and malate (Fig. 37, p. 46) was significantly decreased in injured hearts (Isc, IR, IR+) compared to time controls (TCH 50, TCH 60) in no-treatment mitochondria (Fig. 37A, p. 46). Ex-vivo P188 post-conditioning did not improve ATP synthesis, as no increase from IR to IR+ could be seen. Figure 37B (p. 46) shows an increase in mitochondria from Isc treated with PEG compared to no treatment. Otherwise, neither P188 nor PEG showed improvement nor deterioration of mitochondrial function when given during isolation of mitochondria in all groups.

Complex II

As seen in Figure 38A (p.47), ATP synthesis in no-treatment mitochondria decreased after IR compared to TCH 60 and in Isc compared to TCH 50 with the complex II-specific substrate succinate in the presence of complex I inhibitor rotenone. This suggests significant damage to the cardiac mitochondria by both ischemic and IR injury. Moreover, no difference between IR+ and TCH 60 could be detected, indicating a slight increase in mitochondrial ATP synthesis after ex-vivo P188 post-conditioning. This improvement was not significant compared to IR. In Isc hearts, mitochondrial treatment with both P188 and PEG showed a similar increase in ATP synthesis compared to no-treatment mitochondria (Fig. 38B, p. 47). In contrast, neither P188 nor PEG had an effect on mitochondrial function in hearts subjected to IR in this assay (Fig. 38C, p. 47). This was matched in IR+ hearts treated with PEG, while P188 reduced ATP synthesis, suggesting deteriorating mitochondrial function when both ex-vivo and mitochondrial P188 treatment was administered.

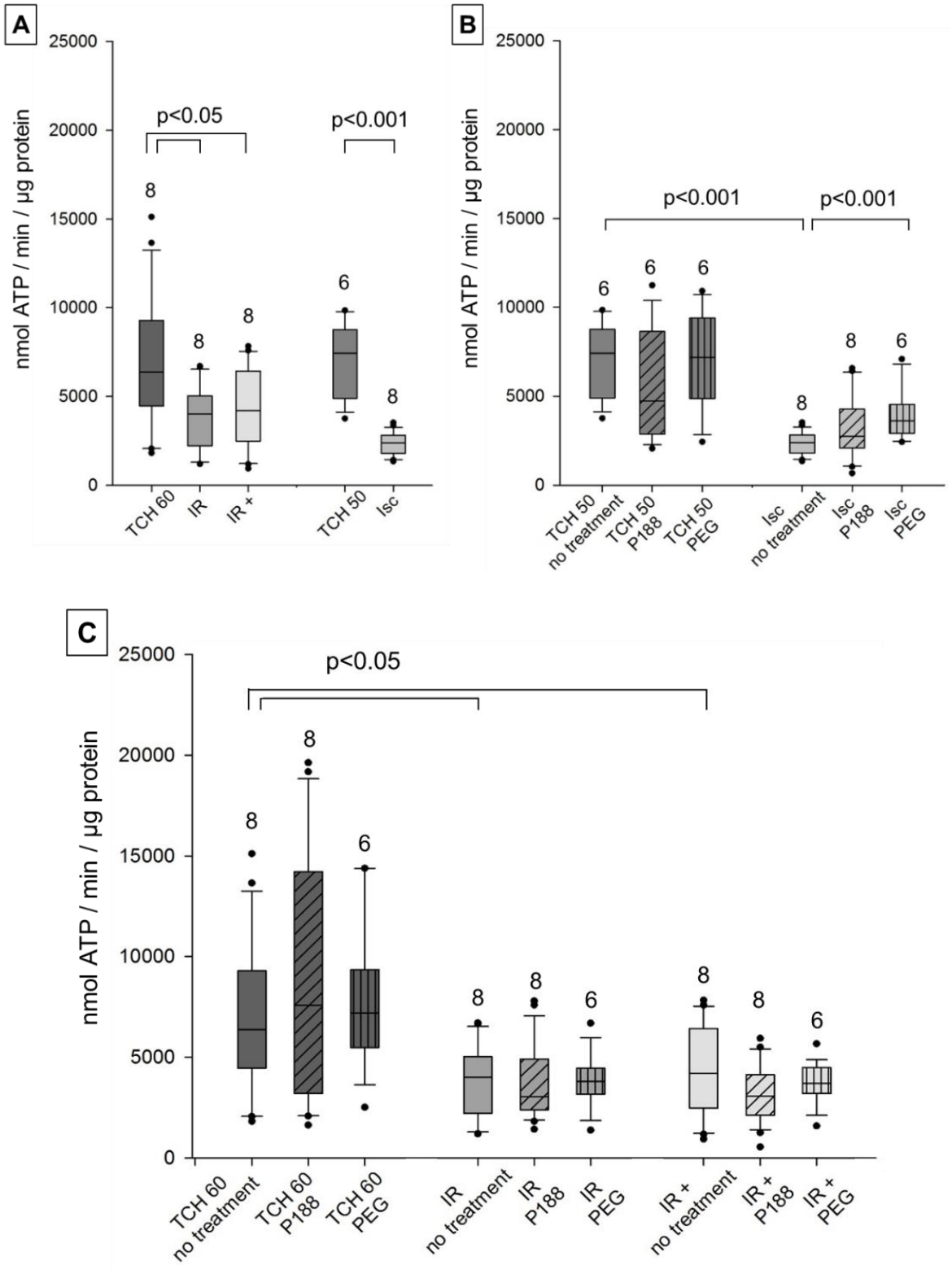

Figure 37: Mitochondrial adenosine triphosphate (ATP) synthesis (nmol ATP / min / µg protein) with complex I substrates in isolated cardiac mitochondria. Mitochondria subjected to ischemia (Isc), ischemia reperfusion (IR), IR with P188 during reperfusion (IR+), only perfusion (time control hearts [TCH] 50 min and 60 min). **A**: Mitochondria isolated with isolation buffer (IB/ no treatment). **B**: Mitochondria isolated with no treatment, IB containing 1 mM P188 or 1 mM PEG for Isc and TCH 50 hearts. **C**: Treated and untreated mitochondria for IR, IR+ and TCH 60 hearts. N in triplicates. Brackets indicate statistically significant difference TCH dark grey, injured hearts lighter grey. Hatching shows mitochondrial treatment: no treatment (no hatching), P188 (diagonal lines), PEG (vertical lines).

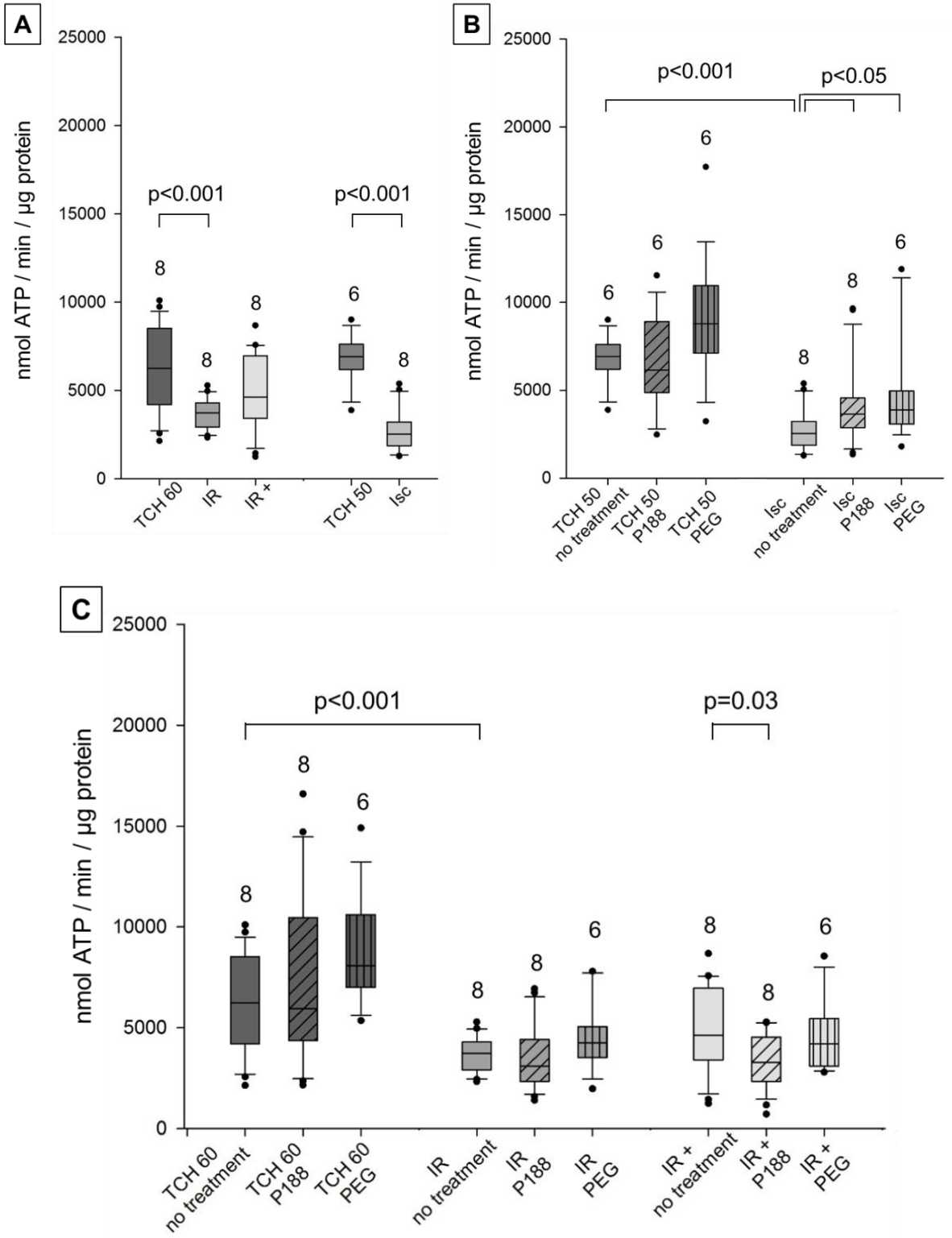

Figure 38: Mitochondrial adenosine triphosphate (ATP) synthesis (nmol ATP / min / µg protein) with complex II substrate in isolated cardiac mitochondria. Mitochondria subjected to ischemia (Isc), ischemia reperfusion (IR), IR with P188 during reperfusion (IR+), only perfusion (time control hearts [TCH] 50 min and 60 min). **A**: Mitochondria isolated with isolation buffer (IB/ no treatment). **B**: Mitochondria isolated with no treatment, IB containing 1 mM P188 or 1 mM PEG for Isc and TCH 50 hearts. **C**: Treated and untreated mitochondria for IR, IR+ and TCH 60 hearts. N in triplicates. Brackets indicate statistically significant difference TCH dark grey, injured hearts lighter grey. Hatching shows mitochondrial treatment: no treatment (no hatching), P188 (diagonal lines), PEG (vertical lines).

4.2.2. Mitochondrial O_2-Consumption

Data for mitochondrial respiration are shown as RCI which was calculated as the ratio of state 3 to state 4 respiration. The individual states of respiration are also shown to allow a clearer comprehension of changes in RCI.

Complex I

Respiratory Control index

RCI with the complex I-specific substrates pyruvate and malate was significantly decreased in Isc hearts compared to TCH 50 in no-treatment mitochondria, while no statistically significant difference could be found among TCH 60, IR and IR+ (Fig. 39A, p. 50). This suggests that RCI recovers with reperfusion and that additional IR injury could not be found in this assay. Mitochondrial PEG treatment showed a marginally reduced RCI in all injured hearts (Isc, IR, IR+) that was not significant and was not mirrored in time controls (TCH 50, TCH 60). Mitochondrial treatment with P188, however, showed no direct mitochondrial effect – neither improvement nor deterioration – on RCI in all five groups (Fig. 39B, C; p. 50).

State 3 Respiration

State 3 respiration was significantly decreased in mitochondria isolated from Isc and IR hearts compared to time controls in no-treatment mitochondria, so a quantifiable damage could be found after both ischemia and reperfusion.

However, TCH 60 and IR+ were similar, suggesting a slight increase in state 3 respiration after P188 post-conditioning. This was not shown to be significant compared to IR (Fig. 40A, p. 51). In Figure 40B and 40C (p. 51) an increase in state 3 respiration is shown in TCH 50 with mitochondrial PEG treatment compared to no-treatment that was not reproduced in TCH 60. Treatment of mitochondria with P188, but not PEG, increased state 3 respiration in Isc and IR hearts compared to time controls suggesting a benefit of P188 treatment in damaged hearts. This effect was not seen in IR+ groups.

State 4 Respiration

State 4 respiration was similar in time controls and injured hearts in no-treatment mitochondria. A trend of increase in state 4 respiration could be seen in IR+ (Fig. 41A, p. 52) possibly pointing towards light uncoupling by ex-vivo P188 post-conditioning. As seen in Figure 41B (p.52), mitochondria from TCH 50 showed an increase in state 4 respiration when treated with PEG compared to no mitochondrial treatment. A similar trend, that was not shown to be significant, could be seen in TCH 60. Mitochondrial treatment with either P188 or PEG increased state 4 respiration in Isc and IR groups compared to no mitochondrial treatment. However, IR+ mitochondria treated with PEG only showed a significant increase in state 4 respiration compared to P188 treatment which was marginally decreased compared to no-treatment.

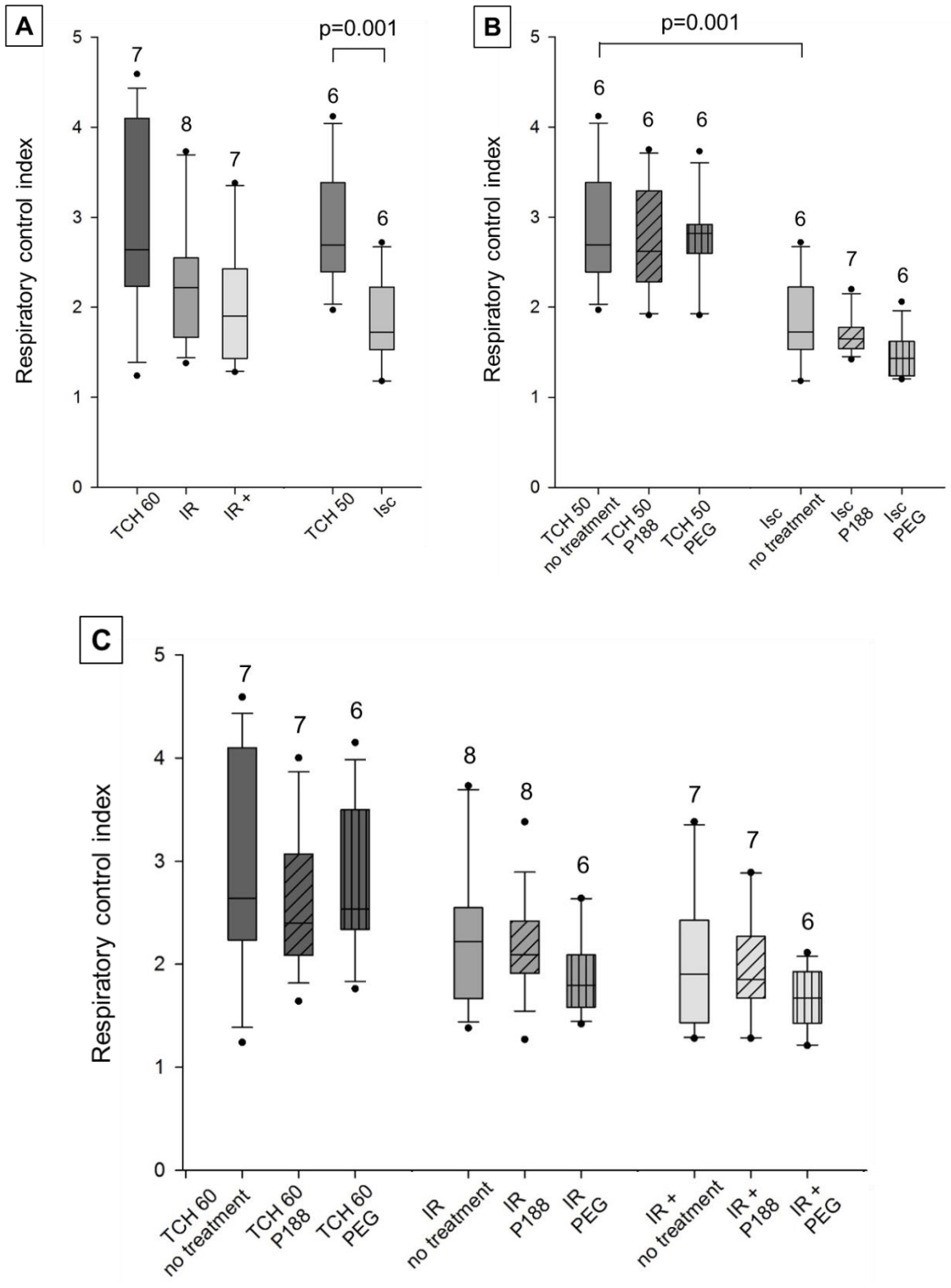

Figure 39: Mitochondrial respiratory control index (RCI) with complex I substrates in isolated cardiac mitochondria. RCI calculated as respiratory state 3 / state 4. Mitochondria subjected to ischemia (Isc), ischemia reperfusion (IR), IR with P188 during reperfusion (IR+), only perfusion (time control hearts [TCH] 50 min and 60 min). **A**: Mitochondria isolated with isolation buffer (IB/ no treatment). **B**: Mitochondria isolated with no treatment, IB containing 1 mM P188 or 1 mM PEG for Isc and TCH 50 hearts. **C**: Treated and untreated mitochondria for IR, IR+ and TCH 60 hearts. N in duplicates. Brackets indicate statistically significant difference TCH dark grey, injured hearts lighter grey. Hatching shows mitochondrial treatment: no treatment (no hatching), P188 (diagonal lines), PEG (vertical lines).

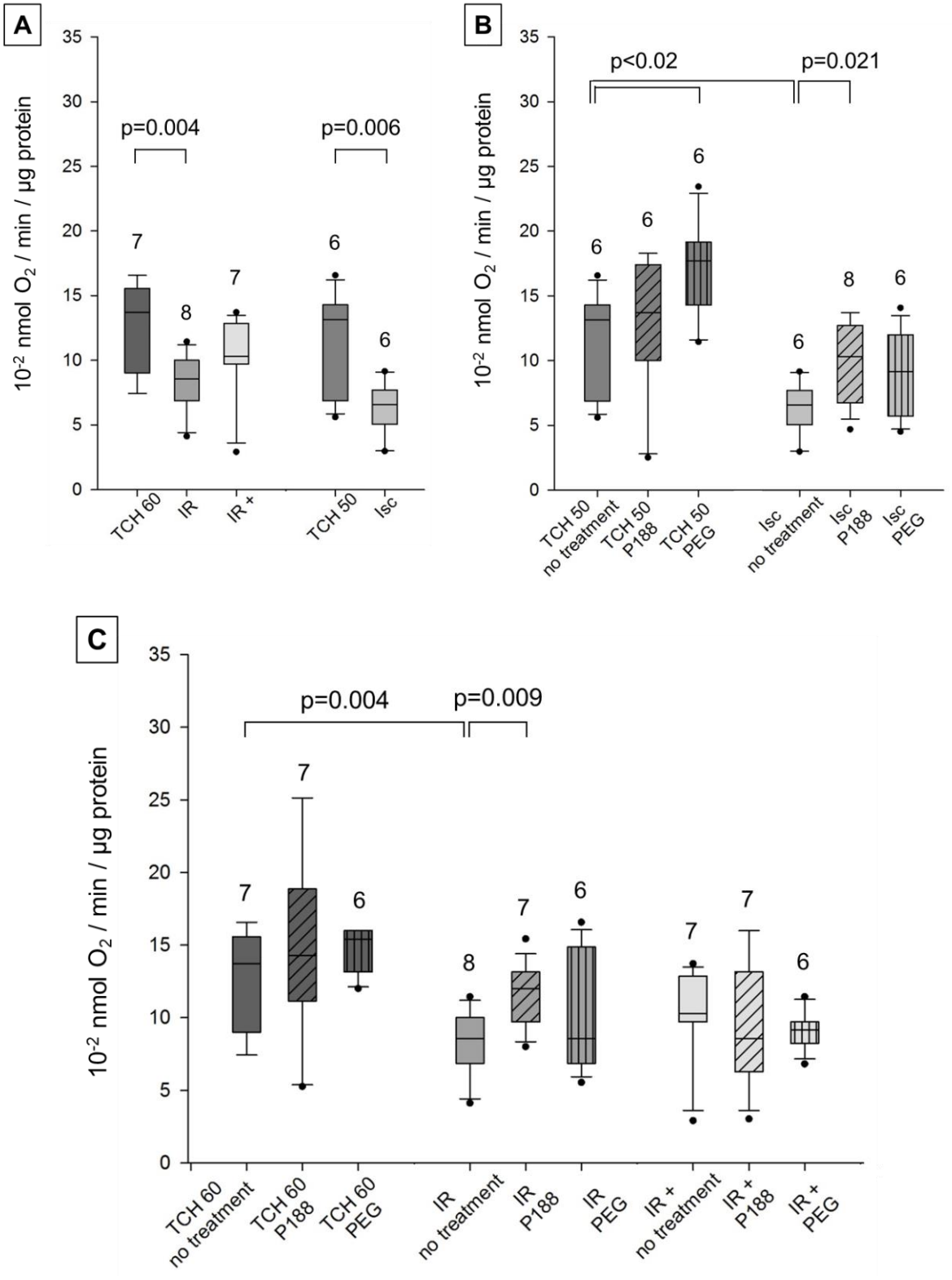

Figure 40: Mitochondrial respiratory state 3 (10^{-2} nmol O_2 / min / µg protein) with complex I substrates in isolated cardiac mitochondria. Mitochondria subjected to ischemia (Isc), ischemia reperfusion (IR), IR with P188 during reperfusion (IR+), only perfusion (time control hearts [TCH] 50 min and 60 min). **A**: Mitochondria isolated with isolation buffer (IB/ no treatment). **B**: Mitochondria isolated with no treatment, IB containing 1 mM P188 or 1 mM PEG for Isc and TCH 50 hearts. **C**: Treated and untreated mitochondria for IR, IR+ and TCH 60 hearts. N in duplicates. Brackets indicate statistically significant difference TCH dark grey, injured hearts lighter grey. Hatching shows mitochondrial treatment: no treatment (no hatching), P188 (diagonal lines), PEG (vertical lines).

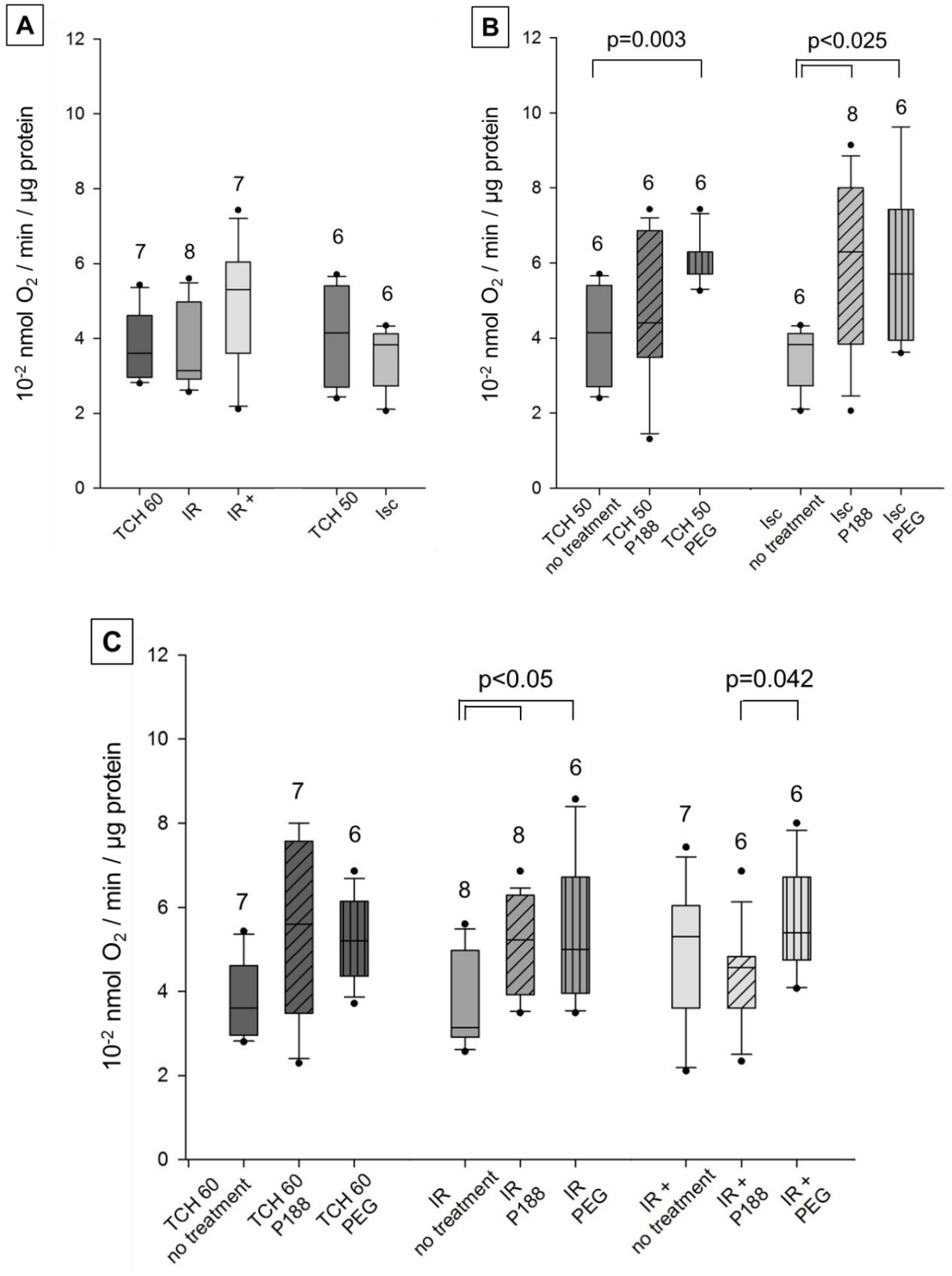

Figure 41: Mitochondrial respiratory state 4 (10^{-2} nmol O_2 / min / µg protein) with complex I substrates in isolated cardiac mitochondria. Mitochondria subjected to ischemia (Isc), ischemia reperfusion (IR), IR with P188 during reperfusion (IR+), only perfusion (time control hearts [TCH] 50 min and 60 min). **A**: Mitochondria isolated with isolation buffer (IB/ no treatment). **B**: Mitochondria isolated with no treatment, IB containing 1 mM P188 or 1 mM PEG for Isc and TCH 50 hearts. **C**: Treated and untreated mitochondria for IR, IR+ and TCH 60 hearts. N in duplicates. Brackets indicate statistically significant difference TCH dark grey, injured hearts lighter grey. Hatching shows mitochondrial treatment: no treatment (no hatching), P188 (diagonal lines), PEG (vertical lines).

Complex II

Respiratory Control Index

In complex II experiments, RCI was significantly reduced in Isc and IR+ but not in IR hearts compared to time controls (TCH 50, TCH 60). Similar to complex I, an ischemic injury could be measured but, in contrast to complex I, an IR injury was also seen. However, this suggests that ex-vivo P188 post-conditioning had a negative effect on the mitochondria. Neither mitochondrial treatment showed effects on RCI in all groups (Fig. 42B, C, p. 54).

State 3 Respiration

Similar to complex I, state 3 respiration was significantly decreased in mitochondria isolated from Isc and IR hearts compared to time controls with the complex II-specific substrate succinate in the presence of complex I inhibitor rotenone.

TCH 60 and IR+ were similar, indicating a slight increase in state 3 respiration after P188 post-conditioning. This was not significant compared to IR (Fig. 43A, p. 55). A direct mitochondrial effect of P188 and PEG could only be observed in Isc hearts compared to no-treatment mitochondria (Fig. 43B, p. 55) but neither in time control nor IR or IR+ (Fig. 43C, p. 55).

State 4 Respiration

Fig. 44A (p. 56) shows that state 4 respiration in no-treatment mitochondria was similar in time controls (TCH 50, TCH 60) and injured hearts (Isc, IR, IR+) with the complex II-specific substrate succinate in the presence of complex I inhibitor rotenone. This would suggest that changes in state 4 respiration are not the driving force in RCI changes. Mitochondrial treatment with either P188 or PEG showed a non-significant trend to increase in Isc and IR and a trend to decrease in IR+ which was only significant in mitochondrial PEG treatment compared to no-treatment mitochondria (Fig. 44B, 44C; p. 56). This could point towards a possible decrease in mitochondrial uncoupling in pretreated hearts with continued higher osmolarity.

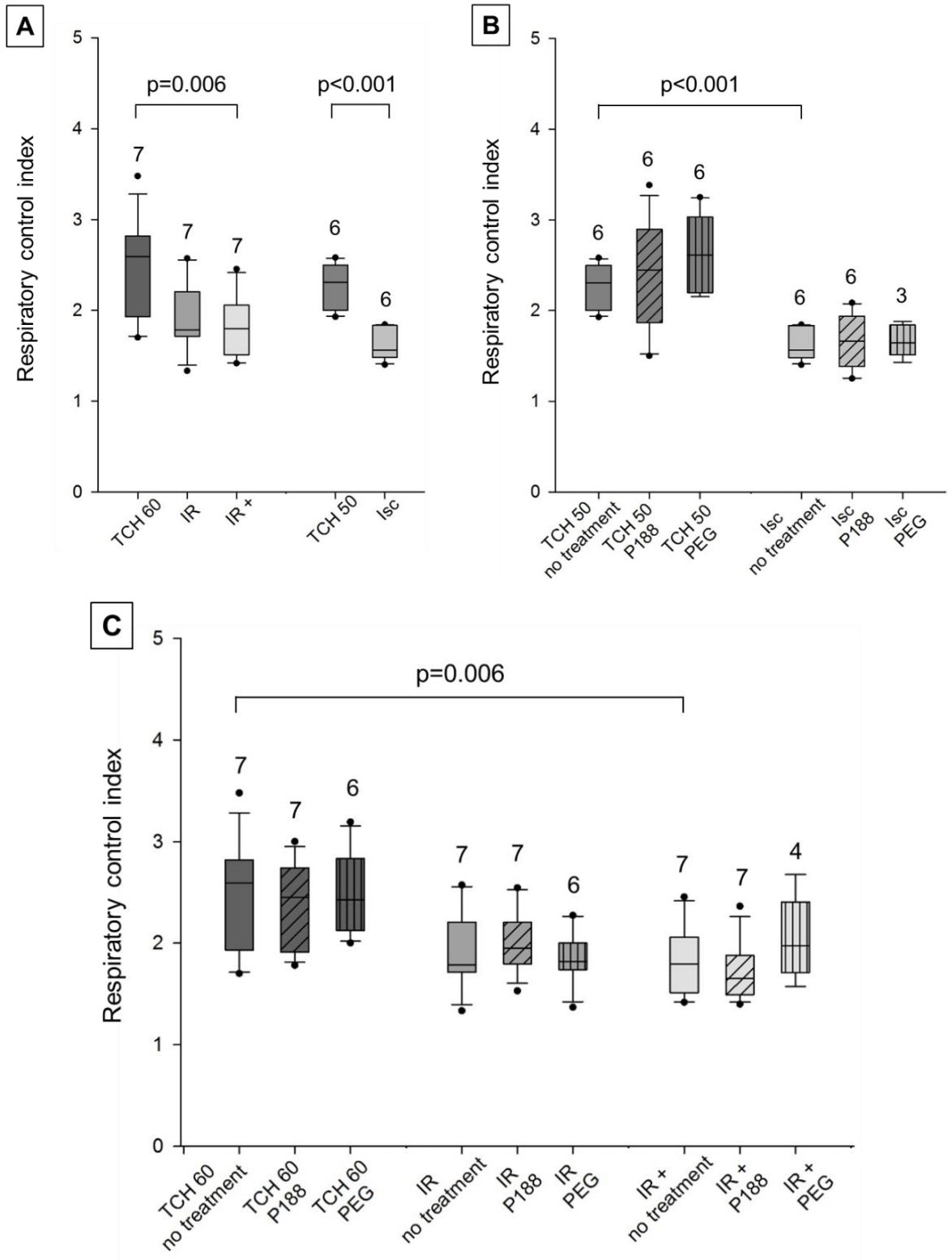

Figure 42: Mitochondrial respiratory control index (RCI) with complex II substrate in isolated cardiac mitochondria. RCI calculated as respiratory state 3 / state 4. Mitochondria subjected to ischemia (Isc), ischemia reperfusion (IR), IR with P188 during reperfusion (IR+), only perfusion (time control hearts [TCH] 50 min and 60 min). **A**: Mitochondria isolated with isolation buffer (IB/ no treatment). **B**: Mitochondria isolated with no treatment, IB containing 1 mM P188 or 1 mM PEG for Isc and TCH 50 hearts. **C**: Treated and untreated mitochondria for IR, IR+ and TCH 60 hearts. N in duplicates. Brackets indicate statistically significant difference TCH dark grey, injured hearts lighter grey. Hatching shows mitochondrial treatment: no treatment (no hatching), P188 (diagonal lines), PEG (vertical lines).

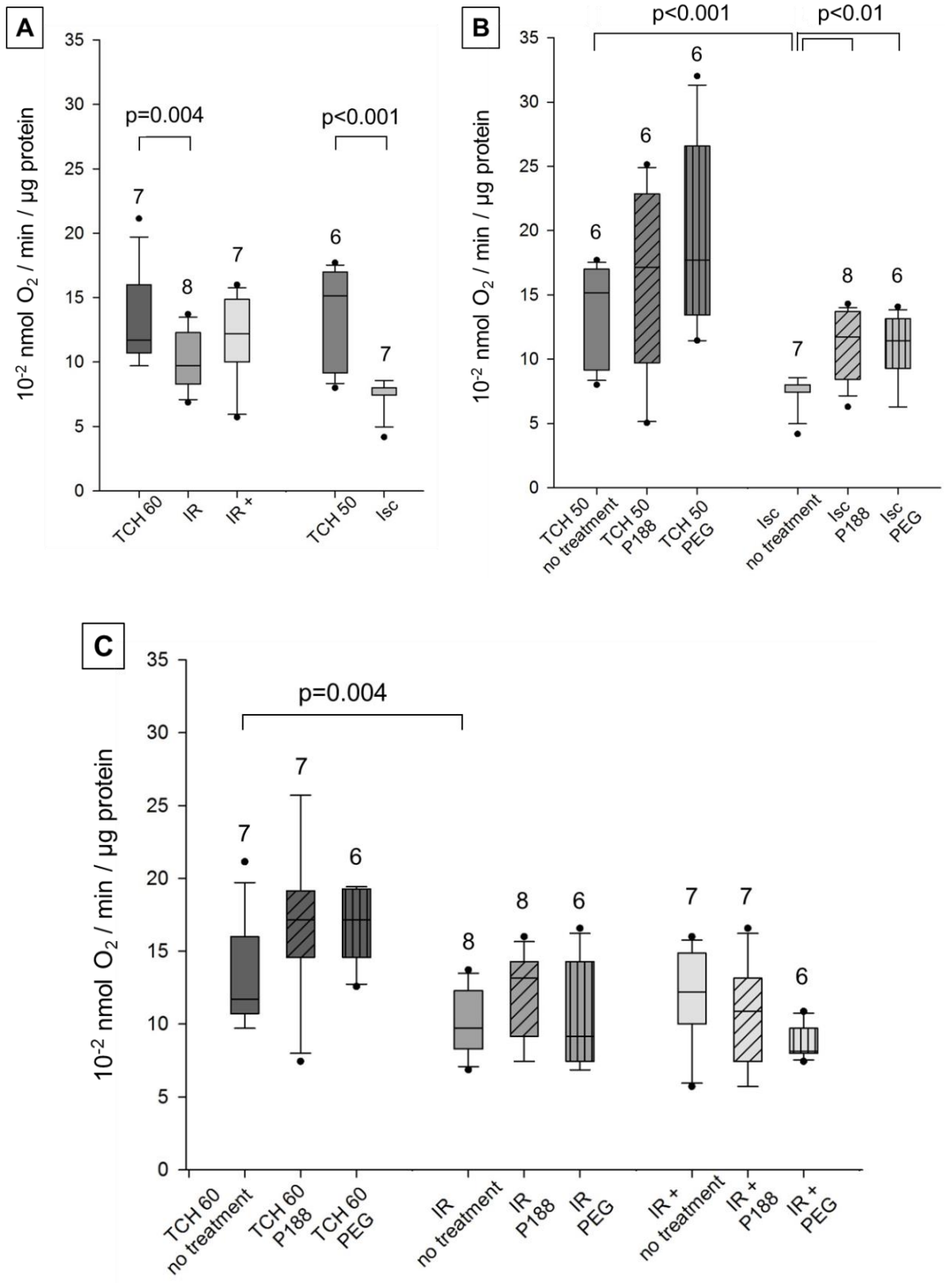

Figure 43: Mitochondrial respiratory state 3 (10^{-2} nmol O_2 / min / µg protein) with complex II substrate in isolated cardiac mitochondria. Mitochondria subjected to ischemia (Isc), ischemia reperfusion (IR), IR with P188 during reperfusion (IR+), only perfusion (time control hearts [TCH] 50 min and 60 min). **A**: Mitochondria isolated with isolation buffer (IB/ no treatment). **B**: Mitochondria isolated with no treatment, IB containing 1 mM P188 or 1 mM PEG for Isc and TCH 50 hearts. **C**: Treated and untreated mitochondria for IR, IR+ and TCH 60 hearts. N in duplicates. Brackets indicate statistically significant difference TCH dark grey, injured hearts lighter grey. Hatching shows mitochondrial treatment: no treatment (no hatching), P188 (diagonal lines), PEG (vertical lines).

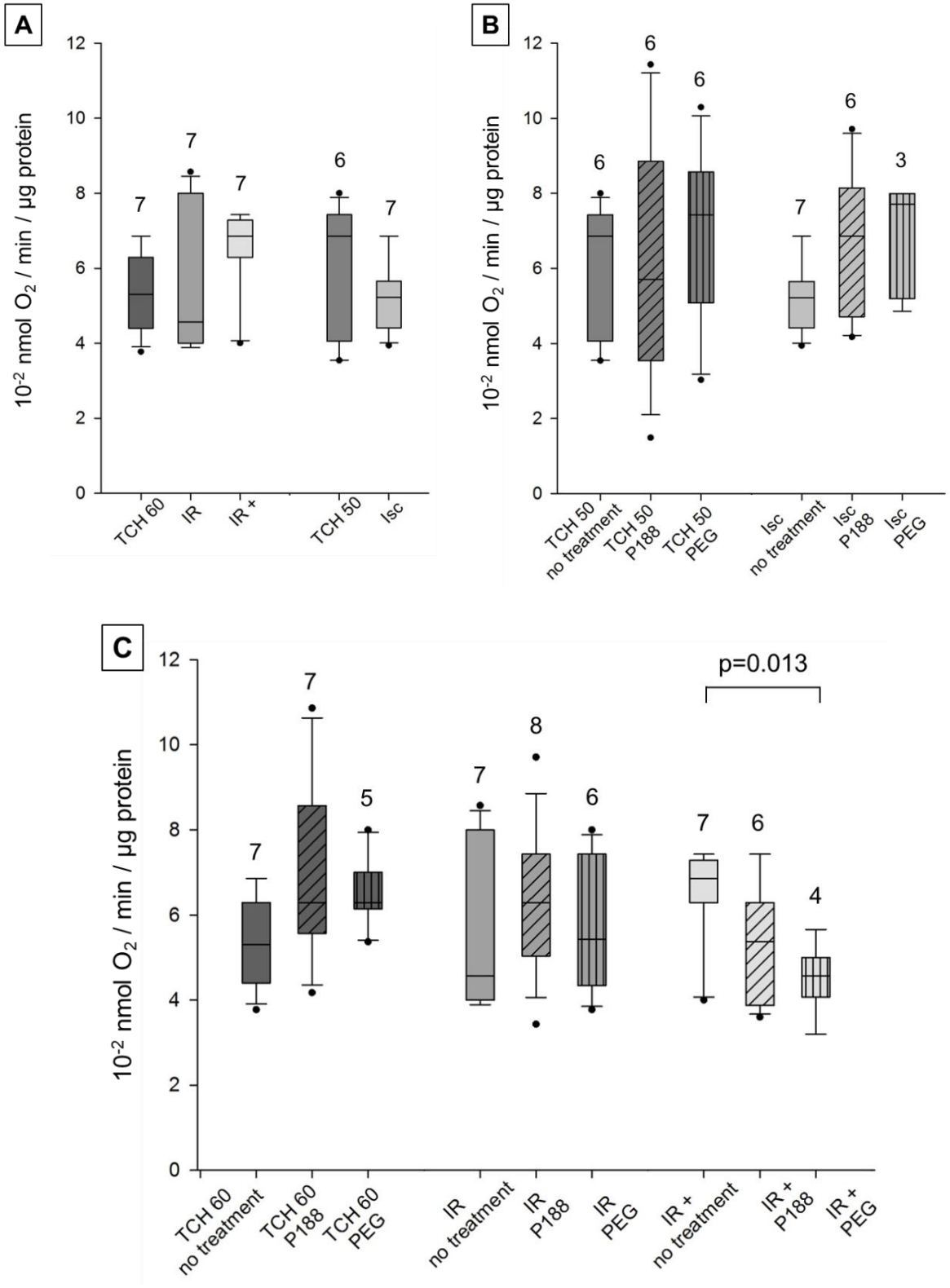

Figure 44: Mitochondrial respiratory state 4 (10^{-2} nmol O_2 / min / µg protein) with complex II substrate in isolated cardiac mitochondria. Mitochondria subjected to ischemia (Isc), ischemia reperfusion (IR), IR with P188 during reperfusion (IR+), only perfusion (time control hearts [TCH] 50 min and 60 min). **A**: Mitochondria isolated with isolation buffer (IB/ no treatment). **B**: Mitochondria isolated with no treatment, IB containing 1 mM P188 or 1 mM PEG for Isc and TCH 50 hearts. **C**: Treated and untreated mitochondria for IR, IR+ and TCH 60 hearts. N in duplicates. Brackets indicate statistically significant difference TCH dark grey, injured hearts lighter grey. Hatching shows mitochondrial treatment: no treatment (no hatching), P188 (diagonal lines), PEG (vertical lines).

4.2.3. Mitochondrial Calcium Retention Capacity

Complex I

Mitochondrial CRC was similar in time controls (TCH 50, TCH 60) and injured hearts (Isc, IR, IR+) with complex I-specific substrates pyruvate and malate (Fig. 45A, p. 58). When compared to Figure 46 (p. 59), CRC was lower in all groups for complex I than complex II. CRC increased with mitochondrial PEG treatment compared to no-treatment in TCH 50, Isc and IR groups (Fig. 45B, C; p. 58). Additionally, mitochondrial PEG treatment increased CRC significantly compared to P188 in Isc hearts. P188 treatment did not improve or damage membrane integrity with complex I specific substrates in all groups.

Complex II

As mentioned above, CRC was higher in complex II experiments than complex I. Accordingly, damage to the heart did show decrease in mitochondrial membrane integrity. However, CRC was only reduced in Isc but not IR and IR+ groups compared to time controls in no-treatment mitochondria (Fig. 46A, p. 59). This concludes that IR injury could not be observed in this assay. Mitochondrial treatment consistently showed no statistically significant difference in TCH60, Isc and IR. However, PEG treatment significantly increased CRC compared to no-treatment mitochondria in TCH 50 (Fig. 46B, p. 59) with a similar, not significant, trend observable in TCH 60 (Fig. 46C, p. 59). As seen in Figure 46C (p. 59), CRC was reduced in mitochondria treated with PEG compared to P188 in IR+. Finally, neither ex-vivo nor mitochondrial P188 treatment showed a significant effect in either group.

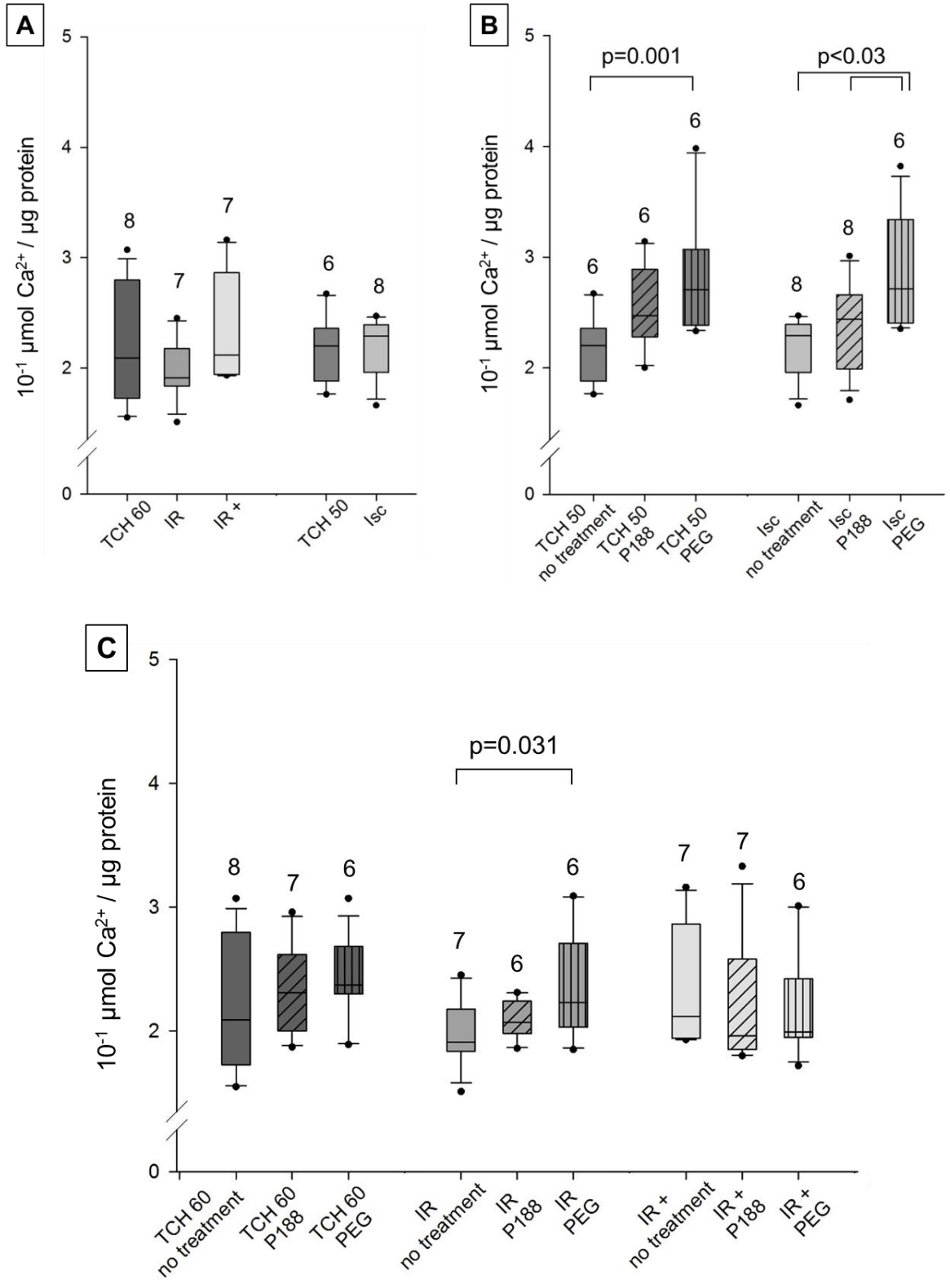

Figure 45: Mitochondrial calcium retention capacity (CRC) (10^{-1} µmol Ca^{2+} / µg protein) with complex I substrates in isolated cardiac mitochondria. Mitochondria subjected to ischemia (Isc), ischemia reperfusion (IR), IR with P188 during reperfusion (IR+), only perfusion (time control hearts [TCH] 50 min and 60 min). **A**: Mitochondria isolated with isolation buffer (IB/ no treatment). **B**: Mitochondria isolated with no treatment, IB containing 1 mM P188 or 1 mM PEG for Isc and TCH 50 hearts. **C**: Treated and untreated mitochondria for IR, IR+ and TCH 60 hearts. N in duplicates. Brackets indicate statistically significant difference TCH dark grey, injured hearts lighter grey. Hatching shows mitochondrial treatment: no treatment (no hatching), P188 (diagonal lines), PEG (vertical lines).

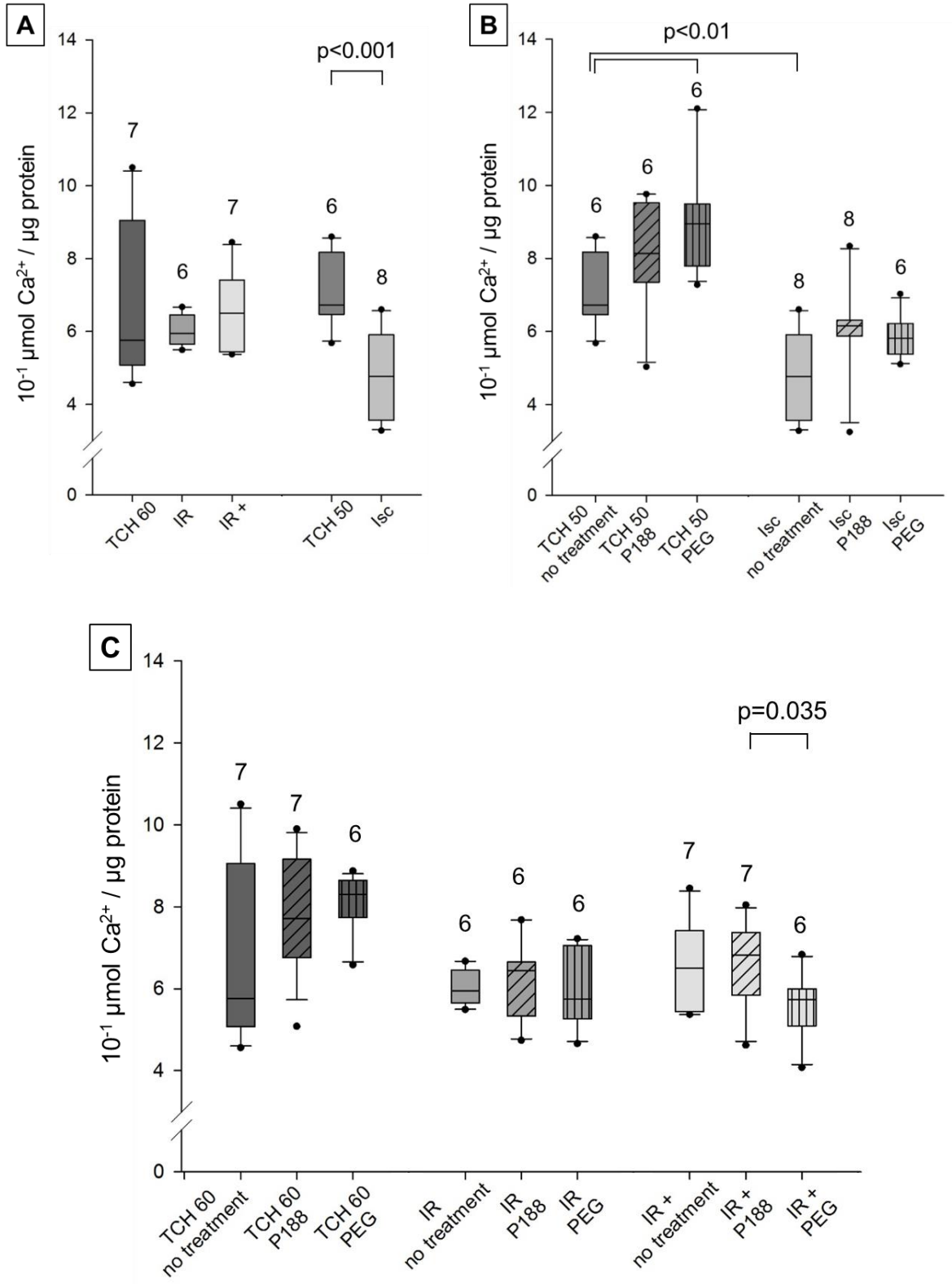

Figure 46: Mitochondrial calcium retention capacity (CRC) (10^{-1} µmol Ca^{2+} / µg protein) with complex II substrate in isolated cardiac mitochondria. Mitochondria subjected to ischemia (Isc), ischemia reperfusion (IR), IR with P188 during reperfusion (IR+), only perfusion (time control hearts [TCH] 50 min and 60 min). **A**: Mitochondria isolated with isolation buffer (IB/ no treatment). **B**: Mitochondria isolated with no treatment, IB containing 1 mM P188 or 1 mM PEG for Isc and TCH 50 hearts. **C**: Treated and untreated mitochondria for IR, IR+ and TCH 60 hearts. N in duplicates. Brackets indicate statistically significant difference TCH dark grey, injured hearts lighter grey. Hatching shows mitochondrial treatment: no treatment (no hatching), P188 (diagonal lines), PEG (vertical lines).

5. Discussion

Cardiac IR injury consists of a primary ischemic injury as well as a secondary reperfusion injury that exacerbates tissue damage [9]. Notwithstanding, any amount of cardiomyocytes salvaged through reperfusion is invaluable in limiting infarct size and long-term complications right up to heart failure [8]. Mitochondria sustain cardiac function but have also been shown as source and target of IR injury in the heart. This highlights the importance of treatment for reperfusion injury, e.g. through membrane stabilizers such as P188, to recover both cellular and mitochondrial function.

This study inflicted IR injury on rat isolated hearts and evaluated possible P188 effects during the clinically relevant time of reperfusion. Cardiac mitochondria were isolated and treated with P188 or PEG to assess direct mitochondrial protection. While a quantifiable ischemic injury was found in mitochondria, further deterioration of mitochondrial function after reperfusion was not. P188 did not consistently improve myocardial or mitochondrial function.

5.1. Myocardial Function

Myocardial function was measured in ex-vivo hearts during ischemia and reperfusion. As expected, myocardial function decreased in all injured groups equally during the ischemic period. However, this study showed no statistically significant improvement in diastolic and systolic pressure, developed LVP, contractility, heart rate, RPP or coronary flow by P188 post-conditioning.

Generally speaking, the first few minutes of ischemia are the time frame until mitochondrial OXPHOS is completely inhibited and the cell is switched over to anaerobic glycolysis entirely [7,12]. This is a turning point in cardiac injury, as the efficiency in ATP synthesis lags severely behind that of OXPHOS. Myocardial cells, especially, have a high turn-over in energy [12]. Correspondingly, the data in this study show that functional data such as the systolic pressure, devLVP, contractility and RPP are close to 0% bl after 3 min and after 5 min of ischemia the heart stops contracting.

Of all functional data collected, only systolic pressure returned to baseline levels during 10 min of reperfusion. Diastolic pressure increased with reperfusion, and all other variables improved compared to ischemia but did not reach baseline levels of time controls.

An abrupt rise in diastolic pressure at the beginning of reperfusion can be observed while contractile function hasn't recovered yet. This is expression of myofibrillar hypercontracture that contributes to lethal myocardial reperfusion injury [14]. The higher the diastolic pressure during reperfusion and the longer contractility is impaired, the more cellular damage results. Hearts with P188 post-conditioning show a trend towards lower diastolic pressure throughout reperfusion that is statistically not significant and does not reach time control levels. It is therefore unlikely that P188 post-conditioning prevents hypercontracture in this study. However, it is possible that the membrane sealing traits of P188 limit membrane rupture that ensues from it.

Hypercontracture is defined as the "forceful uncontrolled contraction" [12] that occurs upon reperfusion when the cell faces a drastic increase in cytosolic Ca^{2+} that develops during ischemia. At the same time, the cell is re-energized and the pH rises abruptly which leads to re-activation of the contractile apparatus [9]. Apart from a rise in diastolic pressure, this can also be seen as sudden spikes at the beginning of reperfusion in heart rate, devLVP, contractility and RPP. Due to the simultaneous contraction of all viable myocardial cells, membrane disruption ensues in the intact organ by virtue of the tight cell-cell-contacts. It is further enhanced by the already fragile cytoskeleton after the ischemic interval [9]. This is seen in the subsequent decrease in devLVP, contractility, HR and RPP and might be a first expression of irreversible damage. Other studies have shown that IR injury could be reduced by inhibiting the contractile machinery in the first few minutes of reperfusion [104–106].

The data of this study suggest that hearts reperfused with P188 might show a more even recovery. While not significant, P188-treated hearts had a trend towards better function for at least a period of time during reperfusion, e.g. contractility. This could imply a lesser extent of hypercontracture which might be beneficial in long-term outcome that was not investigated in this study. As hypercontracture leads to lethal reperfusion injury through membrane disruption, the cell could benefit from P188's membrane stabilizing properties when given over a longer period of time.

The RPP is an indication for myocardial workload and energy demand. By including HR and blood pressure, it correlates well with myocardial oxygen consumption and can be used to define the response of the coronary circulation to myocardial metabolic demands [107]. The high initial peak in RPP upon reperfusion shows an increase in myocardial energy demand which is higher in IR than IR+. However, untreated hearts

showed a steeper fall in energy demand and stayed below P188-post-conditioned hearts for the rest of reperfusion. Thus, the high energy demand in the first few minutes might actually exacerbate hypercontracture and damage, subsequently reducing energy demand through cell death.

Similarly, coronary flow also depicted a statistically non-significant trend towards a decrease in IR+ hearts for the whole duration of reperfusion. A lower cardiac output might actually lower the stress on the heart and could also be beneficial for long-term outcome.

In previous studies of ex-vivo IR models in the Riess laboratory, P188 post-conditioning has been shown to be cardioprotective in rats [78,79] when administered for 120 min during reperfusion. According to Watanabe et al. [108], P188 pretreatment is not only dose- but also time-dependent, and 10 min with 1 mM were not enough to show cardiac protection. This might very well be applicable to post-conditioning as well and could explain lack of protection of P188 on myocardial function in this model. However, this study's aim was to assess mitochondrial function, and hearts were taken out of the Langendorff apparatus after only 10 min of reperfusion to obtain values of mitochondrial function [109].

In conclusion, this ex-vivo model clearly shows IR injury but could not recreate the benefits of P188 on myocardial function from previous studies in rat and mice isolated hearts [31,78,79,89]. To elucidate whether P188 post-conditioning increases myocardial energy demand long-term, longer reperfusion periods would have to be investigated ex-vivo, as well as long-term outcome in in-vivo models.

5.2. Mitochondrial Function

Mitochondria from the ex-vivo heart were treated with P188 or PEG during the process of isolation and mitochondrial function was assessed in ATP synthesis, CRC and O_2-consumption. The results are very heterogeneous; thus, with a small sample size the data can only roughly point in one direction.

While a study from 2020 showed P188 to improve yield during isolation of cardiomyocytes [110], this study could not detect an increase in mitochondrial yield with P188 (data not shown).

Time controls (TCH 50 and 60) were verified against freshly excised hearts in a preliminary collection of data that is also not shown here. Mitochondrial function of TCH 60 and TCH 50 was compared to mitochondrial function of hearts that had not been connected to the Langendorff apparatus with no apparent differences. Thus, it was concluded that TCH 60 and TCH 50 are appropriate controls for the injured hearts in this study.

Mitochondrial function in IR groups throughout most assays showed a slight improvement compared to Isc groups. This might imply that, while cellular and functional damage is exacerbated during 10 min of reperfusion, it is not enough time for visible mitochondrial damage to occur. During IR, the initial damage occurs on a cellular level, which later compromises mitochondrial function. Mitochondria can exacerbate the cellular damage with ROS production, mPTP opening and the release of apoptotic factors. Irreversibility ensues due to membrane damage, ATP deprivation, loss of cellular ionic gradients, Ca^{2+}-overload and the resulting activation of proteases and phospholipases [17]. Moreover, energy of the remaining functional mitochondria boosts cellular injury through, e.g. hypercontracture [12]. This further shows that reperfusion is a double-edged sword and, while it is imperative to improve outcome after ischemia, it also has the opposite effect on a cellular level, making treatment of IR injury essential for better care [8].

Preliminary data from the Riess laboratory in isolated mitochondria from rat isolated hearts showed no direct mitochondrial protection after 1 h incubation with 100 µM P188 after isolation and concluded that P188 might only show a positive effect on mitochondria when given immediately upon reperfusion [89]. However, the current study also did not show direct protective effect on mitochondria when P188 or PEG were given immediately upon reperfusion. This could mean that any observed recovery of mitochondrial function is only an indirect effect of P188 derived from overall cellular protection.

5.2.1. Mitochondrial ATP Synthesis

Measuring the rate of ATP synthesis in a bioluminescent assay showed that the damage observed in myocardial function was also reflected in mitochondrial ATP synthesis. ATP synthesis in IR and Isc was significantly lower than in the respective time controls in both complexes. Generally speaking, and as evidenced by the data in

this study, ATP synthesis is lower during ischemia, compared to both time control and reperfusion. This is easily explained by ATP being synthesized only through anaerobic glycolysis and, additionally, by the ATP synthase starting to work in reverse and hydrolyzing ATP to keep up membrane potential [59].

P188 post-conditioning showed a non-significant trend towards improved ATP synthesis in complex II. Albeit the box plot indicated relatively heterogenous data, the median of IR+ was higher than IR and still lower than TCH 60. The reason that this was not mirrored in complex I could be that complex I is more vulnerable to acidosis [27] and a main source for ROS during IR [17]. This means that complex I is more easily uncoupled, and, while mitochondrial O_2-consumption recovers, ATP synthesis lags behind.

Surprisingly, the biggest impact of both mitochondrial treatments was observed in mitochondria from ischemic hearts. PEG significantly improved ATP synthesis in both complex I and II, while P188 only showed a trend to do so in complex I, but was significant in complex II. The higher osmolarity of the mitochondrial treatment might delay cell swelling and membrane disruption in, as of yet, reversibly injured cells just as hyperosmotic reperfusion has been shown to improve cellular function [111,112]. This could point towards mitochondria going through a reperfusion period of sort during the isolation process in which treatment might still be possible. A possible reperfusion activity was limited as far as possible by keeping mitochondria on ice for the whole duration of the isolation process. This finding could be promising for an approach in pre-conditioning with CCMS as has been shown to be beneficial by Watanabe et al. [108] as ischemic tissue might be susceptible to the membrane stabilizing abilities before the start of reperfusion.

P188 did not elicit a benefit in mitochondria subjected to IR injury, nor could an additive protective effect after both ex-vivo and in-vitro treatment be observed as was hinted at by William et al. [89]. To the contrary, a significant decrease in ATP synthesis in complex II was observed in IR+ mitochondria treated with additional P188 and a similar tendency, albeit not significant, was mirrored in complex I. This observation, though unsatisfactory, is not entirely surprising. Double P188 treatment might have caused an overload of P188 in the mitochondria, exceeding P188's critical micelle concentration [113]. A high concentration of the amphiphilic molecule leads to the formation of micelles which in turn reduces the concentration of free P188 molecules that are most

likely to provide protection [77]. This would have prevented P188 from showing a benefit on mitochondria. Moreover, P188 that has been improving cellular and mitochondrial function during reperfusion is also taken up into these micelles, interfering with the previous protective effect of P188 post-conditioning in complex II. PEG treatment does not have the same impact, because PEG does not share the amphiphilic character of P188 and, thus, does not form micelles with P188.

No differences between treatment groups could be observed in IR hearts. A bigger sample size might be able to assert whether P188 has a direct impact on mitochondrial IR injury but with the current set of data, this seems unlikely. Albeit disappointing, this matches recent findings by Pille and Riess in rat isolated brain mitochondria [88].

It should be mentioned that ATP levels take days to normalize after cardiac IR injury [17] and that recordings of ATP synthesis could look vastly different after a longer recovery period. This would require a more long-term in-vivo model and cannot be assessed with this ex-vivo model.

5.2.2. Mitochondrial O_2-Consumption

The kinetics of O_2 utilization during OXPHOS have first been described by Chance and Williams in 1955 [114]. They defined state 3 as a state with high extra-mitochondrial ADP levels and ATP synthesis, evidenced by high O_2-consumption. Concurrently, state 4 was defined as a state with low extra-mitochondrial ADP levels, no ATP synthesis and O_2-consumption corresponding solely to H^+-leakage [114,115]. In the experimental setting of this study, state 3 was initiated through addition of ADP which was transformed to ATP through OXPHOS, illustrated by a rapid O_2-consumption. State 4 was reached once all ADP was dissipated. RCI is calculated as the state 3 to state 4 ratio and is a measure of coupling of O_2-consumption to ATP synthesis. Preservation of RCI is crucial as it has been shown that respiratory dysfunction impedes cardiac recovery after prolonged ischemia [101].

ETC uncoupling is characterized experimentally by a decreased RCI through an increase in state 4 respiration. During uncoupling, the electrochemical gradient of the IMM dissipates, resulting in an increase in O_2-consumption without enhanced ATP synthesis [116,117]. This quickly drains the cell of energy and results in enhanced ROS production [46,61].

The collected data indicate damage in mitochondrial respiration after ischemia and IR compared to TCH. This is seen as a decrease in state 3 but not state 4 respiration that, in turn, leads to a decrease in RCI and is most likely linked to deterioration of respiratory substrate oxidation instead of uncoupling from ATP synthesis [17]. It can therefore be concluded that the RCI is a useful measure to judge mitochondrial damage and changes in mitochondrial O_2-consumption in this study.

As previously mentioned, all mitochondrial data were recorded with complex I- and complex II-specific substrates. In contrast to other researchers [38,118,119], mitochondrial respiration was not found to be particularly reduced for complex I compared to complex II substrates.

In line with previous findings of the Riess study group [89], P188 post-conditioning in the Langendorff heart model did not show improvement of RCI. There was even an inclination of a decrease in RCI after treatment with P188 (IR+) compared to IR. In this study, this was almost exclusively due to a bigger increase in state 4 than state 3 respiration in mitochondria of the post-conditioned hearts. This could suggest uncoupling of mitochondrial respiration due to P188 post-conditioning.

With intracoronary (i.c.) P188 application in a porcine model, Bartos et al. showed near total preservation of mitochondrial respiration through P188 treatment in complex I but not II [38]. The publication does not show whether those changes are mostly due to changes in state 3 or state 4 respiration. This information could be vital in determining whether P188 enhances RCI by enhancing coupling or increasing ATP synthesis and if H^+ leakage can be prevented by stabilization of the IMM by P188. It should be noted that the only prior studies on direct effects of P188 on mitochondrial function in-vitro [88,89] have not been promising so far.

As anticipated based on preliminary data [89], mitochondrial treatment with neither P188 nor PEG had an effect on RCI in TCH. Both P188 and PEG increased state 3 and state 4 respiration to a similar extent. Thus, any increase in ATP synthesis was also matched with a physiologically appropriate increase in H^+-leakage. In contrast, RCI decrease in ischemic hearts occurred primarily through a decrease in state 3 respiration. This was to be expected and has been described previously in mitochondria isolated from ischemic hearts, including rat hearts after 30 min of ischemia [17].

Mitochondrial treatment with P188 showed no impact on RCI in all injured groups and complexes. It is interesting to note that, while P188 increased state 3 and state 4 respiration in Isc and IR hearts, it decreased both states in IR+ hearts, leading to a similar outcome through a different route. It should also be taken into consideration that, due to a large increase in state 4 respiration in P188 post-conditioned hearts with no further mitochondrial treatment, the effects of mitochondrial treatment in state 4 of IR+ hearts are difficult to evaluate and leave no clear conclusion.

In contrast to P188, mitochondrial treatment with PEG decreased RCI by increasing state 4 respiration in injured hearts with complex I specific substrates, suggesting an increase in uncoupling of complex I that P188 did not show. Strangely, when assessed with complex II-specific substrate succinate, mitochondrial PEG treatment shows different results. While neither Isc nor IR showed an impact of PEG on RCI, state 3 and state 4 respiration were both increased in Isc, while they were not at all changed compared to no-treatment in IR hearts. This would suggest that the uncoupling through PEG treatment only occurs in experiments with complex I- but not complex II-specific substrates. This is most prominently displayed in a major decrease in state 4 respiration in IR+ hearts which lead to a slight improvement on RCI through mitochondrial PEG treatment.

There are still many unanswered questions about the gathered data that currently cannot be explained. For example, why does P188 lead to uncoupling when administered ex-vivo but not when isolated mitochondria were treated and why is uncoupling with PEG restricted to complex I?

5.2.3. Mitochondrial Calcium Retention Capacity

Increased mitochondrial Ca^{2+}-concentrations trigger opening of the mPTP which has been linked to mitochondrial dysfunction and is a major determinant of the extent of injury during reperfusion [53]. The CRC is defined as the amount of Ca^{2+} necessary to induce mPTP opening [101]. CRC is exceeded when mitochondria start to extrude Ca^{2+} through the mPTP which is an indication of loss of structural integrity [120]. It can therefore be used to monitor mitochondrial membrane integrity in isolated mitochondria.

First and foremost, mitochondria in all groups showed a much lower CRC with complex I- than complex II-specific substrates. Differences in CRC between complex I and II

have also been found by other study groups. Similar to the present results, Stowe et al. also showed a lower CRC for complex I than II substrates in both damaged and intact mitochondria [120]. In contrast, Bartos et al. showed complex I to be damaged to a greater extent during ischemia than complex II. In their study, the non-ischemic controls of complex I CRC exceeded that of complex II in all groups [38]. It is, as of yet, unknown why the extent of CRC is so divergent for substrates feeding into these two complexes.

In this study, complex I substrates showed no difference between TCH and injured hearts, making this assay inconclusive for documenting IR injury in complex I. A possible explanation might be the aforementioned vulnerability of complex I that lead it to be damaged beyond repair in the isolated heart and mitochondria, leaving no room for further damage to be revealed in this assay. Complex I's vulnerability to acidosis and oxidative damage is also linked to the fact that inhibition of complex I activity upon exposure of mitochondria to ROS is one of the earliest ischemia-induced alterations in mitochondrial function. This may be a cardioprotective reaction to limit Ca^{2+}-overload and ROS production during reperfusion [12,17]. Incidentally, injured, healthy and P188-treated mitochondria showed no difference in a similar assay in isolated mitochondria from a rat brain [88].

In contrast to complex I, ischemic – but not IR – injury could be observed in complex II. This is most likely due to the short reperfusion period of this study in which the benefits of reperfusion could still outweigh its cost. While the mitochondria are already deteriorating – as seen by impairment of specific functions like ATP synthesis and mitochondrial respiration – mitochondrial structural integrity might not yet be compromised.

An interesting trend observable in TCH 50, TCH 60 and Isc mitochondria showed slight, though non-significant, tendency of improvement of CRC with P188 treatment and a significant increase with PEG treatment in complex I. These are the groups most likely to have unruptured membranes. However, the process of removing the heart from the Langendorff set-up and isolating the mitochondria leaves opportunity for damage to cells and cell organelles to occur. Hyperosmotic reperfusion has been shown to limit myocardial injury during reperfusion [9] by limiting the osmotic stress on the cell. Even though the mitochondrial isolation buffer closely resembles iso-osmotic proportions, a slight osmolarity wash-out might still occur during the resuspension of

tissue in buffer leading to cellular dysfunction. The subsequent swelling of the mitochondria can then induce membrane disruption. A hyperosmotic solution limits water influx into cell and organelle by limiting the osmotic gradient. Thus, P188's and PEG's effect on mitochondrial membrane integrity might be due to a decrease in osmotic stress on the mitochondria. It is less clear, why P188 shows less of an increase, though it might also be related to micelle formation. Again, a momentary observation of improved membrane integrity does not necessarily protect specific functions, explaining why the same trend cannot be found in the other assays.

Conversely, IR and IR+ hearts are most likely to show membrane damage at the end of the ex-vivo experiment [9,26,27]. A hyperosmotic solution might actually exacerbate injury of cells and organelles with already damaged membranes by creating water efflux. This would explain deterioration of CRC after mitochondrial PEG treatment in IR+ hearts compared to P188 treatment in complex II studies. In contradistinction, there is no decrease in CRC with mitochondrial P188 treatment, possibly as a result of the membrane sealing capacity of P188, notwithstanding the higher osmolarity.

There are little to no previous studies available to compare these results to. Bartos et al. injected P188 i.c. in-vivo early upon reperfusion and improved CRC but did not see similar results with PEG or delayed P188 treatment [38]. Similar to our own model, isolated brain mitochondria could also not mirror the promising beneficial effects of P188 on CRC [88]. We did show, however, an improvement of ischemic and non-damaged mitochondria with mitochondrial PEG treatment and, albeit less so, P188 treatment. This improvement was only partly echoed in IR and not at all in IR+ hearts.

As mentioned before, we cannot yet sufficiently explain all presented results. Further studies on the specific mechanisms of action of P188 on mitochondrial and cellular membrane are crucial to fully understand how – or if at all – it can be established as a viable treatment option of IR injury. It is unlikely in this scenario, that P188 or PEG lead to a decrease in Ca^{2+} sensitivity of the mPTP which has been identified as a mechanism in ischemic pre- and post-conditioning to increase mitochondrial resistance to Ca^{2+} overload [121,122].

5.3. Study Context

5.3.1. Therapeutic Strategies against Cardiac IR Injury

Prompt reperfusion by PTCA, thrombolytics or cardiopulmonary resuscitation (CPR) continues to be the only method to reduce ischemic damage and improve outcome after cardiac IR injury. It is, therefore, a crucial part of clinical guidelines [123] and has helped decrease the mortality of CHD in the last decades in high-income countries [2,5]. However, the ESC guidelines demonstrate an obvious lack in recommendations for treatment of the secondary injury caused by reperfusion. As mentioned before, promising efforts have been made to reduce IR injury with ischemic pre-, and post-conditioning [32–35,101]. However, other approaches to therapeutic strategies are currently being investigated.

Moderate hypothermia has shown promising effects on neurologic recovery in patients after traumatic brain injury (TBI) in several observational and phase II clinical studies, as well as on neurological outcome after cardiac arrest [124,125], and external cooling can reduce IR injury of skeletal muscle in a pig model [126]. In cardiac injury, hypothermia has shown beneficial outcomes in infarct size, myocardial function and the no-reflow phenomena in models of acute MI in multiple animal models [125,127–129]. This could not be observed in clinical studies so far. It should be noted that most protocols failed to reach the target temperature of 33 °C in patients at the onset of reperfusion [127]. It is also well established, that the benefit of hypothermia decreases significantly with delay and no benefit is shown when hypothermia occurs after reperfusion, making this a difficult approach to implement in a clinical setting [127].

A more viable advance has been made in regards of pharmaceutical intervention, and the impact of anesthetics especially, has been studied for a long time [130]. While not all mechanisms are yet fully understood, it seems that the positive effects are not solely due to their hemodynamic effects but also due to interventions at specifics steps in the pathomechanism of IR. Halothane, for example, has shown protective effects against myocardial IR injury in isolated cardiomyocytes, as well as in ex-vivo rat hearts and in-vivo rabbits by Schlack et al. back in 1997 [131]. More recently, Riess et al. [102] have shown improvement of myocardial dysfunction, and preservation of mitochondrial function with the more timely anesthetic sevoflurane in a pig model of prolonged cardiac arrest. Building on that, Bartos et al. have shown in another pig model of

cardiac arrest that a bundle therapy of stutter CPR, impedance threshold device, sevoflurane, and P188 improves cardiac and neurologic function after 17 min of untreated cardiac arrest in pigs [132]. Halogenated anesthetics, especially, could prove to be vital in improving outcome after cardiac IR injury because of the simplicity in which they could be used, e.g. during out-of-hospital CPR, compared to i.v. administered treatments [102].

For a long time, ROS were believed to be the most significant culprit of reperfusion injury. It has since been established, e.g. by Martindale et al. [31], that oxidative stress alone does not warrant IR injury, so long as membrane integrity is preserved. Nevertheless, free radical scavengers like edaravone [133,134] and antioxidant vitamins like vitamin C [135] are being studied for potential benefits on cardiac IR injury, though with varying degrees of success. Excessive ROS production is still undoubtedly a vital part of mitochondrial IR injury, therefore, mitochondrial-targeted antioxidants could prove promising in the future [28], as could other treatments targeting mitochondria, like CsA [36,37] or CCMS like P188 [31,38,77,87].

5.3.2. Effect of P188 on Cardiac IR injury

Membrane damage is a crucial pathomechanism of IR injury in the heart, and, therefore, membrane stabilization has to be considered when reviewing possible treatment approaches. While several mechanisms of endogenous membrane repair have been discovered, such as dysferlin (*dys*), mitsugumin 53 and thrombospondin 4, these intrinsic pathways are too slow to prevent the lethal complications of large-scale membrane rupture [136]. For this reason, exogenous CCMS like P188 have been evaluated as a treatment option.

Not many in-vitro studies have looked at P188 treatment specifically in a model of cardiac IR injury in isolated cardiomyocytes. There are a few studies examining IR injury in myocytes in striated muscle cells as well as in dystrophic cardiomyocytes like an in-vitro model of Duchene Muscle Dystrophy by Yasuda et al. that has shown P188 to successfully salvage tears in the membrane of dystrophin deficient isolated cardiomyocytes at a concentration of 150 µM [137].

More recently, studies have been conducted subjecting non-dystrophic cardiomyocytes to IR injury. In 2014, Martindale et al. [31] used cells isolated from adult rat ventricles to show P188 in dosages of 1 and 10 µmol/L preserving membrane

integrity after the cells had been subjected to 40 min of ischemia and 1 h of reperfusion without altering the cellular redox state. The authors concluded that an altered redox state is not sufficient to cause IR injury as long as membrane integrity is preserved by CCMS such as P188. Pretreatment with P188 did not show the same benefit, possibly due to wash-out during reperfusion, reinforcing that membrane stabilizers are most useful in the state of reperfusion where membrane damage is thought to majorly occur.

Drawing on these findings, Salzman et al. [77] published their research on a model of IR injury in isolated cardiomyocytes from adult male mice in 2020. They used concentrations from 10 µmol/L to 1 mmol/L of P188 and PEG on cells after 5 h of hypoxia and 2 h of reperfusion. P188 improved cell viability and membrane integrity and reduced Ca^{2+}-influx in injured cells in a dose-dependent manner with a dosage optimum between 100-300 µmol/L while showing no adverse effects on uninjured cells. PEG in the same dosage did not reflect those results. From these findings it can be inferred that the hydrophobic part of P188 is vital for its ability to seal membranes in IR models of isolated cardiomyocytes.

Another interesting study from 2020 found that 150 µmol/L P188 administered during the cannulation process of the Langendorff preparation before primary isolation of rat cardiomyocytes improved survival of the isolated cell without impairing cellular function [110]. The author attributed this to P188's protective effects on the membrane after the short ischemic insult during the Langendorff preparation. It should be noted that P188 did not improve long-term survival of the isolated cell compared to the normal isolation process, which is congruent with the knowledge that P188 squeezes out of the cell after repairing it [85] and can provide no additional benefit other than short-term membrane stabilization.

An important hallmark in experimental cardiac IR injury is the formerly described Langendorff heart model [39,40]. The Riess study group has previously demonstrated P188's ability to salvage myocardial function and reduce infarct size in mice, BN and SS rats [78,79]. The hearts of SD rats used in this study are intermediate in their susceptibility to IR injury in the heart compared to the resilient BN and much more sensitive SS hearts.

Building on these findings, this study administered P188 in a concentration of 1 mM after 20 min of stabilization and 30 min of ischemia. Unlike previous studies that

reperfused the hearts for 120 min, these hearts were taken out of the Langendorff apparatus after only 10 min of reperfusion to conduct mitochondrial experiments before mitochondria were damaged beyond repair. Because of this short reperfusion period in which P188 could work, it is not as surprising that we could not find significant difference between our IR and IR+ groups in myocardial function.

Others, like Martindale et al. [31], have shown improvement on LV function with P188 after 15 min of ischemia and 60 min of reperfusion in both wild type (C57BL/10) and *dys*-deficient mice as a model of cardiomyocytes with impaired sarcolemmal integrity. However, Evans et al. [138] conducted a similar experiment and, while they did show significant improvement with P188 on *dys*-deficient mice, they did not confirm the findings of Martindale et al. in wild type mice. Dissimilar to the model presented here, Evans et al. used a much lower dose of P188 (10 µM) and administered the treatment both during the 20 min stabilization, as well as the 60 min reperfusion period.

Another interesting approach to simulating IR injury in an ex-vivo model that uses P188 pre-treatment has been done by Watanabe et al. in 2003 [108]. The authors pre-conditioned hearts from SD rats with 1 mM for 30 min, followed by a 5 min wash-out, 15 min of perfusion with lysophosphatidylcholine (LPC) and another 20 min wash-out (= reperfusion). LPC accumulates during ischemia because of increased formation from and decreased conversion into phosphatidylcholine. When applied exogenously to the heart, it creates an injury similar to the one observed during IR. Watanabe et al. have shown that LPC creates membrane disruption that is attenuated with P188 pre-conditioning with 1 mM for 30 min. In adaptations of their own protocol they also tested a lower dose (0.24 mM P188 for 30 min) and a shorter time period (1 mM P188 for 10 min) both of which did not prompt similar results. Therefore, it can be surmised that P188's effect is dependent on both time and concentration, at least when used as a pre-treatment. This emphasizes the assumption that 10 min of reperfusion (post-conditioning) with P188 would not be able to salvage myocardial function either.

As compelling as the pre-conditioning approach is, we have deliberately avoided pre-treatment in our study because of the much more clinically appropriate scenario of cardiac IR injury where treatment only becomes available right around the time reperfusion can occur through PTCA or thrombolysis.

The first recorded in-vivo study of P188 in myocardial IR injury was conducted by Justicz et al. in 1991 [139]. The authors tested effects of P188 (48 mg/kg), mannitol and a combination of both on a dog model. After occlusion of the left anterior descending (LAD) coronary artery, treatment was introduced i.v. during the last 15 min of ischemia. The treatment was also given for an additional 45 min during reperfusion and the animals recovered for 24 h before the hearts were harvested. Both P188 and mannitol reduced infarct size by about 50 % individually with another slight decrease when used jointly. The authors also reported a reduction of “distortion of myocardial cell architecture” and largely eliminated contraction band formation with P188 which would be evidence for its cytoprotective effects.

However, when Schaer et al. [82] used a very similar model with a much longer reperfusion period with a P188 bolus (75 mg/kg) administered i.v. at the same time point and then again as continuous i.v. perfusion (150 mg/kg/h) for 4 vs 48 h, they found a reduction of only 25 % in infarct size in the 4 h group but a 42 % reduction in the 48 h group. They surmised that additional injury must occur between 4 and 48 h after reperfusion. It is possible that the difference in concentration, compared to Justicz et al., might have played a role as well.

Moreover, it is highly unlikely that treatment given i.v. during an ischemic period would reach the site of injury in an adequate amount. Peripheral P188 administration has been shown to be less effective than direct intracoronary application [38], much less when there is no blood flow to distribute the drug to the tissue. That is most likely a reason for failure of a follow up study by Kelly et al. [140] in a dog model of prolonged ischemic injury with 3 h of ischemia and 3 h of reperfusion. A P188 bolus (75 mg/kg, i.v.) was given after 1 h of ischemia and a continuous i.v. infusion (150 mg/kg/h) for the last 2 h of ischemia and all throughout reperfusion. They found no increase in collateral blood flow and LV function, nor reduction in infarct size. However, P188 most likely only reached the site of injury with start of reperfusion after 3 h of ischemia and, given that it is only able to seal small tears in the sarcolemma [137] not the massive damages 3 h of no-flow ischemia would have created, it is possible that there simply was not enough left for P188 to salvage.

The rodent and porcine models of recent years have mostly focused on shorter ischemic intervals, as pre-hospital and “door-to-balloon”- time have also been greatly reduced in the last decades [3].

Martindale et al. [31] showed reduction in infarct size and serum cardiac troponin after 30 min ischemia and a 24 h recovery period (= reperfusion) with an i.v. 460 mg/kg P188 infusion in a rodent model. Still, when Evans et al. [138] adapted their protocol to account for chronic treatment in wildtype and *dys*-deficient mice, they found no benefit on infarct size or LV function after two weeks of intraperitoneal P188 injections. The authors suggested that P188 might have been taken up by macrophages which would have lessened its bioavailability in the infarct zone and reduced beneficial effects of the treatment. As of right now, there is only one in-vivo study of P188 long-term effects in a cardiac model. More advances need to be made to find out if different forms of application could increase bioavailability and, just as importantly, whether one-time applications of P188 have long-term beneficial effects on cardiac function and infarct size.

Two promising, albeit both short-term studies, have been done in porcine STEMI models by Sarraf et al. [81] and Bartos et al. [38]. Although injury mechanism and reperfusion time (4 h) were identical and ischemic periods were similar (40 min vs 45 min), the application of P188 was vastly different. Sarraf et al. [81] administered an i.v. bolus of P188 (10 mg) immediately after balloon deflation and continued with a systemic infusion of 250 mg/kg of P188 over 4 h. They reported reduction in infarct size, though area at risk and LV mass showed no difference to control.

Bartos et al. [38], on the other hand, used a different approach with the objective to compare immediate and direct P188 application with delayed and peripheral application, in imitation of the Collaborative Organization for RheothRx Evaluation (CORE) trial [83]. One intervention group was injected an i.c. bolus of P188 (250 mg/kg) immediately upon reperfusion with continued i.c. infusion of P188 (bolus) for the duration of reperfusion. The other invention, similar to the CORE trial, were administered P188 (250 mg/kg, i.v.) starting 30 min after initiation of reperfusion and for the remainder of it. The findings were clear: immediate i.c. P188 treatment reduced infarct size by 68 %, while delayed, peripheral P188 application showed no difference to saline control. It has become apparent, that delivery route and timing of treatment, as well as dosing are crucial in the beneficial effects of P188 on IR injury in the heart.

5.3.3. Effect of P188 on Mitochondrial IR Injury

Mitochondrial injury and dysfunction has long been identified as a crucial part of cell death in IR injury [12,57,87].

In one of the first study of its kind, Bartos et al. [38] isolated cardiac mitochondria from pigs after they underwent 45 min of endovascular occlusion, followed by 4 h of reperfusion. During reperfusion, pigs were treated with either prompt i.c. P188 vs PEG vs saline infusion or a delayed i.v. P188 infusion 30 min after initiation of reperfusion. Mitochondrial function, as assessed via O_2-consumption and CRC, improved significantly after prompt. i.c. P188 reperfusion compared to both PEG and saline control but also delayed peripheral P188 application, shedding new light on the unfavorable outcome of the CORE trial [83] which will be addressed in the next chapter.

While promising, this in-vivo study was not able to elucidate a clear mechanism of action of P188 and whether these effects are due to a direct impact on mitochondria or due to a more generally cytoprotective effect.

A key role of mitochondrial injury during IR lays in the activation of the intrinsic apoptotic pathway wherein pore-formation in the OMM through Bax-protein leads to dissipation of mitochondrial membrane potential and release of cyt c into the cytosol which, together with caspase 9, forms the apoptosome and initiates cell death [141].

In neuronal in-vitro models P188 has been shown to attenuate ischemia-induced dissipation of mitochondrial membrane potential [86,141,142], translocation of Bax to the OMM [87,142], cyt c release [86,87,141,142], as well as improve mitochondrial morphology on light microscopic levels [87]. It did also directly interact with the OMM to inhibit mitochondrial outer membrane permeabilization (MOMP), thereby intervening at and inhibiting the intrinsic apoptotic pathway, as well as excessive autophagy activation that has been shown to be relevant in disproportionate cell death in in-vitro and in-vivo stroke models [86]. MOMP inhibition has also been appertained to direct P188 interaction with the isolated rat cortical mitochondria by Wang et al. [87].

Nonetheless, Shelat et al. [142] have shown almost identical benefits with prompt vs delayed P188 treatment 12 h after occurrence of ischemia in an in-vitro stroke model. Considering that the intrinsic apoptotic pathway is initiated in the first few hours after ischemia, the authors suggest that P188 arrests ongoing apoptosis by modulating other pathomechanisms upstream of MOMP. It should be noted that those experiments

were done in isolated cells which might have camouflaged direct interaction with the mitochondria.

In recent years, a few studies have been conducted with isolated mitochondria to determine direct mitochondrial protection of P188.

A study by Pille and Riess [88] could not duplicate the benefits of P188 in rat isolated brain mitochondria that Wang et al. [87] reported. Tests for mitochondrial function (CRC, ATP synthesis and O_2-consumption) did not improve upon treatment with 250 µM P188 during reperfusion. However, the study designs vary. While Wang et al. selectively created MOMP through tBID application, both the in-vitro application of H_2O_2 and in-vivo asphyxiation described by Pille and Riess touched on a much broader range of mechanisms of IR injury. The authors suggest that the attenuation of MOMP through P188 treatment might not be enough to explain the outstanding improvement of mitochondrial function reported by Bartos et al. [38].

The present study also used a complex injury mechanism that would very closely resemble in-vivo IR injury by subjecting the ex-vivo isolated rat heart to 30 min of ischemia with 10 min of reperfusion. In contrast to Pille and Riess [88], the mitochondria were subjected to both the ischemic injury and reperfusion before they were isolated. This way, we tried to account for mitochondrial damage that might only occur in the intact cell and organ. Similarly to Pille and Riess, an improvement with P188 treatment in the isolated mitochondria could not be found, possibly supporting the theory of other cellular mechanisms playing a crucial part in providing mitochondrial protection.

The concentrations of P188 also varied in previous studies. Wang et al. conducted studies with P188 concentrations from 1 µM to 100 µM and reported the most consistently positive effects with 30 µM, a decrease in MOMP inhibition with 100 µM and no effect below 10 µM [87]. Pille and Riess, who used 250 µM P188 on the isolated mitochondria, suggested that, at higher concentrations, P188 counteracts its own positive impact by partially damaging mitochondria [88]. However, previous data from the Riess study group closely resembling this current study incubated mitochondria in 100 µM P188 after isolating them from an ex-vivo rat heart subjected to IR injury (also 30 min ischemia, 10 min reperfusion) and found no improvement of mitochondrial function, as assessed by ATP synthesis and O_2-consumption, compared to PEG or no

treatment [89]. According to the study by Wang et al. [87] we would have at least expected a slight improvement on mitochondrial function.

The aforementioned study in the Riess lab did, however, show a non-significant trend towards an additive protective effect on ATP synthesis by P188 administration after pretreatment with P188 or PEG [89].

In our study, mitochondria were treated with 1 mM P188, the highest dose of all previously published studies in isolated mitochondria but still in the range of subcritical micelle concentration [113]. Similarly to William et al. [89], it is also the same concentration used in the ex-vivo heart, providing the opportunity to examine whether the reported additive protective effect could be replicated and/ or augmented – which it could not. Nor was a damage to the mitochondria found after mitochondrial P188 treatment.

It is exceedingly clear that more dose-finding studies need to be conducted with P188 on isolated mitochondria, preferably after being subjected to complex IR injury as would occur in the live organ.

Another difference between studies is time until treatment. Both Pille and Riess [88] and William et al. [89] added treatment after isolation of mitochondria whereas this study included P188 treatment into the isolation buffer. This way, mitochondria were exposed to treatment at the earliest possible time, taking into consideration the observation made by Bartos et al. that delayed P188 showed no benefit in mitochondrial function after in-vivo IR injury [38]. Additionally, William at al. [89] incubated mitochondria for 1 h on ice before starting testing for mitochondrial function, potentially giving the isolated mitochondria time to deteriorate in function before it could be assessed [143]. We tried to take into account the potential time-dependent decline in mitochondrial function by rotating the order in which the assays were conducted, as the three assays back-to-back could take between 2 and 3 h to be completed.

A very interesting observation Pille and Riess [88] made, is the detrimental effect of prolonged exposure to room temperature on the isolated mitochondria. Mitochondrial ATP synthesis was significantly decreased after 20 min of room temperature compared to 10 min of incubation at room temperature in all of their groups. An observation also made by Kleinbonga et al. [144] in isolated cardiac mitochondria comparing mitochondrial respiration after 9 min exposure to room temperature compared to

baseline sample. This could have obscured potential effects of P188 that would have been visible on healthier mitochondria. Accordingly, it was ensured here that mitochondria were kept on ice until experiments began.

Neither this study, nor the ones conducted by Pille and Riess [88] and William et al. [89] could show a direct protective effect of P188 on the isolated mitochondria in different study models. However, P188 has been shown to be active at mitochondrial membranes in neurons [87]. MOMP, as well as the breakdown of mitochondrial membrane phospholipids [17] are crucial steps in the pathway to irreversible injury of the cell and, thus, CCMS and other membrane stabilizers should be further investigated.

5.3.4. P188 in the Clinical Context

As P188 has been FDA approved for more than 50 years, there are quite a few clinical studies in which it has been tested on patients with acute MI making use of a variety of formerly described qualities such as: the reduction in blood viscosity and red blood cell aggregation, its synergism with fibrinolytic drugs, its ability to reduce thrombotic coronary occlusion after arterial injury and stent implantation in a porcine model, and its positive impact on IR injury [82]. Only later came the discovery of its potential as membrane stabilizer [136].

In a study by Schaer et al. that used P188 as an adjunct to thrombolysis in patients with suspected MI, a reduction in infarct size and an improvement of LV function with a subsequent lower incidence of reinfarction was shown [82]. A study by O'Keefe, using the same dosages, could not show a similar benefit when using P188 adjunct to PTCA [145]. Another study from Maynard et al. in patients not eligible for either thrombolysis or PTCA could not find a decrease in infarct size either and even demonstrated a lower LV ejection fraction [146]. However, these patients were generally older than in all other studies and had, presumably, longer medical histories. Taken together, these studies suggest that benefit of P188 during reperfusion after MI could depend on its synergism with the fibrinolytic agents used during thrombolysis.

The much cited CORE trial [83], a phase II open label clinical trial with nearly 3,000 patients, could not find a benefit of P188 administration after initiation of reperfusion. The treatment was only started with a certain delay and it has since been established by Bartos et al. [38] that P188 only helps prevent IR injury when administered

immediately upon reperfusion and that delayed as well as peripheral P188 rapidly reduces potential benefits. I.c. application presents with the additional benefit of a more limited effect on other organs, e.g. kidneys.

P188 is renally cleared with an elimination half-life of about 5 h [82] and its safety has been tested repeatedly. Especially studies pre-1996 showed varying results. While Maynard et al. had to terminate their study prematurely due to the occurrence of acute renal dysfunction [146], Schaer et al. reported a reversible increase in serum creatinine levels in some but not all patients [82]. This was most notably in patients aged 65 years and older and in those with elevated creatinine levels at baseline [83]. These effects were dose-dependent. It has since been found that using a purified version of P188 drastically reduces these adverse effects on renal function, making P188 a generally safe substance to use in a clinical setting for up to 72 h [64,136,147,148].

5.3.5. Effect of PEG on IR injury

PEG (8,000 Da) is used in this study, as a basic osmotic control to ensure possible effects observed with P188 do not solely rely on its osmotic properties. It has previously been shown, that PEG does not exhibit the same benefit as P188 after IR injury at the same concentration in isolated myoblasts [149,150], cardiac myocytes [31,77], isolated neurons [87] and an in-vivo pig model of myocardial infarction [38]. This has led to the conclusion that the hydrophobic PPO block that is inherent to P188's triblock structure, but not to PEG, is essential in membrane stabilization. To exclude possible rheologic effects, previous studies have reported that PEG and P188 have the same effects on post-ischemic blood viscosity [38,151] and viscosity in aqueous solution [151].

However, high-molecular-weight PEG (15-20 kDa) has been shown to be cardio-protective [152–154], to prevent ischemia-induced cell swelling in liver tissue [155] and after hemorrhagic shock [156,157]. PEG with a molecular weight of 35 kDa has even been shown to reduce mitochondrial injury after prolonged ischemic injury in an isolated perfused rat liver [158]. This is attributed to PEG acting as a cell-impermeant and a colloidal molecule that increases perfusion pressure and, thus, organ perfusion, e.g. after cardiac arrest [159]. PEG-20k has shown improvement of myocardial and cerebral function, as well as duration of survival after return of spontaneous circulation (ROSC) after cardiac arrest [154,157,159] and presents as a novel therapeutic agent to improve outcome after cardiac IR injury. When administered pre-hospital, the

quicker repayment of the oxygen debt, lactate clearance and re-establishment of oxygen transfer under low volume conditions could safely prolong the time until in-hospital treatment [160].

Establishing this has not been the aim of the current study and, thus, the molecular-weight and concentrations of PEG administered were too low to observe cardiac protection.

5.4. Study Limitations

This study needs to be interpreted within its natural constraints. Potential limitations are: 1) the ex-vivo animal model used cannot fully mirror cardiac IR injury in patients; 2) the time periods of ischemia as well as reperfusion; 3) dosage of P188; 4) end-point assays used to assess mitochondrial function; and 5) the statistical tests used for data analysis.

1) This study used healthy male rodents without the underlying comorbidities and medication that patients usually present with. The latter are confounding factors that might influence cardiac injury as well as protection, as is the fact that the situation evaluated was of acute rather than chronic nature which might alter tissue response. The isolated heart model removes the organ from its natural habitat which might result in a temporary shock and excludes physiological modification through hormonal and neuronal input. However, time controls were validated by testing mitochondrial function of freshly excised hearts in advance, and one of this model's benefits is actually the possibility to look at tissue reaction without extra-cardiac stimuli.

Compared to IR models of isolated myocardial cells, the Langendorff model allows to observe pathophysiological models in an intact, functional organ with all cell types essential in the organ's response to injury instead of only one cell type without its physiological context.

2) No further studies on longer reperfusion times were done. Ischemic injury presents differently than reperfusion injury which is strongly associated with membrane damage. With insufficient reperfusion time, P188's beneficial effect might not have been observable on myocardial function; this short-coming had to be accepted for the sake of generating data for mitochondrial function.

There was also limited to no follow-up time. Mitochondria were isolated and tested immediately after 10 min of reperfusion. Apoptosis as part of IR injury can be enhanced up to 3 days after start of reperfusion [21] so immediate testing might not be able to fully assess results of the intervention. This could likely be the cause of improvement of mitochondrial function in IR compared to Isc groups even though myocardial function did not reflect this. As reperfusion also salvages cells and mitochondrial function, the benefits might outweigh the harm of reperfusion in a shorter follow-up. However, this also eliminates possible confounders like long-term effects such as arrhythmia and reduced LV function [101], as well as possible impairment in the Langendorff apparatus over time.

3) Dose optimization for P188 was not conducted as part of this study. With insufficient dosing, not enough P188 would be available to stabilize all injured membranes and the protective effects would suffer. Availability of single P188 molecules is also reduced when administered in high concentrations because the amphiphilic P188 molecules could form micelles [161]. In in-vitro studies of cardiomyocytes optimal effects on IR injury were observed with 100 µM P188 [72]. However, the Riess laboratory has shown mitochondrial protective effects in ex-vivo hearts with 1 mM P188 during reperfusion and has found no direct mitochondrial effect on IR injury after incubation of isolated cardiac mitochondria with 100 µM P188 [89]. 250 µM P188 also showed no direct mitochondrial effect on rat brain isolated mitochondria [88]. Thus, a concentration of 1 mM P188 was chosen for ex-vivo post-conditioning, as well as mitochondrial treatment. This is still in the range of subcritical micelle concentration for P188 [113].

4) Isolated mitochondria are a great asset to assess mitochondrial function but concerns have been voiced that they do not adequately display normal mitochondrial function but rather put more stress on the already damaged organelle [162]. This has to be considered when analyzing data of these in-vitro experiments. Additionally, it has to be noted that the mere assessment of mitochondrial function might not be able to fully elucidate a direct mechanism of action of P188. Therefore, our results need to be interpreted in the context of the sparse knowledge from previous studies of direct P188 interaction.

5) Due to small sample sizes, given the number of different groups and the nature of this study, and very heterogeneous mitochondrial data, data at large were shown to not be normally distributed, so that only non-parametric statistic tests could be used.

Since these are more conservative, this decreases power and increases the possibility of type II errors.

5.5. Future Outlook

While treatment and outcome of MI have vastly improved in the last decades, there is not yet a satisfactory clinical strategy targeting reperfusion injury [163]. This is, of course, complicated further by the individual's susceptibility to injury as well as the limited time frame available for treatment. It is nevertheless an immense opportunity and obligation for further research to improve patient outcome in the future.

Despite the negative results in this study, the protective benefits of P188 shown in previous studies [38,77–79,87,132] should not simply be dismissed. On the contrary, these findings can be taken as a call to action to achieve a clearer understanding of P188's cellular and mitochondrial effects and the mechanisms they are achieved with. Therefore, a few core themes should be emphasized in the future such as: dose-finding studies in different models of IR injury, a longer reperfusion time and studies evaluating long-term outcome after P188 application. Additionally, findings by Bartos et al. [38] in regards to delivery route and place of application (i.c. vs i.v.) should be taken into account for possible future clinical studies to draw conclusions in a clinically relevant context.

Mitochondrial injury unequivocally plays an important role in cell death following IR injury and should therefore be a substantial part of future investigations to improve outcome after IR injury. Further research is needed to ascertain whether P188 has a direct protective effect on mitochondria or if improvement of mitochondrial function is solely due to overall cell protection, or whether other mechanisms upstream of MOMP and the intrinsic apoptotic pathway are indeed key points of P188's action. For this, more in-vitro studies need to be conducted on isolated mitochondria to substantiate or negate previous findings.

Apart from the triblock copolymer P188 and the homopolymer PEG, another kind of copolymer has been in the center of recent research. Amphiphilic diblock copolymer have been shown to protect the cell membrane after IR injury [149,150]. It is believed that, by eliminating a redundant hydrophilic block from the poloxamer's triblock architecture, the structure-function understanding of interactions with membranes is simplified [151]. This enhances the interaction with the hydrophobic interior of the lipid

bilayer, also known as “anchoring” effect. Apart from potentially sealing membranes with more strength than triblocks, this allows diblocks the pharmacological advantage of showing the same efficacy, as e.g. P188, at a lower dose. [151]. Efficacy of diblocks seems to be very dependent on the different chemical end-groups of the PPO chain. In that regard, the hydrophobic tert-butyl end group on the PPO block has been shown to play a prominent role in aiding cell membrane protection [149,150]. This would allow to pharmacologically engineer a more efficient membrane sealer.

So, while this study focused on the effects of P188 after cardiac IR injury in mitochondria, there is evidence suggesting that other block-copolymers might have a similar, or even increased, beneficial impact on IR injury as well.

5.6. Conclusion

In this model of isolated mitochondria from an ex-vivo rat heart subjected to IR injury, a quantifiable ischemic injury was found in mitochondria. A further exacerbation of mitochondrial function after reperfusion was not consistently observed, but myocardial function did not fully recover with reperfusion, suggesting that tissue damage did occur.

P188 was not found to have beneficial effects on myocardial function in the ex-vivo heart after IR injury, though the reperfusion time was much shorter than that of previous studies. P188 and PEG also did not improve mitochondrial function as assessed by ATP synthesis, O_2-consumption and CRC. These findings stand in contrast to promising studies by Bartos [38], Luo [86,141] and Wang et al. [87] but reflect recent findings by Pille and Riess [88] in rat isolated brain mitochondria.

6.1. Abstract

With high prevalence and mortality, myocardial infarction constitutes a social and economic burden in Germany and worldwide. Current guidelines for MI treatment require prompt reperfusion to salvage heart tissue and minimize short- and long-term complications. However, there are currently no treatments available to attenuate reperfusion injury. Ischemic as well as pharmacological post-conditioning have been identified as important clinical strategies to improve outcome. Membrane stabilizers, like Poloxamer 188 (P188), have been shown to improve myocardial ischemia reperfusion (IR) injury and mitochondrial function but have not yet been proven to directly offer mitochondrial protection. Mitochondrial function is crucial for cardiomyocyte function, and mitochondrial dysfunction plays an important role in myocardial injury.

In this study, hearts from 79 Sprague Dawley rats were isolated and perfused ex-vivo with oxygenated Krebs Buffer for 20 min before 30 min of no-flow ischemia. Hearts were reperfused for 10 min with Krebs buffer or 1 mM P188. Cardiac mitochondria were isolated with 1 mM P188 vs 1 mM polyethylene glycol (PEG) vs vehicle by differential centrifugation. Mitochondrial function was assessed as adenosine triphosphate (ATP) synthesis, oxygen consumption and calcium retention for complex I and II substrates of the respiratory chain.

An improvement of myocardial function with 10 min P188 post-conditioning could not be shown. Direct mitochondrial protection of P188 or PEG could not be observed in this model either. Further research is needed to ascertain whether P188 has a direct protective effect on mitochondria and, if so, on what pathways of IR injury it acts.

6.2. Zusammenfassung

Mit einer sehr hohen Prävalenz und Mortalität stellt der Myokardinfarkt in Deutschland und weltweit eine hohe gesellschaftliche und finanzielle Belastung dar. Die aktuellen Leitlinien fordern eine schnellstmögliche Reperfusion, um ischämisches Gewebe zu retten und Kurz- und Langzeitkomplikationen zu vermindern. Allerdings gibt es bisher keine Behandlungsmöglichkeiten des sekundären Reperfusionschadens.

Ischämische und pharmakologische Post-Konditionierung gelten jedoch als wichtige Strategien um das Outcome nach Ischämie-Reperfusions- (IR) schaden zu verbessern. Membranstabilisierende Moleküle, wie Poloxamer 188 (P188), verbessern in Studien die myokardiale und mitochondriale Funktion. Bisher konnte jedoch noch kein direkter Schutz des Mitochondriums nachgewiesen werden. Mitochondriale Funktion ist vor allem in Zellen mit hohem Energieumsatz, wie den Kardiomyozyten, unverzichtbar und die mitochondriale Dysfunktion spielt eine große Rolle bei der Entstehung des myokardialen Schadens.

Für diese Studie wurden Herzen aus 79 männlichen Sprague Dawley Ratten isoliert. Die Herzen wurden ex-vivo mit oxygenierter Krebs-Lösung für 20 min perfundiert, bevor eine 30-minütige Ischämie induziert wurde. Die Herzen wurden anschließend für 10 min mit Krebs Lösung (KL) oder 1 mM P188 in KL reperfundiert. Die kardialen Mitochondrien wurden mit 1 mM P188 vs 1 mM Polyethylenglycol (PEG) vs Trägersubstanz mittels Differenzialzentrifugation isoliert. Die mitochondriale Funktion wurde als Adenosintriphosphat (ATP) Synthese, Sauerstoffverbrauch und Calcium-Retention für Komplex I und II der Atmungskette bestimmt.

Es konnte keine Verbesserung der myokardialen Funktion mit 10 min P188 Post-Konditionierung gezeigt werden. Direkter Schutz der Mitochondrien mit P188 konnte in diesem Modell ebenfalls nicht nachgewiesen werden. Weitere Forschung ist notwendig, um zu ermitteln ob P188 einen direkten protektiven Effekt auf Mitochondrien hat und, wenn ja, an welchem Pfad des IR Schadens es angreift.

7. References

1. Thygesen, K.; Alpert, J.S.; Jaffe, A.S.; Chaitman, B.R.; Bax, J.J.; Morrow, D.A.; White, H.D. Fourth Universal Definition of Myocardial Infarction (2018). *Circulation* **2018**, *138*, e618-e651.
2. Timmis, A.; Townsend, N.; Gale, C.P.; Torbica, A.; Lettino, M.; Petersen, S.E.; Mossialos, E.A.; Maggioni, A.P.; Kazakiewicz, D.; May, H.T.*; et al.* European Society of Cardiology: Cardiovascular Disease Statistics 2019. *Eur Heart J* **2020**, *41*, 12–85.
3. Deutsche Herzstiftung (Hg.). *32. Deutscher Herzbericht 2020*: *Sektorenübergreifende Versorgungsanalyse zur Kardiologie, Herzchirurgie und Kinderherzmedizin in Deutschland*: Frankfurt a. M., 2021.
4. Yusuf, S.; Hawken, S.; Ôunpuu, S.; Dans, T.; Avezum, A.; Lanas, F.; McQueen, M.; Budaj, A.; Pais, P.; Varigos, J.*; et al.* Effect of potentially modifiable risk factors associated with myocardial infarction in 52 countries (the INTERHEART study): case-control study. *Lancet* **2004**, *364*, 937–952.
5. Finegold, J.A.; Asaria, P.; Francis, D.P. Mortality from ischaemic heart disease by country, region, and age: statistics from World Health Organisation and United Nations. *Int J Cardiol* **2013**, *168*, 934–945.
6. Ardehali, A.; Ports, T.A. Myocardial oxygen supply and demand. *Chest* **1990**, *98*, 699–705.
7. Ošt'ádal, B.; Kolář, F. *Cardiac Ischemia: From Injury to Protection*; Springer US: Boston, MA, 1999.
8. Braunwald, E. Myocardial Reperfusion: A Double-edged Sword? *J Clin Invest* **1985**.
9. Piper, H.M.; Garcia-Dorado, D.; Ovize, M. A fresh look at reperfusion injury. *Cardiovasc Res* **1998**, *38*, 291–300.
10. Krug, A.; Du Mesnil de, R.; Korb, G. Blood supply of the myocardium after temporary coronary occlusion. *Circ Res* **1966**, *19*, 57–62.
11. Ndrepepa, G.; Tiroch, K.; Fusaro, M.; Keta, D.; Seyfarth, M.; Byrne, R.A.; Pache, J.; Alger, P.; Mehilli, J.; Schömig, A.*; et al.* 5-year prognostic value of no-reflow phenomenon after percutaneous coronary intervention in patients with acute myocardial infarction. *J Am Coll Cardiol* **2010**, *55*, 2383–2389.

12. Piper, H.M.; Noll, T.; Siegmund, B. Mitochondrial function in the oxygen depleted and reoxygenated myocardial cell. *Cardiovasc Res* **1994**, *28*, 1–15.
13. Melkonian, E.A.; Schury, M.P. *Biochemistry, Anaerobic Glycolysis*: Treasure Island (FL), 2020.
14. Hausenloy, D.J.; Yellon, D.M. Myocardial ischemia-reperfusion injury: a neglected therapeutic target. *J Clin Invest* **2013**, *123*, 92–100.
15. Avkiran, M.; Marber, M.S. Na+/h+exchange inhibitors for cardioprotective therapy: progress, problems and prospects. *J Am Coll Cardiol* **2002**, *39*, 747–753.
16. Ottolia, M.; Torres, N.; Bridge, J.H.B.; Philipson, K.D.; Goldhaber, J.I. Na/Ca exchange and contraction of the heart. *J Mol Cell Cardiol* **2013**, *61*, 28–33.
17. Borutaite, V.; Toleikis, A.; Brown, G.C. In the eye of the storm: mitochondrial damage during heart and brain ischaemia. *FEBS J* **2013**, *280*, 4999–5014.
18. Di Lisa, F.; Menabò, R.; Canton, M.; Petronilli, V. The role of mitochondria in the salvage and the injury of the ischemic myocardium. *Biochim Biophys Acta* **1998**, *1366*, 69–78.
19. Lee, R.C.; Myerov, A.; Maloney, C.P. Promising therapy for cell membrane damage. *Ann N Y Acad Sci* **1994**, *720*, 239–245.
20. Steenbergen, C.; Hill, M.L.; Jennings, R.B. Volume regulation and plasma membrane injury in aerobic, anaerobic, and ischemic myocardium in vitro. Effects of osmotic cell swelling on plasma membrane integrity. *Circ Res* **1985**, *57*, 864–875.
21. Ong, S.-B.; Gustafsson, A.B. New roles for mitochondria in cell death in the reperfused myocardium. *Cardiovasc Res* **2012**, *94*, 190–196.
22. Maxwell, S.R.J.; Lip, G.Y.H. Reperfusion injury: a review of the pathophysiology, clinical manifestations and therapeutic options. *Int J Cardiol* **1997**, *58*, 95–117.
23. Siegmund, B.; Zude, R.; Piper, H.M. Recovery of anoxic-reoxygenated cardiomyocytes from severe Ca2+ overload. *Am J Physiol* **1992**, *263*, H1262-9.
24. Siegmund, B.; Ladilov, Y.V.; Piper, H.M. Importance of sodium for recovery of calcium control in reoxygenated cardiomyocytes. *Am J Physiol* **1994**, *267*, H506-13.
25. Bond, J.M.; Herman, B.; Lemasters, J.J. Protection by acidotic pH against anoxia/reoxygenation injury to rat neonatal cardiac myocytes. *Biochem Biophys Res Commun* **1991**, *179*, 798–803.

26. Ruiz-Meana, M.; García-Dorado, D.; González, M.A.; Barrabés, J.A.; Soler-Soler, J. Effect of osmotic stress on sarcolemmal integrity of isolated cardiomyocytes following transient metabolic inhibition. *Cardiovasc Res* **1995**, *30*, 64–69.
27. Turrens, J.F. Mitochondrial formation of reactive oxygen species. *J Physiology* **2003**, *552*, 335–344.
28. Szibor, M.; Schreckenberg, R.; Gizatullina, Z.; Dufour, E.; Wiesnet, M.; Dhandapani, P.K.; Debska-Vielhaber, G.; Heidler, J.; Wittig, I.; Nyman, T.A.*; et al.* Respiratory chain signalling is essential for adaptive remodelling following cardiac ischaemia. *J Cell Mol Med* **2020**.
29. Burton, K.P.; McCord, J.M.; Ghai, G. Myocardial alterations due to free-radical generation. *Am J Physiol* **1984**, *246*, H776-83.
30. Bolli, R. Oxygen-derived free radicals and myocardial reperfusion injury: An overview. *Cardiovasc Drugs Ther* **1991**, *5*, 249–268.
31. Martindale, J.J.; Metzger, J.M. Uncoupling of increased cellular oxidative stress and myocardial ischemia reperfusion injury by directed sarcolemma stabilization. *J Mol Cell Cardiol* **2014**, *67*, 26–37.
32. Murry, C.E.; Jennings, R.B.; Reimer, K.A. Preconditioning with ischemia: a delay of lethal cell injury in ischemic myocardium. *Circulation* **1986**, *74*, 1124–1136.
33. Zhao, Z.-Q.; Corvera, J.S.; Halkos, M.E.; Kerendi, F.; Wang, N.-P.; Guyton, R.A.; Vinten-Johansen, J. Inhibition of myocardial injury by ischemic postconditioning during reperfusion: comparison with ischemic preconditioning. *Am J Physiol Heart Circ Physiol* **2003**, *285*, H579-88.
34. Kin, H.; Zhao, Z.-Q.; Sun, H.-Y.; Wang, N.-P.; Corvera, J.S.; Halkos, M.E.; Kerendi, F.; Guyton, R.A.; Vinten-Johansen, J. Postconditioning attenuates myocardial ischemia-reperfusion injury by inhibiting events in the early minutes of reperfusion. *Cardiovasc Res* **2004**, *62*, 74–85.
35. Iliodromitis, E.K.; Georgiadis, M.; Cohen, M.V.; Downey, J.M.; Bofilis, E.; Kremastinos, D.T. Protection from post-conditioning depends on the number of short ischemic insults in anesthetized pigs. *Basic Res Cardiol* **2006**, *101*, 502–507.
36. Piot, C.; Croisille, P.; Staat, P.; Thibault, H.; Rioufol, G.; Mewton, N.; Elbelghiti, R.; Cung, T.T.; Bonnefoy, E.; Angoulvant, D.*; et al.* Effect of cyclosporine on reperfusion injury in acute myocardial infarction. *N Engl J Med* **2008**, *359*, 473–481.

37. Nazareth, W. Inhibition of anoxia-induced injury in heart myocytes by cyclosporin A. *J Mol Cell Cardiol* **1991**, *23*, 1351–1354.
38. Bartos, J.A.; Matsuura, T.R.; Tsangaris, A.; Olson, M.; McKnite, S.H.; Rees, J.N.; Haman, K.; Shekar, K.C.; Riess, M.L.; Bates, F.S.*; et al.* Intracoronary Poloxamer 188 Prevents Reperfusion Injury in a Porcine Model of ST-Segment Elevation Myocardial Infarction. *J Am Coll Cardiol Basic Trans Science* **2016**, *1*, 224–234.
39. Langendorff, O. Untersuchungen am überlebenden Säugethierherzen. *Pflugers Arch* **1895**, *61*, 291–332.
40. Dhein, S. The Langendorff Heart. In *Practical methods in cardiovascular research*: Springer, 2005, pp. 155–172.
41. Klabunde, R. *Cardiovascular Physiology Concepts*; Wolters Kluwer Health/Lippincott Williams & Wilkins, 2011.
42. Hom, J.; Sheu, S.-S. Morphological Dynamics of Mitochondria – A Special Emphasis on Cardiac Muscle Cells. *J Mol Cell Cardiol* **2009**, *46*, 811–820.
43. Brenner, C.; Moulin, M. Physiological roles of the permeability transition pore. *Circ Res* **2012**, *111*, 1237–1247.
44. Bartz, R.R.; Suliman, H.B.; Piantadosi, C.A. Redox mechanisms of cardiomyocyte mitochondrial protection. *Front Physiol* **2015**, *6*, 291.
45. Youle, R.J.; van der Bliek, A.M. Mitochondrial fission, fusion, and stress. *Science* **2012**, *337*, 1062–1065.
46. Rassow, J.; Hauser, K.; Netzker, R.; Deutzmann, R. *Biochemie*, 3rd ed; Georg Thieme Verlag: Stuttgart, 2012.
47. *Mitochondria: Form, function, and disease*; 2020. Available online: www.medicalnewstoday.com/articles/320875 (accessed on 9 Nov, 2021).
48. Torrealba, N.; Aranguiz, P.; Alonso, C.; Rothermel, B.A.; Lavandero, S. Mitochondria in Structural and Functional Cardiac Remodeling. In *Mitochondrial Dynamics in Cardiovascular Medicine*; Santulli, G., Ed.: Springer: Cham, 2017; volumen 982, pp. 277–306.
49. Efremov, R.G.; Baradaran, R.; Sazanov, L.A. The architecture of respiratory complex I. *Nature* **2010**, *465*, 441–445.
50. Neupane, P.; Bhuju, S.; Thapa, N.; Bhattarai, H.K. ATP Synthase: Structure, Function and Inhibition. *Biomol Concepts* **2019**, *10*, 1–10.
51. Mitochondrial Biology Unit. *Subunit composition of ATP synthase | MRC Mitochondrial Biology Unit*; 2020. Available online: https://www.mrc-

mbu.cam.ac.uk/research-groups/walker-group/subunit-composition-atp-synthase (accessed on 9 Nov, 2021).

52. Suzuki, T.; Ueno, H.; Mitome, N.; Suzuki, J.; Yoshida, M. F(0) of ATP synthase is a rotary proton channel. Obligatory coupling of proton translocation with rotation of c-subunit ring. *J Biol Chem* **2002**, *277*, 13281–13285.
53. Halestrap, A.P.; Richardson, A.P. The mitochondrial permeability transition: a current perspective on its identity and role in ischaemia/reperfusion injury. *J Mol Cell Cardiol* **2015**, *78*, 129–141.
54. Bernardi, P.; Petronilli, V. The permeability transition pore as a mitochondrial calcium release channel: a critical appraisal. *J Bioenerg Biomembr* **1996**, *28*, 131–138.
55. Kwong, J.Q.; Molkentin, J.D. Physiological and pathological roles of the mitochondrial permeability transition pore in the heart. *Cell Metab* **2015**, *21*, 206–214.
56. Bernardi, P.; Di Lisa, F. The mitochondrial permeability transition pore: molecular nature and role as a target in cardioprotection. *J Mol Cell Cardiol* **2015**, *78*, 100–106.
57. Chistiakov, D.A.; Shkurat, T.P.; Melnichenko, A.A.; Grechko, A.V.; Orekhov, A.N. The role of mitochondrial dysfunction in cardiovascular disease: a brief review. *Ann Med* **2018**, *50*, 121–127.
58. Campanella, M.; Parker, N.; Tan, C.H.; Hall, A.M.; Duchen, M.R. IF1: setting the pace of the F1Fo-ATP synthase. *Trends Biochem Sci* **2009**, *34*, 343–350.
59. Jonckheere, A.I.; Smeitink, J.A.M.; Rodenburg, R.J.T. Mitochondrial ATP synthase: architecture, function and pathology. *J Inherit Metab Dis* **2012**, *35*, 211–225.
60. Maskarinec, S.A.; Hannig, J.; Lee, R.C.; Lee, K.Y.C. Direct Observation of Poloxamer 188 Insertion into Lipid Monolayers. *Biophys J* **2002**, *82*, 1453–1459.
61. Kessler, R.J.; Tyson, C.A.; Green, D.E. Mechanism of uncoupling in mitochondria: uncouplers as ionophores for cycling cations and protons. *Proc Natl Acad Sci U S A* **1976**, *73*, 3141–3145.
62. Halestrap, A.P. The mitochondrial permeability transition: its molecular mechanism and role in reperfusion injury. *Biochem Soc Symp* **1999**, *66*, 181–203.

63. Wang, J.-Y.; Marks, J.; Lee, K.Y.C. Nature of interactions between PEO-PPO-PEO triblock copolymers and lipid membranes: (I) effect of polymer hydrophobicity on its ability to protect liposomes from peroxidation. *Biomacromolecules* **2012**, *13*, 2616–2623.
64. Moloughney, J.G.; Weisleder, N. Poloxamer 188 (P188) as a Membrane Resealing Reagent in Biomedical Applications. *Recent Pat Biotechnol* **2012**, *6*, 200–211.
65. Marks, J.D.; Pan, C.Y.; Bushell, T.; Cromie, W.; Lee, R.C. Amphiphilic, tri-block copolymers provide potent membrane-targeted neuroprotection. *FASEB J* **2001**, *15*, 1107–1109.
66. Houang, E.M.; Sham, Y.Y.; Bates, F.S.; Metzger, J.M. Muscle membrane integrity in Duchenne muscular dystrophy: recent advances in copolymer-based muscle membrane stabilizers. *Skelet Muscle* **2018**, *8*, 31.
67. Walsh, A.; Mustafi, D.; Makinen, M.; Lee, R. A Surfactant Copolymer Facilitates Functional Recovery of Heat-Denatured Lysozyme. *Ann N Y Acad Sci* **2006**, *1066*, 321–327.
68. Plataki, M.; Lee, Y.D.; Rasmussen, D.L.; Hubmayr, R.D. Poloxamer 188 facilitates the repair of alveolus resident cells in ventilator-injured lungs. *Am J Respir Crit Care Med* **2011**, *184*, 939–947.
69. Adams-Graves, P.; Kedar, A.; Koshy, M.; Steinberg, M.; Veith, R.; Ward, D.; Crawford, R.; Edwards, S.; Bustrack, J.; Emanuele, M. RheothRx (poloxamer 188) injection for the acute painful episode of sickle cell disease: a pilot study. *Blood* **1997**, *90*, 2041–2046.
70. Carr, M.E.; Powers, P.L.; Jones, M.R. Effects of poloxamer 188 on the assembly, structure and dissolution of fibrin clots. *Thromb Haemost* **1991**, *66*, 565–568.
71. Murphy, A.D.; McCormack, M.C.; Bichara, D.A.; Nguyen, J.T.; Randolph, M.A.; Watkins, M.T.; Lee, R.C.; Austen, W.G. Poloxamer 188 protects against ischemia-reperfusion injury in a murine hind-limb model. *Plast Reconstr Surg* **2010**, *125*, 1651–1660.
72. Michele M. Salzman, Benjamin J. Hackel, Frank S. Bates, Jason A. Bartos, Demetris Yannopoulos, and Matthias L. Riess. *Poloxamer 188 Protects Isolated Cardiomyocytes from Hypoxia/Reoxygenation Injury*, 31st ed, 2017.

73. Gu, J.-H.; Ge, J.-B.; Li, M.; Xu, H.-D.; Wu, F.; Qin, Z.-H. Poloxamer 188 protects neurons against ischemia/reperfusion injury through preserving integrity of cell membranes and blood brain barrier. *PLoS One* **2013**, *8*, e61641.
74. Salzman M.M.; Afzal, A.; Cheng Q.; Bates, F.S.; Riess, M.L. *Poloxamer 188 Protects Endothelial Cells From Hypoxia/Reoxygenation Injury - Implications for Cardio- and Neuroprotection After Cardiac Arrest*, 132nd ed, 2015.
75. Lotze, F.P.; Riess, M.L. Poloxamer 188 Exerts Direct Protective Effects on Mouse Brain Microvascular Endothelial Cells in an In Vitro Traumatic Brain Injury Model. *Biomedicines* **2021**, *9*, 1043.
76. Poellmann, M.J.; Lee, R.C. Repair and Regeneration of the Wounded Cell Membrane. *Regen Eng Transl Med* **2017**, *3*, 111–132.
77. Salzman, M.M.; Bartos, J.A.; Yannopoulos, D.; Riess, M.L. Poloxamer 188 Protects Isolated Adult Mouse Cardiomyocytes from Reoxygenation Injury. *Pharmacol Res Perspect* **2020**, *8*, e00639.
78. Salzman, M.; Cheng, Q.; Matsuura, T.; Yannopoulos, D.; Riess, M. Cardioprotection by Poloxamer 188 is Mediated by Nitric Oxide Synthase. *FASEB J* **2015**, *29*, 1026.5.
79. Yannopoulos, D.; Cheng, Q.; Matsuura, T.R.; Riess, M.L. Cardioprotection by Poloxamer One Eight Eight in Rat Isolated Hearts. *Anästh Intensivmed* **2014**, *55*, 213.
80. Schaer, G.L.; Hursey, T.L.; Abrahams, S.L.; Buddemeier, K.; Ennis, B.; Rodriguez, E.R.; Hubbell, J.P.; Moy, J.; Parrillo, J.E. Reduction in reperfusion-induced myocardial necrosis in dogs by RheothRx injection (poloxamer 188 N.F.), a hemorheological agent that alters neutrophil function. *Circulation* **1994**, *90*, 2964–2975.
81. Sarraf, M.; Matsuura, T.; Caldwell, E.; Bates, F.S.; Metzger, J.M.; Yannopoulos, D. Poloxamer 188 Reduces the Infarct Size in Pigs Undergoing ST Elevation Myocadial infarction. *Circulation* **2013**, *128*, A343.
82. Schaer, G.L.; Spaccavento, L.J.; Browne, K.F.; Krueger, K.A.; Krichbaum, D.; Phelan, J.M.; Fletcher, W.O.; Grines, C.L.; Edwards, S.; Jolly, M.K.*; et al.* Beneficial effects of RheothRx injection in patients receiving thrombolytic therapy for acute myocardial infarction. Results of a randomized, double-blind, placebo-controlled trial. *Circulation* **1996**, *94*, 298–307.

83. Effects of RheothRx on mortality, morbidity, left ventricular function, and infarct size in patients with acute myocardial infarction. Collaborative Organization for RheothRx Evaluation (CORE). *Circulation* **1997**, *96*, 192–201.
84. Schmolka, I.R. Physical basis for poloxamer interactions. *Ann N Y Acad Sci* **1994**, *720*, 92–97.
85. Wu, G.; Majewski, J.; Ege, C.; Kjaer, K.; Weygand, M.J.; Lee, K.Y.C. Lipid corralling and poloxamer squeeze-out in membranes. *Phys Rev Lett* **2004**, *93*, 28101.
86. Luo, C.; Li, Q.; Gao, Y.; Shen, X.; Ma, L.; Wu, Q.; Wang, Z.; Zhang, M.; Zhao, Z.; Chen, X.*; et al.* Poloxamer 188 Attenuates Cerebral Hypoxia/Ischemia Injury in Parallel with Preventing Mitochondrial Membrane Permeabilization and Autophagic Activation. *J Mol Neurosci* **2015**, *56*, 988–998.
87. Wang, J.C.; Bindokas, V.P.; Skinner, M.; Emrick, T.; Marks, J.D. Mitochondrial mechanisms of neuronal rescue by F-68, a hydrophilic Pluronic block co-polymer, following acute substrate deprivation. *Neurochem Int* **2017**, *109*, 126–140.
88. Pille, J.A.; Riess, M.L. Potential Effects of Poloxamer 188 on Rat Isolated Brain Mitochondria after Oxidative Stress In Vivo and In Vitro. *Brain Sci* **2021**, *11*, 122.
89. William, K.S.; Salzman, M.M.; Douglas, H.F.; Balzer, C.; Shekar, K.C.; Riess, M.L. Copolymer Treatment Preserves Function of Isolated Cardiac Mitochondria Only When Given Immediately Upon Reperfusion. *Circulation* **2017**, *136*, A19445.
90. Lazar, H.L. High-molecular-weight polyethylene glycol: a new strategy to limit ischemia-reperfusion injury. *J Thorac Cardiovasc Surg* **2015**, *149*, 594–595.
91. Merck KGaA. *Polyethylene Glycol (PEG) Selection Guide* | *Sigma-Aldrich*; 2021. Available online: https://www.sigmaaldrich.com/technical-documents/articles/materials-science/polyethylene-glycol-selection-guide.html (accessed on 9 Nov, 2021).
92. Ray Foster, L.J. PEGylation and BioPEGylation of Polyhydroxyalkanoates: Synthesis, Characterisation and Applications. In.
93. Xu, X.; Philip, J.L.; Razzaque, M.A.; Lloyd, J.W.; Muller, C.M.; Akhter, S.A. High-molecular-weight polyethylene glycol inhibits myocardial ischemia-reperfusion injury in vivo. *J Thorac Cardiovasc Surg* **2015**, *149*, 588–593.
94. Lee, R.C. Cytoprotection by stabilization of cell membranes. *Ann N Y Acad Sci* **2002**, *961*, 271–275.

95. Riess, M.L.; Elorbany, R.; Weihrauch, D.; Stowe, D.F.; Camara, A.K.S. PPARγ-Independent Side Effects of Thiazolidinediones on Mitochondrial Redox State in Rat Isolated Hearts. *Cells* **2020**, *9*.
96. Salzman, M.M.; Cheng, Q.; Deklotz, R.J.; Dulai, G.K.; Douglas, H.F.; Dikalova, A.E.; Weihrauch, D.; Barnes, B.M.; Riess, M.L. Lipid emulsion enhances cardiac performance after ischemia-reperfusion in isolated hearts from summer-active arctic ground squirrels. *J Comp Physiol B, Biochem Syst Environ Physiol* **2017**, *187*, 715–724.
97. Riess, M.L.; Camara, A.K.S.; Chen, Q.; Novalija, E.; Rhodes, S.S.; Stowe, D.F. Altered NADH and improved function by anesthetic and ischemic preconditioning in guinea pig intact hearts. *Am J Physiol Heart Circ Physiol* **2002**, *283*, H53-60.
98. Riess, M.L.; Kevin, L.G.; Camara, A.K.S.; Heisner, J.S.; Stowe, D.F. Dual exposure to sevoflurane improves anesthetic preconditioning in intact hearts. *Anesthesiology* **2004**, *100*, 569–574.
99. Holmuhamedov, E.L.; Wang, L.; Terzic, A. ATP-sensitive K+ channel openers prevent Ca2+ overload in rat cardiac mitochondria. *J Physiology* **1999**, *519 Pt 2*, 347–360.
100. Bradford, M.M. A rapid and sensitive method for the quantitation of microgram quantities of protein utilizing the principle of protein-dye binding. *Anal Biochem* **1976**, *72*, 248–254.
101. Matsuura, T.R.; Bartos, J.A.; Tsangaris, A.; Shekar, K.C.; Olson, M.D.; Riess, M.L.; Bienengraeber, M.; Aufderheide, T.P.; Neumar, R.W.; Rees, J.N.*; et al.* Early Effects of Prolonged Cardiac Arrest and Ischemic Postconditioning during Cardiopulmonary Resuscitation on Cardiac and Brain Mitochondrial Function in Pigs. *Resuscitation* **2017**, *116*, 8–15.
102. Riess, M.L.; Matsuura, T.R.; Bartos, J.A.; Bienengraeber, M.; Aldakkak, M.; McKnite, S.H.; Rees, J.N.; Aufderheide, T.P.; Sarraf, M.; Neumar, R.W.*; et al.* Anaesthetic Postconditioning at the Initiation of CPR Improves Myocardial and Mitochondrial Function in a Pig Model of Prolonged Untreated Ventricular Fibrillation. *Resuscitation* **2014**, *85*, 1745–1751.
103. *Luciferase Reporters | Thermo Fisher Scientific - DE*; 2020. Available online: https://www.thermofisher.com/de/de/home/life-science/protein-biology/protein-biology-learning-center/protein-biology-resource-library/pierce-protein-methods/luciferase-reporters.html (accessed on 5 July, 2020).

104. Garcia-Dorado, D.; Théroux, P.; Duran, J.M.; Solares, J.; Alonso, J.; Sanz, E.; Munoz, R.; Elizaga, J.; Botas, J.; Fernandez-Avilés, F. Selective inhibition of the contractile apparatus. A new approach to modification of infarct size, infarct composition, and infarct geometry during coronary artery occlusion and reperfusion. *Circulation* **1992**, *85*, 1160–1174.
105. Schlack, W.; Uebing, A.; Schäfer, M.; Bier, F.; Schäfer, S.; Piper, H.M.; Thämer, V. Regional contractile blockade at the onset of reperfusion reduces infarct size in the dog heart. *Pflugers Arch* **1994**, *428*, 134–141.
106. Habazettl, H.; PALMISANO, B.; BOSNJAK, Z.; STOWE, D. Initial reperfusion with 2,3 butanedione monoxime is better than hyperkalemic reperfusion after cardioplegic arrest in isolated guinea pig hearts. *Eur J Cardiothorac Surg* **1996**, *10*, 897–904.
107. Gobel, F.L.; Norstrom, L.A.; Nelson, R.R.; Jorgensen, C.R.; Wang, Y. The rate-pressure product as an index of myocardial oxygen consumption during exercise in patients with angina pectoris. *Circulation* **1978**, *57*, 549–556.
108. Watanabe, M.; Okada, T. Lysophosphatidylcholine-induced myocardial damage is inhibited by pretreatment with poloxamer 188 in isolated rat heart. *Mol Cell Biochem* **2003**, *248*, 209–215.
109. Gadicherla, A.K.; Stowe, D.F.; Antholine, W.E.; Yang, M.; Camara, A.K.S. Damage to mitochondrial complex I during cardiac ischemia reperfusion injury is reduced indirectly by anti-anginal drug ranolazine. *Biochimica et Biophysica Acta* **2012**, *1817*, 419–429.
110. Czeiszperger, T.L.; Wang, M.P.; Chung, C.S. Membrane stabilizer Poloxamer 188 improves yield of primary isolated rat cardiomyocytes without impairing function. *Physiol Rep* **2020**, *8*, e14382.
111. Kloner, R.A.; Reimer, K.A.; Willerson, J.T.; Jennings, R.B. Reduction of experimental myocardial infarct size with hyperosmolar mannitol. *Proc Soc Exp Biol Med* **1976**, *151*, 677–683.
112. Garcia-Dorado, D.; Théroux, P.; Munoz, R.; Alonso, J.; Elizaga, J.; Fernandez-Avilés, F.; Botas, J.; Solares, J.; Soriano, J.; Duran, J.M. Favorable effects of hyperosmotic reperfusion on myocardial edema and infarct size. *Am J Physiol* **1992**, *262*, H17-22.

113. Terry, M.A.; Hannig, J.; Carrillo, C.S.; Beckett, M.A.; Weichselbaum, R.R.; Lee, R.C. Oxidative cell membrane alteration. Evidence for surfactant-mediated sealing. *Ann N Y Acad Sci* **1999**, *888*, 274–284.
114. Chance, B.; Williams, G.R. Respiratory enzymes in oxidative phosphorylation. I. Kinetics of oxygen utilization. *J Biol Chem* **1955**, *217*, 383–393.
115. Korzeniewski, B. 'Idealized' state 4 and state 3 in mitochondria vs. rest and work in skeletal muscle. *PLoS One* **2015**, *10*, e0117145.
116. Murray, A.J.; Cole, M.A.; Lygate, C.A.; Carr, C.A.; Stuckey, D.J.; Little, S.E.; Neubauer, S.; Clarke, K. Increased mitochondrial uncoupling proteins, respiratory uncoupling and decreased efficiency in the chronically infarcted rat heart. *J Mol Cell Cardiol* **2008**, *44*, 694–700.
117. Lo Iacono, L.; Boczkowski, J.; Zini, R.; Salouage, I.; Berdeaux, A.; Motterlini, R.; Morin, D. A carbon monoxide-releasing molecule (CORM-3) uncouples mitochondrial respiration and modulates the production of reactive oxygen species. *Free Radic Biol Med* **2011**, *50*, 1556–1564.
118. Xu, A.; Szczepanek, K.; Hu, Y.; Lesnefsky, E.J.; Chen, Q. Cardioprotection by modulation of mitochondrial respiration during ischemia-reperfusion: role of apoptosis-inducing factor. *Biochem Biophys Res Commun* **2013**, *435*, 627–633.
119. Sadek, H.A.; Humphries, K.M.; Szweda, P.A.; Szweda, L.I. Selective inactivation of redox-sensitive mitochondrial enzymes during cardiac reperfusion. *Arch Biochem Biophys* **2002**, *406*, 222–228.
120. Stowe, D.F.; Yang, M.; Heisner, J.S.; Camara, A.K.S. Endogenous and Agonist-induced Opening of Mitochondrial Big Versus Small Ca2+-sensitive K+ Channels on Cardiac Cell and Mitochondrial Protection. *J Cardiovasc Pharmacol* **2017**, *70*, 314–328.
121. Li, J.; Iorga, A.; Sharma, S.; Youn, J.-Y.; Partow-Navid, R.; Umar, S.; Cai, H.; Rahman, S.; Eghbali, M. Intralipid, a clinically safe compound, protects the heart against ischemia-reperfusion injury more efficiently than cyclosporine-A. *Anesthesiology* **2012**, *117*, 836–846.
122. Li, J.; Ruffenach, G.; Kararigas, G.; Cunningham, C.M.; Motayagheni, N.; Barakai, N.; Umar, S.; Regitz-Zagrosek, V.; Eghbali, M. Intralipid protects the heart in late pregnancy against ischemia/reperfusion injury via Caveolin2/STAT3/GSK-3β pathway. *J Mol Cell Cardiol* **2017**, *102*, 108–116.

123. Neumann, F.-J.; Sousa-Uva, M.; Ahlsson, A.; Alfonso, F.; Banning, A.P.; Benedetto, U.; Byrne, R.A.; Collet, J.-P.; Falk, V.; Head, S.J.*; et al.* 2018 ESC/EACTS Guidelines on myocardial revascularization. *Eur Heart J* **2019**, *40*, 87–165.
124. Choi, H.A.; Badjatia, N.; Mayer, S.A. Hypothermia for acute brain injury--mechanisms and practical aspects. *Nat Rev Neurol* **2012**, *8*, 214–222.
125. Naito, H.; Nojima, T.; Fujisaki, N.; Tsukahara, K.; Yamamoto, H.; Yamada, T.; Aokage, T.; Yumoto, T.; Osako, T.; Nakao, A. Therapeutic strategies for ischemia reperfusion injury in emergency medicine. *Acute Med Surg* **2020**, *7*, e501.
126. Simon, M.A.; Tibbits, E.M.; Hoareau, G.L.; Davidson, A.J.; DeSoucy, E.S.; Faulconer, E.R.; Grayson, J.K.; Neff, L.P.; Johnson, M.A.; Williams, T.K. Lower extremity cooling reduces ischemia-reperfusion injury following Zone 3 REBOA in a porcine hemorrhage model. *J Trauma Acute Care Surg* **2018**, *85*, 512–518.
127. Kohlhauer, M.; Berdeaux, A.; Ghaleh, B.; Tissier, R. Therapeutic hypothermia to protect the heart against acute myocardial infarction. *Arch Cardiovasc Dis* **2016**, *109*, 716–722.
128. Ning, X.H.; Xu, C.S.; Song, Y.C.; Xiao, Y.; Hu, Y.J.; Lupinetti, F.M.; Portman, M.A. Hypothermia preserves function and signaling for mitochondrial biogenesis during subsequent ischemia. *Am J Physiol* **1998**, *274*, H786-93.
129. Dae, M.W.; Gao, D.W.; Sessler, D.I.; Chair, K.; Stillson, C.A. Effect of endovascular cooling on myocardial temperature, infarct size, and cardiac output in human-sized pigs. *Am J Physiol Heart Circ Physiol* **2002**, *282*, H1584-91.
130. Kato, R.; Foëx, P. Myocardial protection by anesthetic agents against ischemia-reperfusion injury: an update for anesthesiologists. *Can J Anaesth* **2002**, *49*, 777–791.
131. Schlack, W.; Preckel, B.; Barthel, H.; Obal, D.; Thämer, V. Halothane reduces reperfusion injury after regional ischaemia in the rabbit heart in vivo. *Br J Anaesth* **1997**, *79*, 88–96.
132. Bartos, J.A.; Matsuura, T.R.; Sarraf, M.; Youngquist, S.T.; McKnite, S.H.; Rees, J.N.; Sloper, D.T.; Bates, F.S.; Segal, N.; Debaty, G.*; et al.* Bundled postconditioning therapies improve hemodynamics and neurologic recovery after 17 min of untreated cardiac arrest. *Resuscitation* **2015**, *87*, 7–13.
133. Tsujita, K.; Shimomura, H.; Kawano, H.; Hokamaki, J.; Fukuda, M.; Yamashita, T.; Hida, S.; Nakamura, Y.; Nagayoshi, Y.; Sakamoto, T.*; et al.* Effects of

edaravone on reperfusion injury in patients with acute myocardial infarction. *Am J Cardiol* **2004**, *94*, 481–484.

134. Tsujita, K.; Shimomura, H.; Kaikita, K.; Kawano, H.; Hokamaki, J.; Nagayoshi, Y.; Yamashita, T.; Fukuda, M.; Nakamura, Y.; Sakamoto, T.*; et al.* Long-term efficacy of edaravone in patients with acute myocardial infarction. *Circ J* **2006**, *70*, 832–837.
135. Spoelstra-de Man, A.M.E.; Elbers, P.W.G.; Oudemans-van Straaten, H.M. Making sense of early high-dose intravenous vitamin C in ischemia/reperfusion injury. *Crit Care* **2018**, *22*, 70.
136. Houang, E.M.; Bartos, J.; Hackel, B.J.; Lodge, T.P.; Yannopoulos, D.; Bates, F.S.; Metzger, J.M. Cardiac Muscle Membrane Stabilization in Myocardial Reperfusion Injury. *J Am Coll Cardiol Basic Trans Science* **2019**, *4*, 275–287.
137. Yasuda, S.; Townsend, D.; Michele, D.E.; Favre, E.G.; Day, S.M.; Metzger, J.M. Dystrophic heart failure blocked by membrane sealant poloxamer. *Nature* **2005**, *436*, 1025–1029.
138. Evans, S.; Weinheimer, C.J.; Kovacs, A.; Williams, J.W.; Randolph, G.J.; Jiang, W.; Barger, P.M.; Mann, D.L. Ischemia reperfusion injury provokes adverse left ventricular remodeling in dysferlin-deficient hearts through a pathway that involves TIRAP dependent signaling. *Sci Rep* **2020**, *10*, 14129.
139. Justicz, A.G.; Farnsworth, W.V.; Soberman, M.S.; Tuvlin, M.B.; Bonner, G.D.; Hunter, R.L.; Martino-Saltzman, D.; Sink, J.D.; Austin, G.E. Reduction of myocardial infarct size by poloxamer 188 and mannitol in a canine model. *Am Heart J* **1991**, *122*, 671–680.
140. Kelly; Hursey; Patel; Parrillo; Schaer. Effect of Poloxamer 188 on Collateral Blood Flow, Myocardial Infarct Size, and Left Ventricular Function in a Canine Model of Prolonged (3-Hour) Coronary Occlusion and Reperfusion. *J Thromb Thrombolysis* **1998**, *5*, 239–247.
141. Luo, C.-L.; Chen, X.-P.; Li, L.-L.; Li, Q.-Q.; Li, B.-X.; Xue, A.-M.; Xu, H.-F.; Dai, D.-K.; Shen, Y.-W.; Tao, L.-Y.*; et al.* Poloxamer 188 attenuates in vitro traumatic brain injury-induced mitochondrial and lysosomal membrane permeabilization damage in cultured primary neurons. *J Neurotrauma* **2013**, *30*, 597–607.
142. Shelat, P.B.; Plant, L.D.; Wang, J.C.; Lee, E.; Marks, J.D. The membrane-active tri-block copolymer pluronic F-68 profoundly rescues rat hippocampal neurons

from oxygen-glucose deprivation-induced death through early inhibition of apoptosis. *J Neurosci* **2013**, *33*, 12287–12299.

143. Erich Gnaiger; Andrej V. Kuznetsov; Stefan Schneeberger; RÜdiger Seiler; Gerald Brandacher; Wolfgang Steurer; Raimund Margreiter. Mitochondria in the Cold. In *Life in the Cold*: Springer, Berlin, Heidelberg, 2000, pp. 431–442.
144. Kleinbongard, P.; Gedik, N.; Witting, P.; Freedman, B.; Klöcker, N.; Heusch, G. Pleiotropic, heart rate-independent cardioprotection by ivabradine. *Br J Pharmacol* **2015**, *172*, 4380–4390.
145. O'Keefe, J.H.; Grines, C.L.; DeWood, M.A.; Schaer, G.L.; Browne, K.; Magorien, R.D.; Kalbfleisch, J.M.; Fletcher, W.O.; Bateman, T.M.; Gibbons, R.J. Poloxamer-188 as an adjunct to primary percutaneous transluminal coronary angioplasty for acute myocardial infarction. *Am J Cardiol* **1996**, *78*, 747–750.
146. Maynard, C.; Swenson, R.; Paris, J.A.; Martin, J.S.; Hallstrom, A.P.; Cerqueira, M.D.; Weaver, W.D. Randomized, controlled trial of RheothRx (poloxamer 188) in patients with suspected acute myocardial infarction. *Am Heart J* **1998**, *135*, 797–804.
147. Emanuele, M.; Balasubramaniam, B. Differential effects of commercial-grade and purified poloxamer 188 on renal function. *Drugs R D* **2014**, *14*, 73–83.
148. Singh-Joy, S.D.; McLain, V.C. Safety assessment of poloxamers 101, 105, 108, 122, 123, 124, 181, 182, 183, 184, 185, 188, 212, 215, 217, 231, 234, 235, 237, 238, 282, 284, 288, 331, 333, 334, 335, 338, 401, 402, 403, and 407, poloxamer 105 benzoate, and poloxamer 182 dibenzoate as used in cosmetics. *Int J Toxicol* **2008**, *27 Suppl 2*, 93–128.
149. Kim, M.; Haman, K.J.; Houang, E.M.; Zhang, W.; Yannopoulos, D.; Metzger, J.M.; Bates, F.S.; Hackel, B.J. PEO-PPO Diblock Copolymers Protect Myoblasts from Hypo-Osmotic Stress In Vitro Dependent on Copolymer Size, Composition, and Architecture. *Biomacromolecules* **2017**, *18*, 2090–2101.
150. Houang, E.M.; Haman, K.J.; Kim, M.; Zhang, W.; Lowe, D.A.; Sham, Y.Y.; Lodge, T.P.; Hackel, B.J.; Bates, F.S.; Metzger, J.M. Chemical End Group Modified Diblock Copolymers Elucidate Anchor and Chain Mechanism of Membrane Stabilization. *Mol Pharm* **2017**, *14*, 2333–2339.
151. Haman, K. *Development of Model Diblock Copolymer Surfactants for Mechanistic Investigations of Cell Membrane Stabilization*. Ph.D. Thesis., 2015.

152. Malhotra, R.; Valuckaite, V.; Staron, M.L.; Theccanat, T.; D'Souza, K.M.; Alverdy, J.C.; Akhter, S.A. High-molecular-weight polyethylene glycol protects cardiac myocytes from hypoxia- and reoxygenation-induced cell death and preserves ventricular function. *Am J Physiol Heart Circ Physiol* **2011**, *300*, H1733-42.
153. Xianyao Xu, Jennifer L Philip, Abdur Razzaque, James W Lloyd, Charlie M Muller, Shahab A Akhter. High-Molecular-Weight Polyethylene Glycol (PEG) Inhibits Myocardial Ischemia-Reperfusion Injury and Improves Ventricular Function and Survival. *Circulation. 2014;130:A14049*.
154. Yang, J.; Xiao, Y.; Quan, E.Y.; Hu, Z.; Guo, Q.; Miao, C.; Bradley, J.L.; Peberdy, M.A.; Ornato, J.P.; Mangino, M.J.*; et al.* Effects of Polyethylene Glycol-20k on Postresuscitation Myocardial and Cerebral Function in a Rat Model of Cardiopulmonary Resuscitation. *Crit Care Med* **2018**, *46*, e1190-e1195.
155. Parrish, D.; Lindell, S.L.; Reichstetter, H.; Aboutanos, M.; Mangino, M.J. Cell Impermeant-based Low-volume Resuscitation in Hemorrhagic Shock: A Biological Basis for Injury Involving Cell Swelling. *Ann Surg* **2016**, *263*, 565–572.
156. Plant, V.; Parrish, D.W.; Limkemann, A.; Ferrada, P.; Aboutanos, M.; Mangino, M.J. Low-Volume Resuscitation for Hemorrhagic Shock: Understanding the Mechanism of PEG-20k. *J Pharmacol Exp Ther* **2017**, *361*, 334–340.
157. Wickramaratne, N.; Kenning, K.; Reichstetter, H.; Blocher, C.; Li, R.; Aboutanos, M.; Mangino, M.J. Acute resuscitation with polyethylene glycol-20k: A thromboelastographic analysis. *J Trauma Acute Care Surg* **2019**, *87*, 322–330.
158. Bejaoui, M.; Pantazi, E.; Folch-Puy, E.; Panisello, A.; Calvo, M.; Pasut, G.; Rimola, A.; Navasa, M.; Adam, R.; Roselló-Catafau, J. Protective Effect of Intravenous High Molecular Weight Polyethylene Glycol on Fatty Liver Preservation. *Biomed Res Int* **2015**, *2015*, 794287.
159. Ge, W.; Zheng, G.; Ji, X.; He, F.; Hu, J.; Bradley, J.L.; Moore, C.E.; Peberdy, M.A.; Ornato, J.P.; Mangino, M.J.*; et al.* Effects of Polyethylene Glycol-20k on Coronary Perfusion Pressure and Postresuscitation Myocardial and Cerebral Function in a Rat Model of Cardiac Arrest. *J Am Heart Assoc* **2020**, *9*, e014232.
160. Stettler, G.R.; Moore, E.E.; Moore, H.B.; Lawson, P.J.; Fragoso, M.; Nunns, G.R.; Silliman, C.C.; Banerjee, A. Thrombelastography indicates limitations of animal models of trauma-induced coagulopathy. *J Surg Res* **2017**, *217*, 207–212.
161. Hamley, I.W. *Developments in Block Copolymer Science and Technology*; Wiley, 2004.

162. Picard, M.; Taivassalo, T.; Ritchie, D.; Wright, K.J.; Thomas, M.M.; Romestaing, C.; Hepple, R.T. Mitochondrial structure and function are disrupted by standard isolation methods. *PLoS One* **2011**, *6*, e18317.
163. Fordyce, C.B.; Gersh, B.J.; Stone, G.W.; Granger, C.B. Novel therapeutics in myocardial infarction: targeting microvascular dysfunction and reperfusion injury. *Trends Pharmacol Sci* **2015**, *36*, 605–616.

8. Appendix

8.1. Digital Values of Mitochondrial Data

Table Legend: * significant difference TCH 50 vs Isc, as well as TCH 60 vs IR, ** significant difference TCH 60 vs IR+, *** significant difference IR vs IR+, # significant difference no treatment vs P188, † significant difference no treatment vs PEG, ‡ significant difference P188 vs PEG, no p-values correspond to no significant differences between groups.

Table 12: Digital Values of Mitochondrial ATP Synthesis. Complex I (nmol ATP/ min/ mg px)

Group	Treatment	Median	Interquartile range		p-value	n
			1. quartile (Q_1)	3. quartile (Q_3)		
TCH 50	None	7424	4898	8764	* < 0.001	16
	P188	4738	2866	8640		16
	PEG	7178	4877	9390		17
Isc	None	2382	1802	2822	* < 0.001; † < 0.001	22
	P188	2751	2083	4269		21
	PEG	3609	2915	4543	† < 0.001	16
TCH 60	None	6376	4469	9293	* 0.006; ** 0.041	22
	P188	7585	3204	14225		22
	PEG	7210	5490	9343		19
IR	None	4011	2226	5033	* 0.006	21
	P188	3054	2392	4924		22
	PEG	3816	3171	4455		17
IR+	None	4205	2483	6435	** 0.041	23
	P188	3069	2134	4142		22
	PEG	3702	3207	4491		17

Table 13: Digital Values of Mitochondrial ATP Synthesis. Complex II (nmol ATP/ min/ mg px)

Group	Treatment	Median	Interquartile range		p-value	n
			1.quartile (Q_1)	3. quartile (Q_3)		
TCH 50	None	6917	6190	7612	* < 0.001	15
	P188	6141	4873	8900		16
	PEG	8786	7107	10955		18
Isc	None	2527	1872	3219	* < 0.001; # 0.031; † 0.004	22
	P188	3639	2877	4554	# 0.031	22
	PEG	3868	3070	4960	† 0.004	17
TCH 60	None	6240	4197	8521	* < 0.001	22
	P188	5951	4366	10467		21
	PEG	8083	7004	10611		17
IR	None	3736	2914	4299	* < 0.001	20
	P188	3093	2342	4422		21
	PEG	4255	3515	5063		17
IR+	None	4620	3412	6964	# 0.03	22
	P188	3278	2329	4542	# 0.03	22
	PEG	4217	3090	5454		18

Table 14: Digital Values of Mitochondrial Respiratory Control Index. Complex I.

Group	Treatment	Median	Interquartile range		p-value	n
			1.quartile (Q_1)	3.quartile (Q_3)		
TCH 50	None	2.69	2.39	3.38	* 0.001	12
	P188	2.62	2.28	3.29		12
	PEG	2.82	2.60	2.92		11
Isc	None	1.73	1.53	2.23	* 0.001	10
	P188	1.65	1.54	1.77		13
	PEG	1.43	1.24	1.62		12

TCH 60	None	2.64	2.24	4.10		13
	P188	2.40	2.08	3.07		13
	PEG	2.54	2.34	3.50		12
IR	None	2.22	1.67	2.55		13
	P188	2.09	1.91	2.42		15
	PEG	1.80	1.58	2.09		12
IR+	None	1.90	1.43	2.43		12
	P188	1.85	1.67	2.27		15
	PEG	1.67	1.43	1.93		12

Table 15: Digital Values of Mitochondrial Respiratory Control Index. Complex II.

Group	Treatment	Median	Interquartile range		p-value	n
			1.quartile (Q_1)	3.quartile (Q_3)		
TCH 50	None	2.31	2.00	2.50	* < 0.001	11
	P188	2.45	1.87	2.90		12
	PEG	2.61	2.20	3.03		11
Isc	None	1.56	1.48	1.83	* < 0.001	11
	P188	1.66	1.38	1.94		10
	PEG	1.64	1.51	1.84		6
TCH 60	None	2.59	1.93	2.82	** 0.006	14
	P188	2.45	1.91	2.74		14
	PEG	2.43	2.13	2.83		11
IR	None	1.79	1.71	2.21		11
	P188	1.95	1.79	2.21		13
	PEG	1.82	1.74	2.00		11
IR+	None	1.80	1.51	2.06	** 0.006	12
	P188	1.65	1.49	1.88		12
	PEG	1.97	1.71	2.41		8

Table 16: Digital Values of State 3 Respiration. Complex I (10^2 nmol O_2/ min/ µg protein)

Group	Treatment	Median	Interquartile range		p-value	n
			1.quartile (Q_1)	3.quartile (Q_3)		
TCH 50	None	13.1	6.86	14.3	* 0.006; † 0.013	11
	P188	13.7	10.	17.4		13
	PEG	17.7	14.3	19.1	† 0.013	12
Isc	None	6.6	5.04	7.71	* 0.006; # 0.021	10
	P188	10.3	6.71	12.7	# 0.021	14
	PEG	9.14	5.71	12.0		13
TCH 60	None	13.7	9.00	15.6	* 0.004	12
	P188	14.3	11.1	18.9		14
	PEG	15.4	13.1	16.0		11
IR	None	8.6	6.86	10.00	* 0.004; # 0.009	13
	P188	12	9.71	13.1	# 0.009	15
	PEG	8.6	6.86	14.9		12
IR+	None	10.3	9.71	12.9		13
	P188	8.6	6.29	13.1		15
	PEG	9.14	8.25	9.71		12

Table 17: Digital Values of State 3 Respiration. Complex II (10^2 nmol O_2/ min/ µg protein)

Group	Treatment	Median	Interquartile range		p-value	n
			1.quartile (Q_1)	3.quartile (Q_3)		
TCH 50	None	15.1	9.14	17.0	* < 0.001	12
	P188	17.1	9.71	22.9		13
	PEG	17.7	13.4	26.6		12
Isc	None	8.00	7.43	8.00	* < 0.001; # 0.005; †0.01	12
	P188	11.7	8.43	13.7	# 0.005	14

	PEG	11.4	9.29	13.1	†0.01	12
TCH 60	None	11.7	10.7	16.0	* 0.004	14
	P188	17.1	14.6	19.1		14
	PEG	17.1	14.6	19.3		12
IR	None	9.71	8.29	12.3	* 0.004	13
	P188	13.1	9.14	14.3		15
	PEG	9.14	7.43	14.3		11
IR+	None	12.2	10.00	14.9		13
	P188	10.9	7.43	13.1		15
	PEG	8.14	8.00	9.71		11

Table 18: Digital Values of State 4 Respiration. Complex I (10^2 nmol O_2/ min/ µg protein)

Group	Treatment	Median	Interquartile range		p-value	n
			1.quartile (Q_1)	3.quartile (Q_3)		
TCH 50	None	4.14	2.70	5.40	† 0.003	12
	P188	4.40	3.49	6.86		13
	PEG	6.29	5.71	6.29	† 0.003	11
Isc	None	3.83	2.73	4.13	# 0.017, † 0.021	10
	P188	6.29	3.84	8.00	# 0.017	14
	PEG	5.71	3.94	7.43	† 0.021	13
TCH 60	None	3.60	2.96	4.61		12
	P188	5.60	3.49	7.57		14
	PEG	5.20	4.36	6.14		12
IR	None	3.14	2.91	4.97	# 0.047, † 0.019	13
	P188	5.20	3.89	6.29	# 0.047	15
	PEG	5.00	3.96	6.71	† 0.019	12
IR+	None	5.31	3.60	6.04		13
	P188	4.57	3.60	4.83	‡ 0.042	13
	PEG	5.40	4.74	6.71	‡ 0.042	12

Table 19: Digital Values of State 4 Respiration. Complex II (10^2 nmol O_2/ min/ µg protein)

Group	Treatment	Median	Interquartile range		p-value	n
			1.quartile (Q_1)	3.quartile (Q_3)		
TCH 50	None	6.86	4.06	7.43		11
	P188	5.71	3.54	8.86		13
	PEG	7.43	5.09	8.57		11
Isc	None	5.23	4.41	5.66		12
	P188	6.86	4.71	8.14		10
	PEG	7.71	5.20	8.00		6
TCH 60	None	5.31	4.40	6.29		13
	P188	6.29	5.57	8.57		13
	PEG	6.29	6.14	7.00		10
IR	None	4.57	4.00	8.00		11
	P188	6.29	5.03	7.43		14
	PEG	5.43	4.34	7.43		11
IR+	None	6.86	6.29	7.29	† 0.013	12
	P188	5.37	3.87	6.29		12
	PEG	4.56	4.07	5.00	† 0.013	8

Table 20: Digital Values of Calcium Retention Capacity. Complex I (10^{-1} µmol Ca^{2+} / µg protein)

Group	Treatment	Median	Interquartile range		p-value	n
			1.quartile (Q_1)	3.quartile (Q_3)		
TCH 50	None	2.20	1.88	2.36	† 0.001	12
	P188	2.47	2.28	2.89		11
	PEG	2.71	2.39	3.07	† 0.001	12
Isc	None	2.29	1.96	2.39	† 0.002	11
	P188	2.40	1.90	2.46	‡ 0.026	14
	PEG	2.71	2.40	3.34	† 0.002; ‡ 0.026	12

TCH 60	None	2.09	1.72	2.79		14
	P188	2.31	2.00	2.61		13
	PEG	2.37	2.30	2.69		13
IR	None	1.91	1.84	2.17	† 0.031	12
	P188	2.07	1.98	2.24		11
	PEG	2.23	2.03	2.71	† 0.031	11
IR+	None	2.11	1.94	2.86		10
	P188	1.96	1.85	2.58		11
	PEG	1.99	1.95	2.42		11

Table 21: Digital Values of Calcium Retention Capacity. Complex II (10^{-1} µmol Ca^{2+} / µg protein)

Group	Treatment	Median	Interquartile range		p-value	n
			1.quartile (Q_1)	3.quartile (Q_3)		
TCH 50	None	6.72	6.47	8.18	* < 0.001; † 0.006	10
	P188	8.14	7.35	9.53		12
	PEG	8.95	7.80	9.49	† 0.006	11
Isc	None	4.77	3.56	5.91	* < 0.001	12
	P188	6.16	5.87	6.31		15
	PEG	5.81	5.38	6.22		11
TCH 60	None	5.76	5.07	9.06		13
	P188	7.72	6.75	9.16		13
	PEG	8.30	7.74	8.64		12
IR	None	5.95	5.65	6.45		10
	P188	6.44	5.33	6.65		11
	PEG	5.75	5.26	7.06		11
IR+	None	6.50	5.44	7.41		12
	P188	6.82	5.84	7.38	‡ 0.035	10
	PEG	5.74	5.09	6.00	‡ 0.035	11

8.2. Acknowledgements

This work was supported in part by the US Department of Veterans Affairs Biomedical Laboratory R&D Service (I01 BX003482), and by institutional funds to Matthias L. Riess, MD, PhD.

Throughout the process of collecting data and writing this dissertation I have received an abundance of support and assistance.

I would like to thank Prof. Dr. Klaus Hahnenkamp, Clinical Director of the Department of Anesthesiology and Intensive Care Medicine, and Vice President of the Universität Greifswald. He gave me the opportunity to do research in the U.S. and to complete this dissertation in Germany. Without him, this work would not have been possible.

Furthermore, I want to thank Dr. Anke Hahnenkamp, head of the laboratory in the Department of Anesthesiology and Intensive Care Medicine of the Universität Greifswald. Her questions about my work and insights into writing a thesis were invaluable in starting and finishing my writing.

I would like to express extraordinary gratitude to Matthias Riess, MD, PhD, FASA, Professor of Anesthesiology and Pharmacology at the Vanderbilt University Medical Center, head of the Riess laboratory and my supervisor. I started in his laboratory without any previous experience in scientific work and only found patience, encouragement and advice from him throughout this journey – be it on-site in Nashville or back in Germany via countless Zoom sessions. He has taught me most everything I know about hands-on science and has given me the unique opportunity to immerse myself in practical laboratory work as well as fulfill my dream of a semester abroad. I could not have asked for a better mentor.

I would also like to thank William Cleveland, BS, for his just about endless patience with me and the everyday problems I encountered in the laboratory. Without his constant help trouble-shooting and the witty work-place banter my time in the lab would have been a lot less fun and probably much more frustrating. Not to mention his help in analyzing my Langendorff data with R. I would have been lost in the coding jungle without you.

I thank, of course, each member of the Riess laboratory – Claudius Balzer, MD, MS, and Zhu Li, PhD – for working with me and creating a pleasant work-environment. And Claudius, in particular, for showing us around Nashville when we first got there.

Another big thank you to my very dear friend Luise Meyer, MD, who I barely knew when getting to Nashville but who has made everything about life away from home much better than I could have ever hoped for. I will forever cherish the big and small moments we got to spend together during long work hours, simple grocery shopping and our chaotic road trips. I am grateful to call you my friend and I am so proud to see what you have already achieved.

Last but not least, I want to thank my friends and family their unconditional love and patience throughout my entire studies. My family has always been my biggest supporter in achieving my goals and has made my time abroad possible but has made coming home a festivity of its own. Thank you, mom, for checking all the commas in this twice and, dad, for giving me input in how to make my graphs even though you would have rather have me write this thesis in German so you could read it. And I thank my friends and boyfriend for the social support, for pulling me out of my own head when I got frustrated and for being excited with me as I am nearing the finish line.